DIGITAL COMMUNICATION

— Second Edition —

SOLUTIONS MANUAL

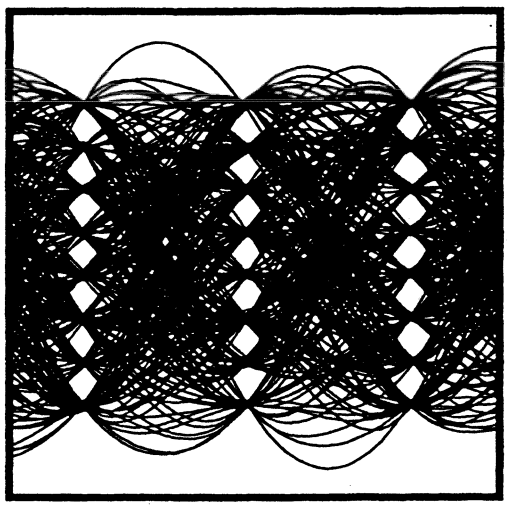

Edward A. Lee
David G. Messerschmitt

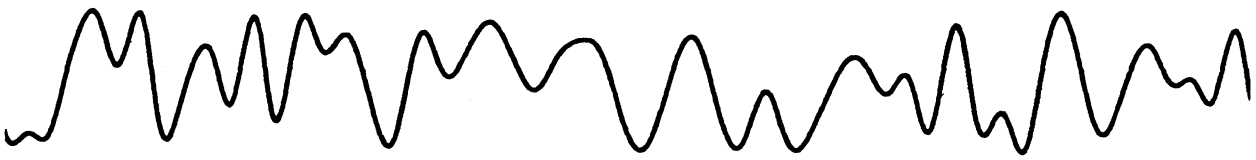

Springer Science+Business Media, LLC

ISBN 978-0-7923-9405-1 ISBN 978-1-4615-3136-4 (eBook)
DOI 10.1007/978-1-4615-3136-4

Printed on acid-free paper.

CONTENTS

CHAPTER 1: SOLUTIONS TO PROBLEMS

1-1.

(a) The overload point of the A/D converter (largest signal that can be accommodated) will be chosen on the basis of the signal statistics and the signal power so as to keep the probability of overload low. Assuming the signal doesn't change, we would want to keep the overload fixed. Hence, the Δ would be halved.

(b) Generally the error signal would be halved in amplitude. This would increase the SNR by $20\log_{10}2 = 6$ dB.

(c) The bit rate would increase by f_s, the sampling rate.

(d) We get, for some constant K,

$$SNR = 6n + K\ , \quad f_b = nf_s\ , \tag{1.1}$$

and thus

$$SNR = \frac{6f_b}{f_s} + K\ . \tag{1.2}$$

In particular, the SNR in dB is directly proportional to the bit rate.

1-2. Each bit error will cause one recovered sample to be the wrong amplitude, which is similar to an added impulse to the signal. This will be perceived as a "pop" or a "click". The size of this impulse will depend on which of the n bits of a particular sample is in error. The error will range from the smallest quantization interval (the least-significant bit in error) to the entire range of signal levels (the sign bit in error).

1-3. The most significant sources will be the anti-aliasing and reconstruction lowpass filters, which will have some group delay, and the propagation delay on the communication medium. Any multiplexes (Chapter 18) will introduce a small amount of delay, as will digital switches (Chapter 18).

1-4. Assume the constant bit rate is larger than the peak bit rate of the source. Then we might artificially increase the bit rate of the source up until it precisely equals the bit rate of the link by adding extra bits. We must have some way of identifying these extra bits at the receiver so that they can be removed. A number of schemes are possible, so here is but one: Divide the source bits in to groups called packets with arbitrary length. Append a unique sequence of eight bits, called a flag, to the beginning and end of each packet, and transmit these packets on the link interspersed with an idle code (say all zeros). The only problem now is to insure that the flag does not occur in the input bit stream. This can be accomplished using coding, with techniques described in Chapter 18.

CHAPTER 2: SOLUTIONS TO PROBLEMS

2-1. We start out with an easy problem! Looking at figure 2-2, when the imaginary part of the impulse response is zero, we see that the system consists of two independent filters, one for real part and one for imaginary part of the input, with no crosstalk. The imaginary part of the impulse response results in crosstalk between the real and imaginary parts.

2-2. Doing the discrete-time part only, write the convolution sum when the input is $e^{j\omega kT}$

$$y_k = \sum_{m=-\infty}^{\infty} e^{j\omega mT} h_{k-m}. \tag{2.142}$$

Changing variables,

$$\begin{aligned} y_k &= \sum_{n=-\infty}^{\infty} e^{j\omega(k-n)T} h_n \\ &= e^{j\omega kT} \sum_{n=-\infty}^{\infty} e^{-j\omega nT} h_n. \end{aligned} \tag{2.143}$$

The output is the same complex exponential multiplied by a sum that is a function of the impulse response of the system h_n and the frequency ω of the input, but is not a function of the time index k. This frequency response

$$H(e^{j\omega T}) = \sum_{n=-\infty}^{\infty} e^{-j\omega nT} h_n \tag{2.144}$$

is recognized as the Fourier transform of the discrete-time signal h_n.

2-3. The output of the impulse generator is defined as

$$w(t) = \sum_{k=-\infty}^{\infty} w_k \delta(t - kT). \tag{2.145}$$

(a)

$$\begin{aligned} Y(j\omega) &= F(j\omega) \sum_{k=-\infty}^{\infty} w_k e^{-j\omega kT} \\ &= F(j\omega) H(e^{j\omega T}) \cdot \frac{1}{T} \sum_{m=-\infty}^{\infty} G(j(\omega + m\frac{2\pi}{T})) X(j(\omega + m\frac{2\pi}{T})) \end{aligned} \tag{2.146}$$

(b) Yes, you can see from a. that if we add two input signals, the output will be a similar superposition.

(c) If $F(j\omega) = 0$ for $|\omega| > \pi/T$ then for $|\omega| \le \pi/T$ we have

$$Y(j\omega) = \frac{1}{T} F(j\omega) H(e^{j\omega T}) G(j\omega) X(j\omega) \tag{2.147}$$

and the system is time-invariant with frequency response $\frac{1}{T} F(j\omega) H(e^{j\omega T}) G(j\omega)$.

2-4. In continuous-time:

$$\begin{aligned}\int_{-\infty}^{\infty} |x(t)|^2 dt &= F.T.\Big[x(t)x^*(t)\Big]_{\omega=0} \\ &= \left[\frac{1}{2\pi}X(j\omega) * X^*(-j\omega)\right]_{\omega=0} \\ &= \frac{1}{2\pi}\int_{-\infty}^{\infty} |X(j\omega)|^2 d\omega .\end{aligned} \tag{2.148}$$

Discrete-time follows similarly.

2-5. We get that the energy of the discrete-time signal is

$$\sum_k |x_k|^2 = \frac{T}{2\pi}\int_{-\pi/T}^{\pi/T} |\sum_m X(j(\omega + m\frac{2\pi}{T}))|^2 d\omega \tag{2.149}$$

and there is evidently no way to relate this to the energy of the continuous-time signal. However, if the continuous-time signal is properly bandlimited, then the sum inside the integral includes one term, and the right hand side is proportional to the energy. In fact, the energy of the discrete-time signal in this case is $1/T^2$ times the energy of the continuous-time signal. As the sampling rate increases, the energy of the discrete-time signal grows without bound, since we have more and more samples in the summation.

2-6. The transfer function is $H(z) = 1 + z^{-1}$ and the frequency response is $H(e^{j\omega T}) = 1 + e^{-j\omega T}$. The output is $y_k = A\cos(\omega_0 kT + \theta)$ where the magnitude response is $A = \sqrt{2(1 + \cos(\omega_0 T))}$ and the phase response is

$$\theta = \tan^{-1}\left[\frac{\sin(\omega_0 T)}{1 + \cos(\omega_0 T)}\right] = \tan^{-1}\left[\frac{2\sin(\frac{\omega_0 T}{2})\cos(\frac{\omega_0 T}{2})}{2\cos^2(\frac{\omega_0 T}{2})}\right] = \frac{\omega_0 T}{2}. \tag{2.150}$$

The phase is linear in ω_0.

2-7. The Fourier transform of a real system is conjugate symmetric, so

$$H(j\omega) = A(\omega)e^{j\theta(\omega)} = H^*(-j\omega) = A(\omega)e^{-j\theta(-\omega)}, \tag{2.151}$$

since $A(\omega) = |H(j\omega)|$ is both non-negative and symmetric. Hence, $\theta(\omega) = -\theta(-\omega)$.

2-8. From problem 2-7 the phase response of a real system is anti-symmetric, so the frequency response of the phase shifter should be

$$H(j\omega) = e^{-j\theta \mathrm{sgn}(\omega)} = \cos(\theta) + j\,\mathrm{sgn}(\omega)\sin(\theta), \tag{2.152}$$

where we have used the symmetry and anti-symmetry of the cos and sin, respectively. This becomes

$$h(t) = \delta(t)\cos(\theta) - \frac{1}{\pi t}\sin(\theta). \tag{2.153}$$

2-9. If $\mathrm{Re}\{\alpha\} > 0$, then we can use the Fourier transform pair

$$y(t) = \frac{1}{jt + \alpha} \leftrightarrow Y(j\omega) = 2\pi e^{\alpha\omega}u(-\omega) \tag{2.154}$$

where $u(\omega)$ is the unit step function. Then we observe that $x(t)$ is $y(t)$ convolved with an impulse stream $\sum_{m=-\infty}^{\infty} \delta(t - mT)$, so its transform is

$$\begin{aligned}X(j\omega) = Y(j\omega)\frac{2\pi}{T}\sum_{m=-\infty}^{\infty} \delta(\omega - \frac{2\pi}{T}m) \\ \frac{2\pi^2}{T}\sum_{m=-\infty}^{0} \delta(\omega - \frac{2\pi}{T}m)e^{2\pi m\alpha/T}.\end{aligned} \tag{2.155}$$

If $\mathrm{Re}\{\alpha\} = 0$, then we can use the transform of $1/jt$, convolving it again with an impulse stream to get

$$\frac{-2\pi^2}{T}\sum_{m=-\infty}^{\infty}\delta(\omega-\frac{2\pi}{T}m)\mathrm{sgn}(\omega). \tag{2.156}$$

2-10. Given $Y(j\omega)=H(j\omega)X(j\omega)$, then if $X(j\omega_0)=0$ then $Y(j\omega_0)=0$.

2-11.

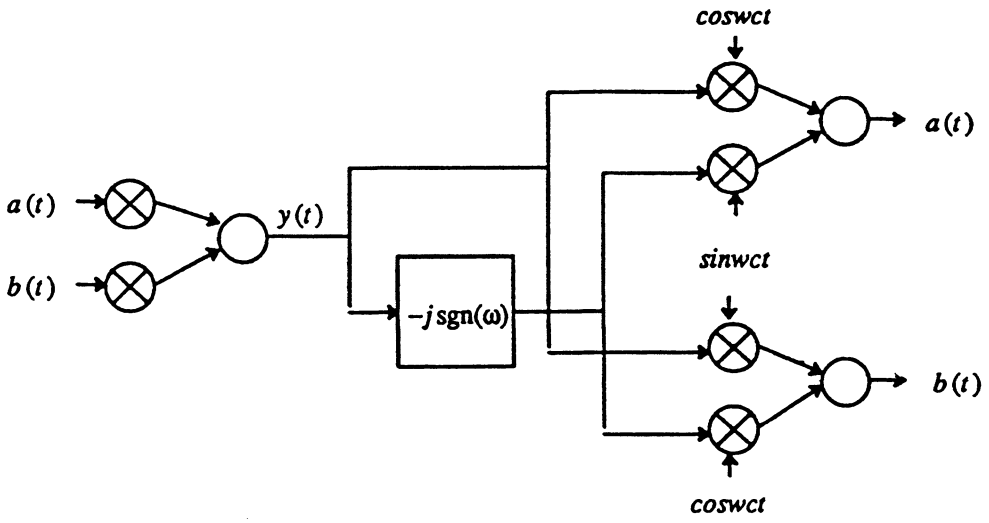

2-12.

(a)

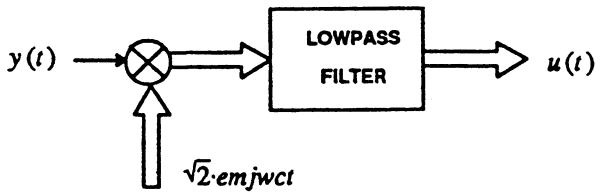

(b)

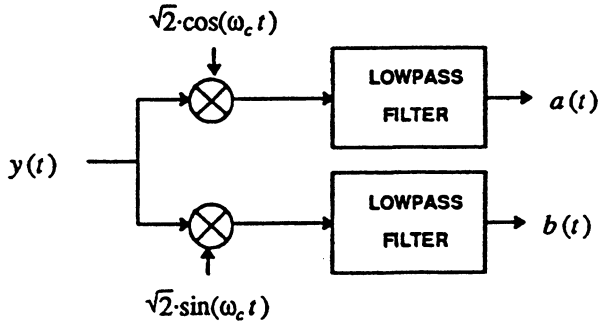

2-13.

(a) From (2.7),

$$y_k=\sum_{m=-\infty}^{\infty}z^m h_{k-m}. \tag{2.157}$$

Changing variables,

$$y_k=\sum_{n=-\infty}^{\infty}z^{k-n}h_n=z^k\sum_{n=-\infty}^{\infty}z^{-n}h_n=z^kH(z). \tag{2.158}$$

Because the system is time invariant, $H(z)$ does not depend on k.

(b) If we constrain z to lie on the unit circle, $|z| = 1$, the two results are identical.

2-14. Let the response to z^k be y_k. By linearity and problem 2-1, if the input to the system is z^{k+m} then the output is $z^m y_k = z^k z^m$. By time invariance the response to that same input is y_{k+m}. Setting these two responses equal,

$$z^m y_k = y_{k+m} \tag{2.159}$$

and setting $k = 0$ we get the desired result

$$y_m = y_0 z^m. \tag{2.160}$$

The transfer function is a complex number y_0, which is evidently a function of z, so we define the notation $y_0 = H(z)$ to reflect this property.

2-15. The Z transform is

$$\begin{aligned} X(z) &= \sum_{m=-\infty}^{\infty} z^{-m} a^m u_m \\ &= \sum_{m=0}^{\infty} (az^{-1})^m. \end{aligned} \tag{2.161}$$

For any b such that $|b| < 1$ we have the identity

$$\frac{1}{1-b} = \sum_{m=0}^{\infty} b^m \tag{2.163}$$

which is easily verified by using long division on the left hand side. Therefore, in the region $|z^{-1}| < \frac{1}{|a|}$, the Z transform is

$$X(z) = \frac{1}{1-az^{-1}}. \tag{2.164}$$

Outside of this region, the Z transform does not exist. If $|a| > 1$, we easily see from (2.102) that the signal goes to infinity as k increases. Not coincidentally, the region in which the Z transform exists does not include the unit circle, implying that the Fourier transform does not exist either.

2-16. If the response of the system to z^t is $y(t)$, then by linearity the response to $z^{t+u} = z^t z^u$ is $z^u y(t)$. By time invariance, the response to z^{t+u} is $y(t+u)$. Setting these two equal, $y(t+u) = t^u y(t)$, and setting $t = 0$, $y(u) = y(0)z^u$.

Clearly $e^{st} = z^t$ if $z = e^s$, i.e., if $s = j\omega$, then $z = e^{j\omega}$, a point on the unit circle.

Substituting into the convolution,

$$y(t) = \int_{-\infty}^{\infty} h(\tau)x(t-\tau)\,d\tau = \int_{-\infty}^{\infty} h(\tau)e^{s(t-\tau)}\,d\tau = e^{st}\int_{-\infty}^{\infty} h(\tau)e^{-s\tau}\,d\tau = e^{st}H(s) \tag{2.165}$$

which implies that $H(s)$ is an eigenvalue of the system.

2-17.

(a)

$$X(z) = \frac{z}{z-a} \tag{2.166}$$

in both cases.

(b) $|z| > |a|$ and $|z| < |a|$ respectively.

(c) $|a| < 1$ and $|a| > 1$ respectively.

2-18. Since

$$\frac{1}{1-az^{-1}} = 1 + az^{-1} + a^2z^{-2} + \cdots \tag{2.167}$$

we get the signal of problem 2-17a, where the ROC is $|az^{-1}| < 1$ or $|z| > |a|$. Also, since

$$-\frac{\frac{z}{a}}{1-\frac{z}{a}} = -\frac{z}{a}(1 + \frac{z}{a} + (\frac{z}{a})^2 + \cdots) \tag{2.168}$$

we get the signal of problem 2-17b where the ROC is $|za^{-1}| < 1$ or $|z| < a$.

2-19. First we perform a partial fraction expansion,

$$X(z) = \frac{A}{z-a} + \frac{B}{z-b} \tag{2.169}$$

where

$$A = \frac{a^2}{a-b}, \quad B = \frac{b^2}{b-a} \ . \tag{2.170}$$

(a) The ROC is $|z| > |b|$, and applying problem 2-17a to both terms in the partial fraction expansion,

$$x_k = A \cdot a^k + B \cdot b^k \tag{2.171}$$

for $k \geq 0$, and zero otherwise.

(b) The ROC must be $|a| < |z| < |b|$ and hence, applying the results of problem 2-17b,

$$x_k = \begin{cases} A \cdot a^k, & k \geq 0 \\ -B \cdot b^k, & k < 0 \end{cases} \tag{2.172}$$

(c) For (a) the signal is not stable because $b^k \to \infty$. This is because the ROC does not include the unit circle. For (b) the ROC does include the unit circle so the signal is stable (this is the only ROC for which the signal is stable).

2-20. Consider the zeros, and the poles will follow similarly. Assume that z_0 is a zero, and hence

$$\sum_{k=0}^{M} b_k z_0^{-k} = 0 \tag{2.173}$$

and taking the conjugate of this equation.

$$\sum_{k=0}^{M} b_k^* (z_0^*)^{-k} = \sum_{k=0}^{M} b_k (z_0^*)^{-k} = 0 \tag{2.174}$$

and we conclude that z_0^* is also a zero.

2-21. The easy terms are

$$H_{\text{zero}}(z) = (1 - jz^{-1})(1 + jz^{-1}) = (1 + z^{-2}) \tag{2.175}$$

$$H_{\min}(z) = \frac{1}{(1 - 0.5e^{j\pi/8}z^{-1})(1 - 0.5e^{-j\pi/8}z^{-1})} = \frac{1}{1 - \cos(\pi/8)z^{-1} + 0.25z^{-2}} \tag{2.176}$$

but the maximum-phase term requires some more work. Writing one maximum-phase zero in monic form,

$$(1 - \frac{3}{2}e^{j\pi/8}z^{-1}) = z^{-1} \cdot (-\frac{3}{2}e^{j\pi/8})(1 - \frac{2}{3}e^{-j\pi/8}z) \tag{2.177}$$

and considering both zeros we get $L = -2, B = (-2/3)^2 = \frac{4}{9}$, and

$$H_{\max}(z) = 1 - \frac{4}{3}\cos(\pi/8)z + \frac{4}{9}z^2 \ . \tag{2.178}$$

2-22.

(a) Let

$$A(z) = \frac{z^{-1} - c^*}{1 - cz^{-1}} \tag{2.179}$$

and note that $G(z) = H(z)A(z)$. $A(z)$ is allpass (see example 2-9), so

$$|G(e^{j\omega T})| = |H(e^{j\omega T})|\,|A(e^{j\omega T})| = |H(e^{j\omega T})| \ . \tag{2.180}$$

It has the effect of moving a zero $|c| < 1$ outside the unit circle without changing the magnitude response.

(b) Using the hint, h_k can be obtained by putting f_k through transfer function $(1 - cz^{-1})$, so

$$h_k = f_k - cf_{k-1} \ . \tag{2.181}$$

Similarly g_k can be obtained by putting f_k through transfer function $(z^{-1} - c^*)$,

$$g_k = f_{k-1} - c^* f_k \ . \tag{2.182}$$

Calculating the difference between the energy in each sample in h_k and g_k,

$$|h_k|^2 - |g_k|^2 = |f_k - cf_{k-1}|^2 - |f_{k-1} - c^* f_k|^2 = (1 - |c|^2)(|f_k|^2 - |f_{k-1}|^2) \tag{2.183}$$

and calculating the difference in energy for the first N samples,

$$\sum_{k=0}^{N} (|h_k|^2 - |g_k|^2) = (1 - |c|^2)|f_N|^2 \geq 0 \tag{2.184}$$

exploiting the fact that f_k is causal (why?), and $|c| < 1$, and hence $f_{-1} = 0$.

2-23. Using the allpass transfer function in example 2-9 with $|c| < 1$, define a signal w_k with Z transform $X(z)/(1 - cz^{-1})$. Note that w_k is causal also (why?). Then x_k is obtained by putting w_k through a system with transfer function $(1 - cz^{-1})$ and y_k is obtained by system $(z^{-1} - c^*)$. From here, the derivation is identical to problem 2-22, with the result

$$\sum_{k=0}^{N} (|x_k|^2 - |y_k|^2) = (1 - |c|^2)|w_N|^2 \geq 0 \tag{2.185}$$

2-24. Using (2.44) to factor $H(z)$ into the product of minimum-phase and maximum-phase transfer functions,

$$H(z) = Bz^L H_{\min}(z)H_{\max}(z)H_{\text{zero}}(z) = Bz^L H_{\min}(z)H^*_{\max}(1/z^*)\frac{H_{\max}(z)}{H^*_{\max}(1/z^*)}H_{\text{zero}}(z) \ . \tag{2.186}$$

Now note that $H^*_{\max}(1/z^*)$ is minimum phase, and from example 2-11 $H_{\max}(z)/H^*_{\max}(1/z^*)$ is allpass. Furthermore, z^L is allpass. Hence,

$$H_{\text{allpass}}(z) = z^L \frac{H_{\max}(z)}{H^*_{\max}(1/z^*)} \tag{2.187}$$

and

$$H_{\min}'(z) = BH_{\min}(z)H^*_{\max}(1/z^*) \ . \tag{2.188}$$

2-25. $H^*(j\omega)$.

2-26.

(a) The norm of both signals is unity. The inner product is

$$\langle S_1, S_2 \rangle = \int_{-\infty}^{\infty} s_1(t)s_2(t)\,dt = 1\cdot\frac{3}{4} - 1\cdot\frac{1}{4} = \frac{1}{2} \ . \tag{2.189}$$

(b)

$$\|S_1 + S_2\|^2 = \int_{-\infty}^{\infty} (s_1(t) + s_2(t))^2\,dt = 4\cdot\frac{3}{4} + 0\cdot\frac{1}{4} = 3 \ . \tag{2.190}$$

(c) There are many possibilities, but here is one:

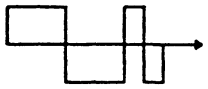

(d) Define an orthonormal basis for the subspace spanned by S_1 and S_2 as:

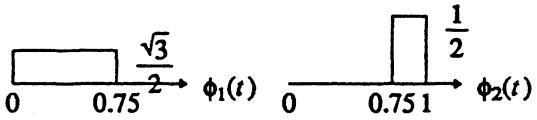

A signal orthogonal to S_1 that is a linear combination of Φ_1 and Φ_2 is $2\cdot\Phi_1 - \frac{2}{\sqrt{3}}\cdot\Phi_2$.

(e) The projection of S_5 on the two basis vectors is

$$\langle S_5,\Phi_1\rangle = -\frac{\sqrt{3}}{8} \quad \langle S_5,\Phi_2\rangle = -\frac{1}{8} \tag{2.191}$$

and hence the projection on the subspace is $-\frac{\sqrt{3}}{8}\cdot\Phi_1 - \frac{1}{8}\cdot\Phi_2$.

2-27.

(a) Clearly if two signals are bandlimited, then their weighted sum is also bandlimited.

(b) Let X be in the subspace. By Parseval's theorem (problem 2-4), for any $Y\varepsilon B$,

$$\int_{-\infty}^{\infty} x(t)y^*(t)\,dt = \frac{1}{2\pi}\int_{-W}^{W} X(j\omega)Y^*(j\omega)\,d\omega = 0. \tag{2.192}$$

Clearly, this is satisfied if and only if $X(j\omega) = 0$ for $|\omega| \le W$.

(c) Let this projection be P, then $\langle S_1 - P, Y\rangle = 0$ for all $Y\varepsilon B$. From (b) this implies that $S_1(j\omega) = P(j\omega)$ for $|\omega| \le W$, and of course since $P\varepsilon B$, we must have that $P(j\omega) = 0$ for $|\omega| > W$. Hence,

$$S_1(j\omega) = \int_0^1 e^{-j\omega t}\,dt = \frac{1-e^{-j\omega}}{j\omega} \tag{2.193}$$

and

$$p(t) = \frac{1}{2\pi}\int_{-1}^{1} \frac{1-e^{-j\omega}}{j\omega} e^{j\omega t}\,d\omega. \tag{2.194}$$

Unfortunately this integral cannot be evaluated in closed form.

2-28. Let $X_1\varepsilon M_1$ and $X_2\varepsilon M_2$. An element of $M_1 \oplus M_2$ can be written in the form $X_1 + X_2$. Hence it suffices to show that

$$\langle X-(P_{M_1}(X) + P_{M_2}(X)), X_1 + X_2\rangle = 0 \tag{2.195}$$

Expanding the left side, it equals

$$\langle X-P_{M_1}(X), X_1\rangle - \langle P_{M_2}(X), X_1\rangle + \langle X - P_{M_2}(X), X_2\rangle - \langle P_{M_1}(X), X_2\rangle \tag{2.196}$$

But by the definition of projection

$$\langle X - P_{M_1}(X), X_1\rangle = \langle X - P_{M_2}(X), X_2\rangle = 0 \tag{2.197}$$

and because M_1 and M_2 are orthogonal subspaces

$$\langle P_{M_2}(X), X_1\rangle = \langle P_{M_1}(X), X_2\rangle = 0 \tag{2.198}$$

and hence the result is established.

2-29. Defining

$$z^{-k}\cdot\mathbf{H} <-> h(t-kT)\ , \tag{2.199}$$

the Schwarz inequality states that

$$|\rho_h(k)| \le \|\mathbf{H}\|\cdot\|z^{-k}\cdot\mathbf{H}\| \tag{2.200}$$

and since it is easy to verify that the signal and its time-translate have identical norms, this becomes the desired result.

2-30. Multiplying out the magnitude squared in (2.97) we get

$$\frac{T}{2\pi}\int_{-\pi/T}^{\pi/T}\log[1-2a\cos(\theta-\omega T)+a^2]\,d\omega\,. \tag{2.201}$$

Changing variables, this can be written

$$\frac{1}{2\pi}\int_{\theta-\pi}^{\theta+\pi}\log(1-2a\cos\omega+a^2)\,d\omega\,. \tag{2.202}$$

Since $\cos\omega$ is periodic, the kernel of the integral is periodic. Since we are integrating over one period, we can rewrite this as

$$\frac{1}{2\pi}\int_{-\pi}^{\pi}\log(1-2a\cos\omega+a^2)\,d\omega\,. \tag{2.203}$$

Finally, since $\cos\omega$ is symmetric, this is equal to (2.98).

CHAPTER 3: SOLUTIONS TO PROBLEMS

3-1. Taking the first derivative,

$$\frac{\partial}{\partial s}\Phi_X(s)=\Phi_X(s)(\mu+\sigma^2 s) \tag{3.265}$$

and setting $s=0$ we get $E[X]=\mu$. Similarly, the second derivative is

$$\frac{\partial^2}{\partial s^2}\Phi_X(s)=\frac{\partial}{\partial s}\Phi_X(s)(\mu+\sigma^2 s)+\Phi_X(s)\sigma^2 \tag{3.266}$$

and again setting $s=0$ we get $E[X^2]=(\mu^2+\sigma^2)$. The variance is therefore σ^2.

3-2. We can use (3.17) and carry out the integral.

3-3.

$$\sqrt{2\pi}Q(y) = \int_y^\infty \frac{1}{\alpha}(\alpha e^{-\alpha^2/2} d\alpha)$$

$$= \frac{1}{\alpha}(-e^{-\alpha^2/2})\Big|_\alpha^\infty - \int_y^\infty \frac{1}{\alpha^2} e^{-\alpha^2/2} d\alpha \tag{3.267}$$

$$= \frac{1}{\alpha} e^{-\alpha^2/2})\Big|_\alpha^\infty - \int_y^\infty \frac{1}{\alpha^2} e^{-\alpha^2/2} d\alpha .$$

The bounds then follow from the fact that

$$0 < \int_y^\infty \frac{1}{\alpha^2} e^{-\alpha^2/2} d\alpha \le \frac{1}{y^3} \int_y^\infty \alpha e^{-\alpha^2/2} d\alpha = \frac{1}{y^3} e^{-\alpha^2/2} . \tag{3.268}$$

3-4.

(a) Defining the MSE as ε^2,

$$\varepsilon^2 = E[|X - aY|^2] = E[|X|^2] + |a|^2 E[|Y|^2] - 2\mathrm{Re}\{a^* E[XY^*]\} \tag{3.269}$$

and taking the derivative with respect to the real and imaginary parts,

$$\mathrm{Re}\{a\} E[|Y|^2] = \mathrm{Re}\{E[XY^*]\} \tag{3.270}$$

$$\mathrm{Im}\{a\} E[|Y|^2] = \mathrm{Im}\{E[XY^*]\} \tag{3.271}$$

or

$$a = E[XY^*]/E[|Y|^2] . \tag{3.272}$$

(b) The problem can be restated as: Find the vector in the subspace spanned by $\{\mathbf{Y}\}$ that is closest to $\mathbf{X}$.

(c) By the orthogonality principle,

$$\langle \mathbf{X} - a\cdot\mathbf{Y}, \mathbf{Y} \rangle = 0 \tag{3.273}$$

or

$$a = \langle \mathbf{X}, \mathbf{Y} \rangle / \langle \mathbf{Y}, \mathbf{Y} \rangle = E[XY^*]/E[|Y|^2] . \tag{3.274}$$

3-5.

(a) Noting that

$$\begin{aligned} E|E_k'|^2 &= E|E_k' - E_k + E_k|^2 \\ &= E|E_k' - E_k|^2 + E|E_k|^2 + 2\mathrm{Re}\{(E_k' - E_k)E_k^*\} . \end{aligned} \tag{3.275}$$

Since the filters generating both E_k and E_k' have unity coefficients at delay zero, the filter generating $(E_k' - E_k)$ has a zero coefficient at delay zero, and this signal is a function of only *past* inputs $X_{k-1}, X_{k-2}, \cdots$, and in view of property (3.184), the third term in (3.275) must in fact be zero.

(b) Since E_k is a linear combination of $X_k, X_{k-1}, \cdots$, it follows from (3.184) that

$$E[E_{k+m}E_k^*] = R_E(m) = 0 , \quad m > 0, \tag{3.276}$$

and since the autocorrelation function has conjugate symmetry, it follows that $R_E(m) = 0$ for all $m \neq 0$.

3-6.

(a) The problem can be restated as: Given a sequence of vectors $\mathbf{X}_k$, $-\infty < k < \infty$, with inner products

$$R_X(m) = \langle \mathbf{X}_{k+m}, \mathbf{X}_k \rangle \tag{3.277}$$

that are independent of k, given a subspace M spanned by $\{\mathbf{X}_{k-m}, m > 0\}$, find the vector $\hat{\mathbf{X}}_k$ in M that is closest to the vector $\mathbf{X}_k$, with error vector $\mathbf{E}_k = \mathbf{X}_k - \hat{\mathbf{X}}_k$.

(b) By the projection theorem, for every vector $\mathbf{Y} \in M$, we must have that

$$\langle \mathbf{E}_k, \mathbf{Y} \rangle = 0 \tag{3.278}$$

and in particular

$$\langle \mathbf{E}_k, \mathbf{X}_{k-m} \rangle = 0, m > 0. \tag{3.279}$$

Thus the prediction error vector is orthogonal to the past (the vectors used in the prediction estimation). Since $E_{k-m} \in M$, $m > 0$, it follows that

$$\langle \mathbf{E}_k, \mathbf{E}_{k-m} \rangle = 0, m > 0, \tag{3.280}$$

or equivalently $R_E(m) = 0, m \neq 0$.

3-7.

$$R_Y(0) = \mathrm{E}[|Y_k|^2] = \mathrm{E}[|X(kT)|^2]. \tag{3.281}$$

Observe that since $X(t)$ is WSS

$$R_X(0) = \mathrm{E}[|X(t)|^2] = \mathrm{E}[|X(t+\tau)|^2] \tag{3.282}$$

for any τ. Define

$$\tau = kT - t \tag{3.283}$$

and the result follows.

3-8. Mechanically,

$$\mathrm{E}[A_p A_q A_r A_s] = \delta_{pq}\delta_{rs} + \delta_{pr}\delta_{qs} + \delta_{ps}\delta_{qr} - 2\delta_{pq}\delta_{pr}\delta_{ps}. \tag{3.284}$$

3-9. Observe that from (3.64)

$$\int_{\omega_a}^{\omega_b} S_X(j\omega)d\omega = \int_{-\infty}^{\infty} S_Y(j\omega)d\omega, \tag{3.285}$$

and from the definition of the power spectrum,

$$R_Y(\tau) = \frac{1}{2\pi}\int_{-\infty}^{\infty} S_Y(j\omega)e^{j\omega\tau}d\omega, \tag{3.286}$$

from which the first result follows. To show that $S_X(j\omega)$ is non-negative everywhere, assume it is negative over some region from ω_a to ω_b. Then note that

$$\int_{\omega_a}^{\omega_b} S_X(j\omega)d\omega \tag{3.287}$$

must also be negative, which implies that $R_Y(0)$ is negative. But

$$R_Y(0) = \int_{-\infty}^{\infty} y^2(\tau)d\tau \tag{3.288}$$

which must be non-negative, a contradiction.

3-10. The power spectrum is

$$N_0 \cdot |F(e^{j\omega T})|^2 = N_0 \cdot F(e^{j\omega T})F^*(e^{j\omega T}) \tag{3.289}$$

where $F(e^{j\omega T})$ is the discrete-time Fourier transform of $f(kT)$. Since the inverse Fourier transform of $F^*(e^{j\omega T})$ is $f^*(-kT)$, the result follows immediately.

3-11.

$$\begin{aligned} R_{XY}(\tau) &= \mathrm{E}[X(t+\tau)Y^*(t)] \\ &= \mathrm{E}[Y^*(p-\tau)X(p)] = R_{YX}^*(-\tau). \end{aligned} \tag{3.290}$$

No it may be complex-valued.

3-12. If the steady state probabilities exist they must satisfy

$$p(j) = \sum_{i \in \Omega_T} p(j|i)p(i)\,, \tag{3.291}$$

and also must satisfy

$$\sum_{j \in \Omega_T} p(j) = 1\,. \tag{3.292}$$

Define the row vector of state probabilities

$$\pi_k = [p_k(0), \cdots, p_k(M)]\ . \tag{3.293}$$

Then the system of equations in (3.96) can be written more concisely as

$$\pi_{k+1} = \pi_k \mathbf{P}. \tag{3.294}$$

The condition that the state probabilities don't change through a state transition gives the desired steady-state probabilities.

3-13.

(a) The signal flow graph is shown below:

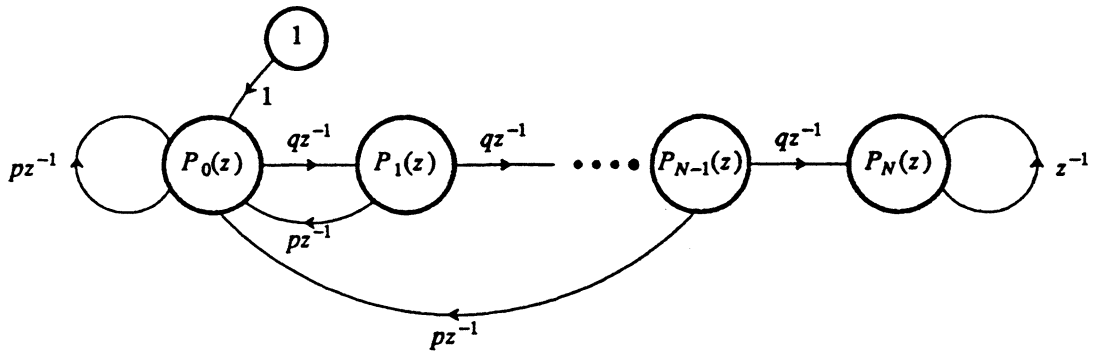

(b) The corresponding equations are

$$P_0(z) = 1 + \sum_{i=0}^{N-1} pz^{-1}P_i(z) \tag{3.295}$$

$$P_i(z) = qz^{-1}P_{i-1}(z)\ ,1 \le i \le N-1 \tag{3.296}$$

$$P_N(z) = qz^{-1}P_{N-1}(z) + z^{-1}P_N(z)\,. \tag{3.297}$$

Solving these equations and using the identity

$$\sum_{i=0}^{N-1} r^i = \frac{1-r^N}{1-r} \tag{3.298}$$

we get the result.

(c) This follows directly by differentiation.

(d) For this case,

$$f_N \simeq q^{-N} \tag{3.299}$$

which is what we would expect. The probability of a head is q, the probability of N heads in a row is q^N, and on a relative frequency basis N heads in a row will occur once out of q^{-N} trials.

3-14.

$$\begin{aligned} p(\psi_0,\psi_1,\cdots,\psi_n) &= p(\psi_n \mid \psi_{n-1},\cdots,\psi_0)p(\psi_{n-1},\cdots,\psi_0) \\ &= p(\psi_n \mid \psi_{n-1})p(\psi_{n-1},\cdots,\psi_0) \\ &= p(\psi_n \mid \psi_{n-1})p(\psi_{n-1} \mid \psi_{n-2}\cdots,\psi_0)p(\psi_{n-2},\cdots,\psi_0) \\ &= p(\psi_n \mid \psi_{n-1})p(\psi_{n-1} \mid \psi_{n-2})p(\psi_{n-2},\cdots,\psi_0) = \cdots \end{aligned}$$

3-15.

$$p(\psi_n \mid \psi_{n+1},\cdots,\psi_{n+m}) = \frac{p(\psi_n,\psi_{n+1},\cdots,\psi_{n+m})}{p(\psi_{n+1},\cdots,\psi_{n+m})}.$$

Using the result in problem 3-14 on both the numerator and denominator and canceling the terms that are equal, this becomes

$$\begin{aligned} p(\psi_n \mid \psi_{n+1},\cdots,\psi_{n+m}) &= \frac{p(\psi_{n+1} \mid \psi_n)p(\psi_n)}{p(\psi_{n+1})} \\ &= p(\psi_n \mid \psi_{n+1}). \end{aligned}$$

3-16.

$$\begin{aligned} p(\psi_n,\psi_s \mid \psi_r) &= \frac{p(\psi_n,\psi_r,\psi_s)}{p(\psi_r)} \\ &= p(\psi_n \mid \psi_r)\left[\frac{p(\psi_r \mid \psi_s)p(\psi_s)}{p(\psi_r)}\right], \end{aligned}$$

where the last equality follows from problem 3-14. The result now follows using Bayes' rule.

3-17. The signal flow graph is in shown in figure 3-22a. The set of equations governing this signal flow graph is

$$P_0(z) = 0.5z^{-1}P_0(z) + 0.5z^{-2}P_1(z) + 1 \tag{3.300}$$

$$P_1(z) = 0.5z^{-1}P_1(z) + 0.5P_0(z). \tag{3.301}$$

Solving these linear equations for $P_0(z)$,

$$P_0(z) = \frac{1-0.5z^{-1}}{1-z^{-1}} = \frac{1}{1-z^{-1}} - 0.5z^{-1}\frac{1}{1-z^{-1}}.$$

Inverting the Z transform (using problem 2-15),

$$p_k(0) = u_k - 0.5u_{k-1},$$

where u_k is the unit step. This is sketched in figure 3-22 (b). Computing $P_1(z)$ similarly,

$$P_1(z) = 0.5z^{-1}\frac{1}{1-z^{-1}}.$$

Inverting the Z transform, again using problem 2-15,

$$p_k(1) = 0.5u_{k-1}.$$

The Markov chain is not stationary.

3-18. The Markov state diagram is shown in figure 3-23 (a).

(a) The diagram shows the independence required for the random process to be Markov, assuming that the coin tosses are independent of one another.

(b) The signal flow graph is shown in figure 3-23 (b).

(c) Writing the set of equations and solving them,

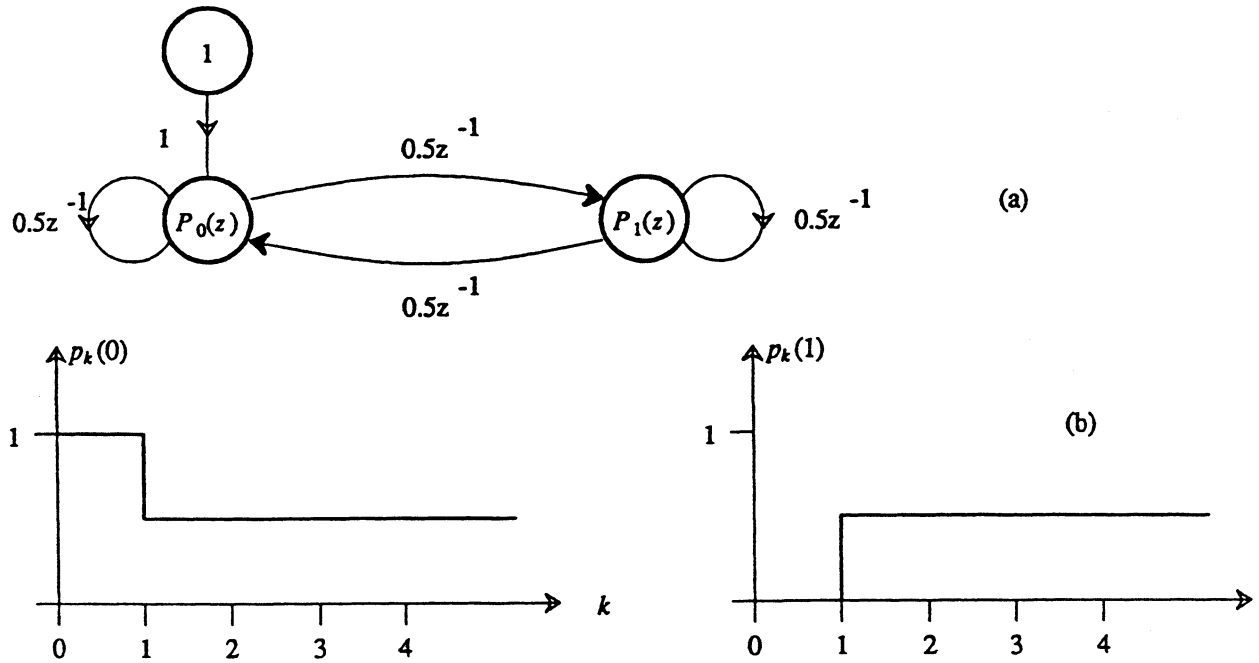

Figure 3-22. (a) The signal flow graph describing the state probabilities of the parity check example when the initial state is zero. (b) The state probabilities as a function of k.

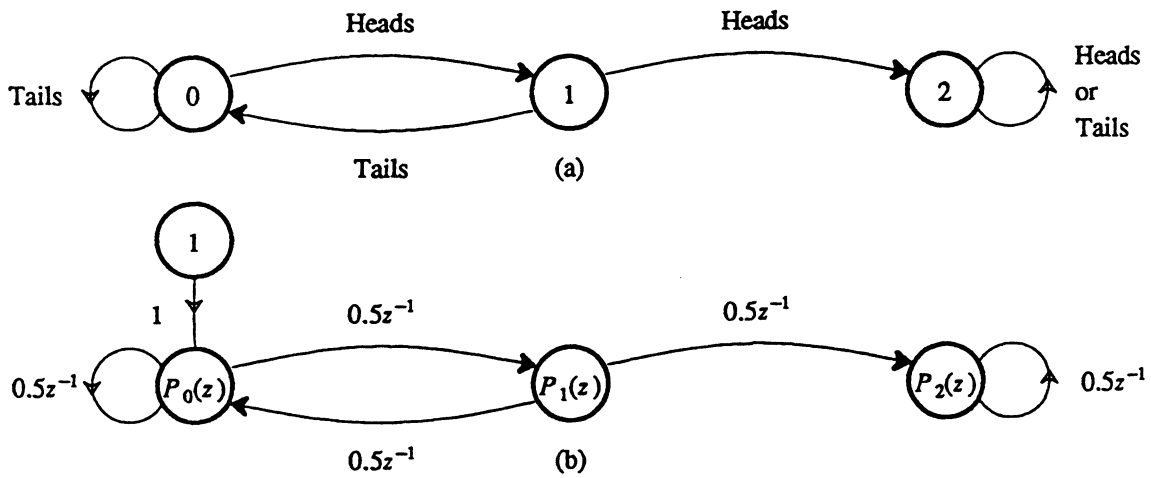

Figure 3-23. (a) Markov chain description of the coin toss experiment of problem 3-18. (b) Signal flow graph.

$$\frac{P_2(z)}{1} = \frac{z}{4z^3 - 6z^2 + z + 1} \tag{3.302}$$

3-19. Starting with (3.121), calculating the optimum value of s, we get for the first bound

$$\frac{x}{a} = e^s \tag{3.303}$$

and finally plugging into the bound we get the result.

3-20. This follows immediately from the fact that $N(t_1)$ is Poisson distributed with parameter $a = \lambda t_1$. Hence from (3.120) we get

$$E[N(t_1)] = \lambda t_1 \tag{3.304}$$

$$\text{Var}[N(t_1)] = \lambda t_1. \tag{3.305}$$

3-21. Writing the joint probability as a conditional probability, the desired probability is

$$p_{N(t_2)|N(t_1)}(k+n\,|\,k) \cdot p_{N(t_1)}(k) \ . \tag{3.306}$$

The left term is the probability of n arrivals in time interval $(t_2 - t_1)$, or

$$\frac{[\lambda(t_2 - t_1)]^n}{n!} e^{-\lambda(t_2 - t_1)} \tag{3.307}$$

and the second probability is

$$\frac{(\lambda t_1)^k}{k!} e^{-\lambda t_1}. \tag{3.308}$$

Taking the product, the result follows immediately.

3-22. The process is governed by the differential equation

$$\frac{dq_j(t)}{dt} = (j-1)\lambda q_{j-1}(t) - j\lambda q_j(t) \tag{3.309}$$

which has Laplace transform

$$Q_j(s) = \frac{q_j(0) + (j-1)\lambda Q_{j-1}(s)}{(s + j\lambda)} \tag{3.310}$$

and iterating we get

$$Q_j(s) = \frac{\lambda^{j-1}(j-1)!}{(s+\lambda)(s+2\lambda)\cdots(s+j\lambda)}. \tag{3.311}$$

It is non-trivial to derive, but the inverse Laplace transform is

$$q_j(t) = e^{-\lambda t}(1 - e^{-\lambda t})^{j-1}. \tag{3.312}$$

3-23.

(a) Since the mean value of $N(t)$ is given by (3.135), differentiating this integral we get the desired expression.

(b) This also follows easily from the fact that the expectation of the convolution is the convolution of the expectation.

(c) This again follows directly from the interchangeability of expectation and differentiation.

(d) We will just derive the first equation, the second is similar. First note that

$$\begin{aligned} R_{WX}(t_1,t_2) &= E[w(t_1)X(t_2)] \\ &= E[w(t_1)\int h(\tau)w(t_2-\tau)\,d\tau] \\ &= \int h(\tau)R_{WW}(t_1,t_2-\tau)\,d\tau \end{aligned}$$

which we recognize as a convolution in the second argument of the autocorrelation function.

3-24. Note that

$$E[N(t_1)(N(t_2)-N(t_1))] = E[N(t_1)N(t_2)] - E[N^2(t_1)]. \tag{3.313}$$

Independence implies that the expectation of the product is the product of the expectations

$$\begin{aligned} E[N(t_1)(N(t_2)-N(t_1))] &= E[N(t_1)]E[N(t_2)-N(t_1)] \\ &= \Lambda(t_1)(\Lambda(t_2)-\Lambda(t_1)). \end{aligned} \tag{3.314}$$

Since $N(t)$ is a Poisson random variable, from (3.135)

$$E[N^2(t_1)] = \Lambda^2(t_1) + \Lambda(t_1) \tag{3.315}$$

from which the result follows immediately with some minor algebraic manipulation.

3-25. Noting that $R_{NN}(t_1,t_2)$ is continuous at $t_1 = t_2$, take the derivative first with respect to t_2,

$$R_{N\dot{N}}(t_1,t_2) = \frac{\partial R_{NN}(t_1,t_2)}{\partial t_2} = \begin{cases} \Lambda(t_1)\lambda(t_2), & t_1 < t_2 \\ (1+\Lambda(t_1))\lambda(t_2), & t_1 \geq t_2 \end{cases} \tag{3.316}$$

Now take the derivative with respect to t_1, first noting that there is a discontinuity of size $\lambda(t_2)$ at $t_1 = t_2$,

$$R_{\dot{N}\dot{N}}(t_1,t_2) = \frac{\partial R_{N\dot{N}}(t_1,t_2)}{\partial t_1} = \lambda(t_1)\lambda(t_2) + \lambda(t_2)\delta(t_1 - t_2). \tag{3.317}$$

Finally, we convolve this result with first $h(t_1)$ and then $h(t_2)$ to obtain the autocorrelation of shot noise. First convolving with $h(t_1)$,

$$R_{\dot{N}\dot{N}}(t_1,t_2) * h(t_1) = [\lambda(t_1) * h(t_1)]\lambda(t_2) + \lambda(t_2)h(t_1 - t_2) \tag{3.318}$$

and then convolving with $h(t_2)$, we obtain (3.199).

3-26. Substituting a constant rate into the autocorrelation of (3.198), the autocorrelation is

$$R_{XX}(t_1,t_2) = \lambda^2 H^2(0) + \lambda \int h(-u)h(t_2 - t_1 - u)\,du \tag{3.319}$$

which is a function of $\tau = t_2 - t_1$ and hence the autocorrelation is

$$R_X(\tau) = \lambda^2 H^2(0) + \lambda h(\tau) * h(\tau). \tag{3.320}$$

Taking the Fourier transform of this expression we get the power spectrum,

$$S_X(\omega) = 2\pi\lambda^2 H^2(0)\,\delta(\omega) + \lambda |H(j\omega)|^2. \tag{3.321}$$

Note that the power spectrum has a d.c. term, corresponding to the expected value of the shot noise, and a term proportional to the magnitude-squared of the filter transfer function (as expected).

3-27. The expected value of the shot noise is

$$E[X(t)] = \lambda_0 \int_{-\infty}^{t} h(\tau)\,d\tau \tag{3.322}$$

which is proportional to the step function.

3-28. If the filter has impulse response $h(t)$ and transfer function

$$H(j\omega) = A(\omega)e^{j\phi(\omega)} \tag{3.323}$$

then the response of the filter to λ_0 is $\lambda_0 A(0)$ and the response to the sinusoid is $\lambda_1 A(\omega_1)\cos(\omega_1 t + \phi(\omega_1))$. The mean value is the sum of these two signals.

3-29. The outputs are still obviously equally probable, $p(0) = p(1) = \frac{1}{2}$. From figure 3-20 we can calculate $P_{111}(z)$,

$$P_{111}(z) = \frac{1 - qz^{-1}}{1 - (qz^{-1} + qz^{-1} + p^2 z^{-2}) + q^2 z^{-2}} \tag{3.324}$$

$$S_X^+(z) = 0.5 \cdot \frac{1 - qz^{-1}}{(1 - z^{-1})(1 - (1-2p)z^{-1})} . \tag{3.325}$$

Recognizing that $\mu_X = ½$ and subtracting $\frac{0.25}{1 - z^{-1}}$ from (3.325) we get

$$S_X^+(z) - \frac{0.25}{1 - z^{-1}} = \frac{0.25}{1 - (1-2p)z^{-1}} . \tag{3.326}$$

Calculating the two-sided spectrum, we get

$$S_X(z) = \frac{0.25}{1 - (1-2p)z^{-1}} + \frac{0.25}{1 - (1-2p)z} - 0.25 \tag{3.327}$$

which simplifies to the desired result.

CHAPTER 4: SOLUTIONS TO PROBLEMS

4-1. The entropy is 0.81 bits. The rate is $R = 0.81$ bits/second. There are many possibilities for the coder. Here is one. Pair the coin flips and represent them as follows:

FLIPS	BITS
TT	0
TH	10
HT	110
HH	111

The first occurs with probability 9/16, the second and third with probability 3/16 and the last with probability 1/16. The expected number of bits per flip-pair is therefore 1.67, or 0.844 bits per flip, which is close to the rate of the source, but not equal.

4-2.

$$H(X) = \frac{1}{2}\log_2(2) + \frac{1}{4}\log_2(4) + \frac{1}{8}\log_2(8) + \frac{1}{8}\log_2(8) = 1.75 . \tag{4.65}$$

$$R = 175 \text{ trials/second} . \tag{4.66}$$

A coder that will work is given by the following table.

outcome	bits
a_1	0
a_2	10
a_3	110
a_4	111

The average number of bits per trial is

$$\frac{1}{2}\cdot 1 + \frac{1}{4}\cdot 2 + \frac{1}{8}\cdot 3 + \frac{1}{8}\cdot 3 = 1.75 . \tag{4.67}$$

4-3. Suppose that $p_i = p_Y(y_i)$ where the set of y_i for $i \in \{1,2,\cdots,M\}$ is the alphabet for the random variable Y. Define the random variable $X = q_i/p_i$. In other words, an outcome $Y = y_i$ results in the outcome $X = x = q_i/p_i$. By Jensen's inequality,

$$\mathrm{E}[\log_2 X] \le \log_2 \mathrm{E}[X] \tag{4.68}$$

but

$$\begin{aligned} \mathrm{E}[\log_2 X] &= \sum_{i=1}^{M} p_i \log_2 \frac{q_i}{p_i} \\ &= \sum_{i=1}^{M} p_i \log_2 q_i - \sum_{i=1}^{M} p_i \log_2 p_i \end{aligned} \tag{4.69}$$

and

$$\mathrm{E}[X] = \sum_{i=1}^{M} q_i = \alpha. \tag{4.70}$$

The p-q inequality follows.

4-4. Let $q_i = 1/K$ in the p-q inequality and the result follows easily.

4-5. The size of the set over which X has positive probability is less than or equal to 2^n, so the result follows immediately from exercise 4-1.

4-6.

(a) It is easy to show that the input and output of this channel are statistically independent, and from this that

$$H(X|Y) = H(X), \quad H(Y|X) = H(Y), \tag{4.71}$$

$$I(X,Y) = 0. \tag{4.72}$$

(b) Since the mutual information is zero independent of the input probability distribution, the capacity is also zero.

4-7.

(a) For this noiseless channel, the output is equal to the input, so

$$H(X|Y) = 0, \quad H(Y|X) = 0, \tag{4.73}$$

$$I(X,Y) = H(X) = H(Y). \tag{4.74}$$

(b) The capacity is the maximum of $H(X)$ over the input distribution, which is one bit because the input has alphabet size of two.

4-8.

(a) We get

$$I(X,Y) = H(Y) + p\log_2 p + (1-p)\log_2(1-p). \tag{4.75}$$

(b) Capacity is achieved when $H(Y)$ is maximized. By direct calculation,

$$H(Y) = -p\log_2 p - (1-p)\log_2(1-p) - q(1-p)\log_2 q - (1-q)(1-p)\log_2(1-q) \tag{4.76}$$

where q is the probability of the first input and $(1-q)$ is the probability of the second. This quantity is maximized when the inputs are equally likely ($q = ½$), and the capacity is

$$C_s = 1 - p \tag{4.77}$$

The center output is called an erasure, and tells us nothing about what the channel input is, so it is not surprising that the capacity approaches zero as $p \to 1$.

4-9.

(a) This follows from

$$\sum_i p_i \log_2 \frac{q_i}{p_i} \le \sum_i p_i \left(\frac{q_i}{q_i} - 1\right) = 0 \tag{4.78}$$

where we have used the inequality $\log x \le x - 1$.

(b) Substitute a uniform distribution $q_i = 1/K$, and the bound follows immediately.

4-10.

(a) The channel has binary input and output, so all we need to show is symmetry. To do this, we solve part b.

(b) The number of transitions from 0 to 1 or vice versa is binomially distributed. As long as there are an even number of such crossovers, then the output of the channel will be the same as the input. The probability of this occurring is

$$p_{Y|X}(0|0) = p_{Y|X}(1|1) = \sum_{\substack{m=0 \\ m \text{ even}}}^{L} K_m (1-p)^{L-m} p^m \tag{4.79}$$

where

$$K_m = \binom{L}{m} = \frac{L!}{m!(L-m)!} . \tag{4.80}$$

Similarly, a channel error occurs if there are an odd number of crossovers, which occurs with probability

$$p_{Y|X}(1|0) = p_{Y|X}(0|1) = \sum_{\substack{m=1 \\ m \text{ odd}}}^{L} K_m (1-p)^{L-m} p^m . \tag{4.81}$$

(c)

$$p_{X|Y}(0|0) = p_{X|Y}(1|0) = p_{X|Y}(0|1) = p_{X|Y}(1|1) = \tfrac{1}{2} \quad \text{as} \quad L \to \infty . \tag{4.82}$$

4-11. Suppose X has distribution p_i and Y has distribution q_i. Then

$$\begin{aligned} H(X) &= -\sum_{i=1}^{K} p_i \log_2 p_i \\ &\le -\sum_{i=1}^{K} p_i \log_2 q_i , \end{aligned} \tag{4.83}$$

where the inequality follows from problem 4-9. Meanwhile,

$$\begin{aligned} H(Y) &= -\sum_{i=1}^{K} q_i \log_2 q_i \\ &= -(p_1 - \delta)\log_2 q_1 - (p_2 + \delta)\log_2 q_2 - \sum_{i=3}^{K} p_i \log_2 q_i \\ &= -\sum_{i=1}^{K} p_i \log_2 q_i + [\delta \log_2 q_1 - \delta \log_2 q_2] . \end{aligned} \tag{4.84}$$

Since $p_1 > p_2$, we have that $q_1 > q_2$, and the term in brackets in non-negative, so by comparing with (4.83) we get that $H(Y) \ge H(X)$.

4-12.

(a)

$$H(X) = -\int_{-a}^{a} \frac{1}{2a} \log_2 \frac{1}{2a} dx = -\log_2 \frac{1}{2a} . \tag{4.85}$$

(b) The variance of X is

$$\sigma^2 = \mathrm{E}[X^2] = \int_{-a}^{a} \frac{1}{2a} x^2 dx = \frac{1}{3}a^2 . \tag{4.86}$$

Hence we can write

$$a = \sqrt{3}\sigma \tag{4.87}$$

and

$$H(X) = \log_2(2\sqrt{3}\sigma) . \tag{4.88}$$

The entropy of a Gaussian is given by (4.21),

$$H(Y) = \log_2(\sigma\sqrt{2\pi e}) . \tag{4.89}$$

Since $2\sqrt{3} < \sqrt{2\pi e}$, then $H(X) < H(Y)$.

4-13. Let the random vector Z denote the ordered pair (X,Y). The set of all possible pairs of outcomes of Z is in $\Omega_X \times \Omega_Y$. Number the possible outcomes (in any order) from 1 through M, where M is the size of Ω_X multiplied by the size of Ω_Y. Then let z_i denote a particular pair of outcomes (x,y), where $1 \le i \le M$. Then define

$$p_i = p_{X,Y}(x,y) \tag{4.90}$$

Further, define

$$q_i = p_X(x)p_Y(y) . \tag{4.91}$$

These p_i and q_i satisfy the constraints of the p-q inequality. The p-q inequality then yields

$$-I(X,Y) = -\sum_{i=1}^{M} p_i \log_2 \frac{p_i}{q_i} \le \log_2 \sum_{i=1}^{M} q_i = \alpha. \tag{4.92}$$

Hence,

$$\begin{aligned} I(X,Y) \ge \alpha &= \log_2 \left[\sum_{x \in \Omega_x} \sum_{y \in \Omega_y} p_X(x)p_Y(y) \right] \\ &= \log_2 \left[\left[\sum_{x \in \Omega_x} p_X(x) \right] \left[\sum_{y \in \Omega_y} p_Y(y) \right] \right] = \log_2 1 = 0. \end{aligned} \tag{4.93}$$

The second and third inequalities follow easily, using (3.27) for the third. The inequalities are equalities when X and Y are independent.

4-14. This follows easily with repeated application of the definition of conditional probability.

4-15. Using the inequality $\log_e(x) \le (x-1)$,

$$C \le \frac{N}{2} \cdot \log_e 2 \cdot \frac{\sigma_x^2}{N\sigma^2} = \log_2\sqrt{e} \cdot \frac{\sigma_x^2}{\sigma^2} . \tag{4.94}$$

Thus, as the number of degrees of freedom increases, the capacity approaches a constant. As we increase N we have in effect more parallel channels to transmit over, and hence the factor of N. However, since the total input power is constrained to σ_x^2, the transmitter is forced to reduce the power in each parallel channel, and hence the SNR on each channel decreases. In the limit, these two effects precisely balance one another.

4-16. The implication of (4.47) is that for any set of outcomes $x_1, \cdots, x_n$,

$$\frac{1}{n}(x_1 + \cdots + x_n) \simeq \mathrm{E}[X] \tag{4.95}$$

with high probability. Let $X_i = \log_2 Y_i$. Then

$$\mathrm{E}[\log_2 Y] \simeq \frac{1}{n}\log_2(y_1 \cdots y_n) \tag{4.96}$$

with high probability. The result follows from this.

4-17. Define the random variable Y to have value 5 with probability 1/6 and value 1/5 with probability 5/6. Then the money left after playing the game n times is

$$M_n = 100 \prod_{i=1}^{n} Y_i \tag{4.97}$$

where Y_i is a sequence of independent trials of the random variable Y. Now, because of independence,

$$\mathrm{E}[M_n] = 100 \prod_{i=1}^{n} \mathrm{E}[Y_i] = 100. \tag{4.98}$$

Surprisingly, this does not imply that the game is fair. From (4.39), with high probability, a set of outcomes $y_1, \cdots, y_n$ satisfies

$$M_n = 100 \prod_{i=1}^{n} Y_i \approx \left[2^{\mathrm{E}[\log_2 Y]} \right]^n \approx [0.34]^n. \tag{4.99}$$

This certainly goes to zero as n gets large. I wouldn't play the game, at least not repeatedly.

4-18. The better estimate is (b). The argument is similar to that in the solution to problem 4-17.

CHAPTER 5: SOLUTIONS TO PROBLEMS

5-1. Note: We will make in this solution the additional assumption that the characteristic impedance of the line is real-valued.

At some point on the line, let the complex voltage and impedance be V and I respectively. Then the instantaneous power at that point is

$$\mathrm{Re}\{ Ve^{j\omega t} \}\mathrm{Re}\{ Ie^{j\omega t} \} = \frac{1}{4}(VIe^{j2\omega t} + V^* I^* e^{-j2\omega t} + 2\mathrm{Re}\{ VI^* \}). \tag{5.106}$$

Evidently, the average power at this point is $\frac{1}{2}\mathrm{Re}\{ VI^* \}$.

At any given point on the line, the voltage and current are

$$V(x) = V_+(e^{-\gamma x} + \Gamma e^{\gamma x}) \quad I(x) = \frac{V_+}{Z_0}(e^{-\gamma x} - \Gamma e^{\gamma x}). \tag{5.107}$$

At the termination and input to the line, the complex power is

$$V(0)I^*(0) = \frac{|V_+|^2}{Z_0^*}(1 - |\Gamma|^2 + 2j\mathrm{Im}\{\Gamma\}) \tag{5.108}$$

$$V(-L)I^*(-L) = \frac{|V_+|^2}{Z_0^*}(e^{2\alpha L} - |\Gamma|^2 e^{-2\alpha L}) + 2j\mathrm{Im}\{\Gamma e^{-2j\beta}\}). \tag{5.109}$$

Taking the real part of each term is simplified by the assumption that Z_0 is real, in which case the ratio of the power into the termination to the power into the line is

$$\frac{\frac{1}{2}\mathrm{Re}\{ V(0)I^*(0) \}}{\frac{1}{2}\mathrm{Re}\{ V(-L)I^*(-L) \}} = \frac{1 - |\Gamma|^2}{e^{2\alpha L} - |\Gamma|^2 e^{-2\alpha L}}. \tag{5.110}$$

It might make sense if this ratio was maximized when the reflection coefficient is zero, and indeed it is. Letting the value of this ratio be ε for $\Gamma = 0$ and ε' otherwise,

$$\varepsilon' = \varepsilon \frac{1 - |\Gamma|^2}{1 - |\Gamma|^2 \varepsilon^2}. \tag{5.111}$$

Since $\varepsilon < 1$, it is easily shown that $\varepsilon' \leq \varepsilon$, thereby establishing that the maximum power transfer from input to termination occurs when $\Gamma = 0$, or $Z_L = Z_0$. (Note that then Z_0 is not real-valued, the termination should be the conjugate of the characteristic impedance, and surprisingly under these conditions there is a reflection.)

For this termination, the input to the line has impedance Z_0, and as is well known the maximum power transfer to the line input will occur when the generator has the same impedance Z_0, again under the assumption that Z_0 is real-valued. This can also be verified simply for this assumption.

5-2. From figure 5-5 we have that

$$\lambda = \frac{2\pi}{\beta} \tag{5.112}$$

and from (5.6) we have

$$\omega = v\beta. \tag{5.113}$$

Eliminating β from these two equations, we get the desired relation.

5-3.

(a) The configuration of a single bridged tap is shown in figure 5-44a, where the bridged tap is modeled as a shunt impedance Z_B. This is an accurate model where the shunt impedance is equal to the input impedance of the bridged tap. From example 5-9 we know that this impedance is

$$Z_B = Z_0 \frac{1 + \Gamma e^{2\gamma L_3}}{1 - \Gamma e^{2\gamma L_3}} \tag{5.114}$$

where L_3 is the length of the bridged tap. Because of assumption of matched termination, the line can for purposes of analysis be split up into two pieces as shown in figure 5-44b and figure 5-44c. In figure 5-44a the section of line after the bridged tap has input impedance Z_0 from example 5-9, so we simply replace it by that impedance. From example 5-10 we know that the voltage across the bridged tap, V_B, is given by

$$V_B = \frac{1 + \Gamma}{2} e^{-\gamma L_1} V_{in} \tag{5.115}$$

where, from example 5-8

$$1 + \Gamma = \frac{2Z_B}{2Z_B + Z_0}. \tag{5.116}$$

Now figure 5-44c models the transmission line from the bridged tap, where the source voltage is now known, to the termination. From example 5-10, the output voltage is

$$\begin{aligned} V_{out} &= e^{-j\gamma L_2} V_B \\ &= \frac{1 + \Gamma}{2} e^{-\gamma(L_1 + L_2)} V_B \end{aligned} \tag{5.117}$$

The effect of the bridged tap is the extra term $1 + \Gamma$, which can be calculated for any given bridged tap length.

(b) From example 5-9, the input impedance of a very long transmission line is the characteristic impedance,

$$Z_B = Z_0 \tag{5.119}$$

and for this case,

$$1 + \Gamma = \frac{2}{3}. \tag{5.120}$$

For this case, the attenuation due to the bridged tap is frequency independent, and simply attenuates all frequencies by the same factor $20.\log_{10}(\frac{2}{3}) = -3.5$ dB. For this case, a fraction $\frac{4}{9}$ of the power goes down

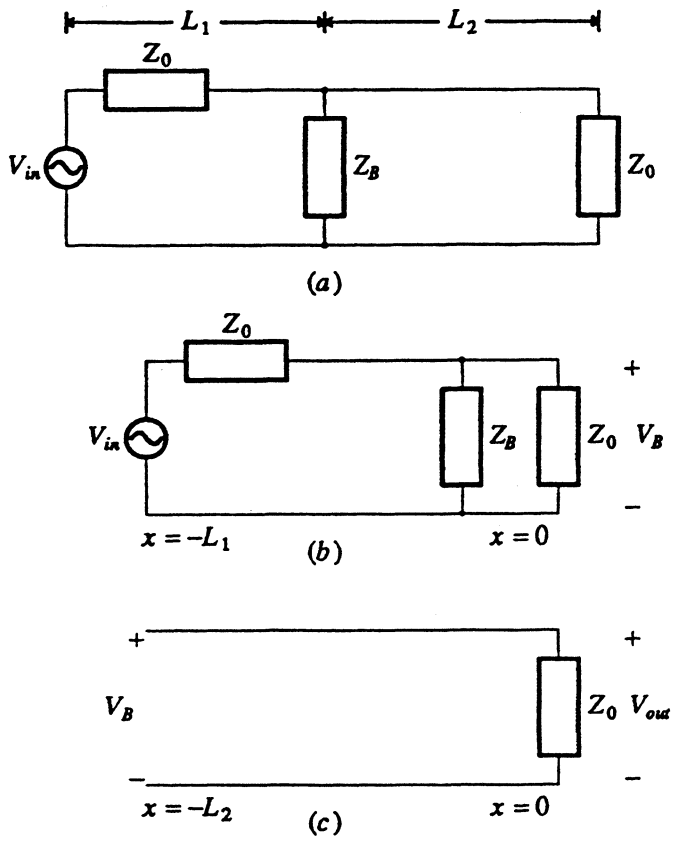

Figure 5-44. Model for analysis of bridged tap. a. A bridged tap as a shunt impedance. b. A model replacing the line after the bridged tap by the characteristic impedance. c. A model for the section of line after the bridged tap.

the bridged tap, never to return, an equal amount goes to the load, and the remaining factor $\frac{1}{9}$ is reflected from the bridged tap back to the load due to the impedance mismatch.

(c) For bridged taps of lesser length, unless the bridged tap is terminated, the effect is much more complicated than the fixed loss of b. The effect can be modeled using the techniques described in appendix 4-B. Intuitively, we expect that a part of the energy traveling down the line will enter the bridged tap, be reflected off the end of the bridged tap, and return to travel down the main line. This energy will be delayed, with larger delay for longer taps, and attenuated, with larger attenuation for longer taps. Thus, for a transmitted pulse, the effect will be a "ghost pulse" which follows the main pulse at the receiver, plus an attenuation of the main pulse. As the bridged tap gets longer, this ghost pulse will be delayed more and will get smaller. In the limit of a long bridged tap, the ghost pulse will be absent.

(d) As the bridged tap approaches zero, the ghost pulse gets larger in amplitude and shorter in delay relative to the main pulse. Due to its short delay, it adds constructively to the main pulse, boosting its amplitude. In the limit, it gets the main pulse amplitude back up to where it would be in the absence of the bridged tap.

5-4. From Snell's law, assuming the index of refraction of the incident medium is unity,

$$\sin(\theta_2) = \frac{\sin(\theta_1)}{n_1} \tag{5.121}$$

and total internal reflection will result if

$$\sin(\phi) > \frac{n_2}{n_1}. \tag{5.122}$$

Further, from the geometry, since θ_2 and ϕ form two angles of a right triangle,

$$\sin^2(\theta_2) + \sin^2(\phi) = 1. \tag{5.123}$$

Manipulating these equations, we get the desired result.

5-5.

(a) Since the path length is proportional to the hypotenuse of a right triangle with side proportional to the length of the fiber, the result follows immediately.

(b) The result follows from the manipulation of the equations

$$\sin(\theta_2) = \frac{\sin(\theta_1)}{n_1} \tag{5.124}$$

$$\sin^2(\theta_1) < n_1^2 - n_2^2. \tag{5.125}$$

5-6. Since a picosec is 10^{-12} seconds and a GHz is 10^9 Hz, if we normalize everything to GHz and nsec (10^{-9} sec) we get

$$\frac{1}{2D} = 3.3 \text{ km–GHz/psec} \cdot 10^3 \text{ psec/nsec} = 3300 \text{ km–(GHZ)}^2 . \tag{5.126}$$

Hence we get

$$L \cdot R^2 < 3000 \tag{5.127}$$

where R is the bit rate in GHz and L is the repeater spacing in kilometers. Therefore we get the following table for L vs. R.

L (km)	R (GHz)
1	57
10	18
100	5.7
1000	1.8

Notice how dramatically the maximum bit rate drops as the repeater spacing increases due to the linearly increasing dispersion as the spacing increases.

5-7.

(a) The number of received photons per second is $\frac{P}{h\nu}$, and therefore the number of received photons per bit is

$$N = \frac{P}{Rh\nu}. \tag{5.128}$$

(b) If N is constant, we get

$$P = NRh\nu \tag{5.129}$$

and the necessary optical power is proportional to the bit rate.

(c)

$$P = \frac{NRhc}{\lambda} = 4.4 \cdot 10^{-9} \text{ watts} \tag{5.130}$$

which equals -53.6 dBm.

(d) The allowable attenuation is 53.6 dB, so the distance is 268 km.

5-8.

(a) Starting with the formula of problem 5-7,

$$\frac{P}{10^{-3}} = R_{Mb} \cdot \frac{10^9 Nhc}{\lambda} \tag{5.131}$$

where the left side is the power expressed in mwatts and

$$R_{Mb} = \frac{R}{10^6}. \tag{5.132}$$

Taking the logarithm and substituting numerical values, the result follows.

(b) 230 and 180 km respectively.

5-9. The 20 vs. 2000 reduction in the number of photons reduces the receiver power by $10\log_{10}(100) = 20$ dB. We have also increased the launched power by 20 dB. This additional 40 dB gives us an additional 40/0.2 = 200 km in distance, or changes 230 and 180 to 430 and 380 km respectively. The range has been approximately doubled! Repeater spacings of 300 km are being seriously sought in undersea cable systems.

5-10. The number of parallel repeatered lines will be B_T/B and the number of repeaters in each line will be L_T/L. Hence, the total number of repeaters is

$$N = \frac{B_T \cdot L_T}{B \cdot L}. \tag{5.133}$$

This is obviously minimized by maximizing $B \cdot L$.

5-11.

(a) We have that

$$\gamma_0 L = 10\log_{10}\frac{P_T}{P_R} = 10\log\frac{P_T}{10^{-3}} - 10\log\frac{P_R}{10^{-3}} = 0 - P_{dBm}. \tag{5.134}$$

(b) The equation becomes

$$L = 329 - 5\cdot\log_{10} R_{Mb}. \tag{5.135}$$

We get the following table:

R_{Mb} (Mb	s)
1	329
10	324
100	319
1000	314
10,000	309

Observe that the repeater spacing is only very weakly dependent on the bit rate. Of course, as the rate increases eventually dispersion will become the dominant impairment.

(c) The LR product is

$$L \cdot R_{Mb} = R_{Mb}(329 - 5\log_{10} R_{Mb}) \tag{5.136}$$

which is a monotonically increasing function of bit rate. Hence, we can minimize the number of repeaters by increasing the bit rate as much as possible, until we reach a dispersion-limited region. This is because the repeater spacing penalty in increasing the bit rate is so small that the best way to decrease the number of repeaters is to transmit at the maximum rate.

5-12. First the voltage source: If a voltage $v(t)$ is in series with the resistor R, then a voltage $v(t)/2$ appears across a matched termination, also with resistance R. The power in a bandwidth B Hz in the matched termination is the available power, and is equal to $v^2(t)/4R$. Setting the expectation of this, or the average power, equal to kT_nB, we get the desired result.

Next the current source: If a current $i(t)$ is in series with the resistance R, the current through a matched termination with resistance R is also $i(t)$, and the instantaneous power in that termination in bandwidth B is $i^2(t)R$. Setting this equal to kT_nB, we get an available power of kT_nB/R.

5-13. The wavelength from (5.31) is $\lambda = 0.05$ meters, the gain is $G = 10^4$, and thus the area is

$$A = \frac{G\lambda^2}{4\pi\eta} = 2.84 \text{ meters}. \tag{5.137}$$

Since this area is $\pi d^2/4$ where d is the diameter, we get $d = 1.9$ meters.

5-14. The parameters staying constant are d, A_T, and A_R. Expressing the total loss in terms of these quantities, we get

$$\frac{P_R}{P_T} = \eta_R \eta_T \frac{A_R A_T}{2d^2\lambda^2}. \tag{5.138}$$

The loss is minimum for the short wavelength end, which is the high frequency end. This is because the antenna presents a larger effective crossection in relation to the wavelength at this end of the band. The difference in loss is proportional to the square of the ratio of the frequencies, or in dB

$$20\log_{10}\frac{6.03}{5.97} = 0.043 \text{ dB}. \tag{5.139}$$

For all practical purposes the loss is independent of frequency.

5-15.

(a) Since from (5.28) we have

$$\gamma_0 d = 10\log_{10}\frac{P_T}{P_R}, \tag{5.140}$$

increasing P_T by an order of magnitude *adds* an additional $10/\gamma_0$ to the repeater spacing. For example, if $\gamma_0 = 0.2$ for a fiber system, we can add 50 km to the repeater spacing. As the spacing gets longer, this increment in spacing will get less and less significant.

(b) From (5.48),

$$d = K\sqrt{\frac{P_T}{P_R}} \tag{5.141}$$

and increasing the transmitted power by an order of magnitude increases the repeater spacing by a factor of about 3.1. Hence, the transmitted power plays a much bigger role in the repeater spacing or distance between antennas than for transmission lines.

5-16. This loss corresponds to (5.48) for the case of perfect efficiency and unity antenna gains. Hence,

$$\text{Loss(dB)} = 20\log_{10}\frac{4\pi d_{\text{km}}\cdot 10^3}{\lambda} \tag{5.142}$$

where

$$\lambda = \frac{c}{f_{\text{GHz}}\cdot 10^9}. \tag{5.143}$$

Substituting for the constants, we get the result.

5-17. Equating the total noise power at the output of figure 5-42a. and b.,

$$kT_2B + kT_1B + kT_1BG = kT_3BG \tag{5.144}$$

we get

$$T_3 = T_1 + \frac{T_2}{G}. \tag{5.145}$$

Note how the noise referenced to the input is decreased by the gain of the amplifier. Further note that the noise temperatures add for two noise sources with no intermediate gain.

5-18. The IF noise source can be referenced to the input to the RF amplifier with noise temperature $\frac{T_{IF}}{G_{RF}}$. Hence, the total noise referenced to the input has temperature

$$T_{in} + T_{RF} + \frac{T_{IF}}{G_{RF}}. \tag{5.146}$$

Note that any noise in the IF amplifier is inherently less significant than noise introduced at the input or RF amplifier.

5-19. The excess distance for the reflected path is approximately

$$\frac{2h^2}{d} = 1.66 \text{ meters} \tag{5.147}$$

and the excess delay (and hence the delay spread) is therefore about 5.5 nsec. The reciprocal of the delay spread is 180 MHz, and assuming the narrowband model is valid over 1% of this bandwidth, that would be 1.8 MHz.

5-20.

(a) The spectrum will become asymmetric about the carrier, with more power concentrated at frequencies near $(\omega_c + kv)$

(b) The spectrum will fill out in the middle and get smaller near $(\omega_c \pm kv)$, but still be close to symmetric about the carrier frequency.

5-21. There are two oscillators, the worst case $|f_c - f_d| < 3\,Hz$. This means that each oscillator should not deviate more than 1.5 Hz from the nominal frequency 1 MHz, implying 1.5 parts per million accuracy.

5-22.

$$y(t) = \text{Re}\{ s(t)e^{j[\omega_c t + \omega_0 - a\cos(\omega_0 t)]} \}. \tag{5.148}$$

CHAPTER 6: SOLUTIONS TO PROBLEMS

6-1. Using (6.4), we can write

$$H(j\omega) = G(j\omega)B(j\omega). \tag{6.280}$$

Using the result of appendix 3-A, we can write the power spectrum of the received signal as

$$S_R(j\omega) = \frac{1}{T}|H(j\omega)|^2 S_A(e^{j\omega T}) = \frac{\sigma_A^2}{T}|G(j\omega)B(j\omega)|^2 = \frac{\sigma_A^2}{T}|G(j\omega)|^2 B(j\omega). \tag{6.281}$$

Using appendix 2-A

$$G(j\omega) = e^{-j\omega T/2} T \frac{\sin(\omega T/2)}{\omega T/2}, \tag{6.282}$$

so

$$|G(j\omega)|^2 = \frac{\sin^2(\omega\pi/W)}{\omega^2/4}. \tag{6.283}$$

The power spectrum $S_R(j\omega)$ is sketched below:

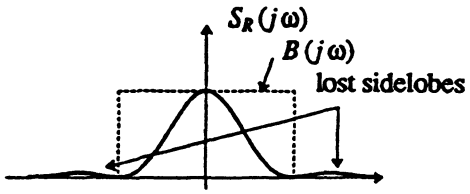

The distortion is due to the loss of the sidelobes of $G(j\omega)$ when it is multiplied by $B(j\omega)$.

6-2. From appendix 3-A, the transmit power spectrum for baseband PAM is

$$S_S(j\omega) = \frac{1}{T}|G(j\omega)|^2 S_A(e^{j\omega T})$$

$$= \begin{cases} T; & 0 \le |\omega| \le (1-\alpha)\pi/T \\ \frac{T}{4}\left[1 - \sin\left[\frac{T}{2\alpha}(|\omega| - \frac{\pi}{T})\right]\right]^2; & (1-\alpha)\frac{\pi}{T} \le |\omega| \le (1+\alpha)\frac{\pi}{T}, \\ 0; & |\omega| > (1+\alpha)\pi/T \end{cases} \tag{6.284}$$

from (6.25). Considering only positive ω, the transmit power is

$$\begin{aligned} R_S(0) &= \frac{1}{\pi}\int_0^\infty S_S(j\omega)d\omega \\ &= \frac{1}{\pi}\int_0^{(1-\alpha)\pi/T} T d\omega + \frac{1}{\pi}\int_{(1-\alpha)\pi/T}^{(1+\alpha)\pi/T} \frac{T}{4}\left[1 - \sin\left[\frac{T}{2\alpha}(\omega - \frac{\pi}{T})\right]\right]^2 d\omega \\ &= (1-\alpha) + \int_{(1-\alpha)}^{(1+\alpha)} \frac{1}{4}\left[1 - \sin\left[\frac{\Omega\pi}{2\alpha} - \frac{\pi}{2\alpha}\right]\right]^2 d\Omega \end{aligned} \tag{6.285}$$

which is independent of T.

6-3. The minimum bandwidth pulse has bandwidth π/T radians/sec. or $1/2T$ Hz, where $1/T$ is the symbol rate. The bandwidth of a pulse with 50% excess bandwidth is $1.5/2T$ in Hz. We require that

$$\frac{1.5}{2T} \le 1500 \tag{6.286}$$

which implies that the maximum symbol rate is $\frac{1}{T} = 2000$ symbols per second.

6-4.

(a) X_k is white, $R_X(k) = \delta_k$, so $S_X(e^{j\omega T}) = 1$. Further,

$$A_k = X_k - X_{k-1}. \tag{6.287}$$

Taking Z-transforms,

$$A(z) = X(z)(1 - z^{-1}). \tag{6.288}$$

Define

$$H(z) = \frac{A(z)}{X(z)} = 1 - z^{-1} \tag{6.289}$$

so

$$H(e^{j\omega T}) = 1 - e^{-j\omega T}. \tag{6.290}$$

Hence

$$\begin{aligned} S_A(e^{j\omega T}) &= S_X(e^{j\omega T})\,|H(e^{j\omega T})|^2 \\ &= |1-e^{-j\omega T}|^2 \\ &= 2-2\cos(\omega T)\,. \end{aligned} \tag{6.291}$$

The sketch is shown in the following figure.

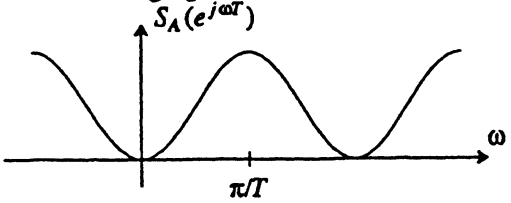

(b) Here is a well-labeled, careful sketch:

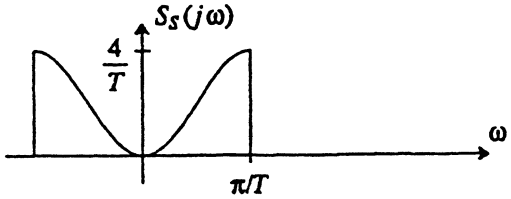

(c)

$$\begin{aligned} S(t) &= \sum_{m=-\infty}^{\infty}(X_m - X_{m-1})g(t-mT) \\ &= \sum_{m=-\infty}^{\infty} X_m g(t-mT) - \sum_{m=-\infty}^{\infty} X_m g(t-mT-T) \\ &= \sum_{m=-\infty}^{\infty} X_m[g(t-mT)-g(t-mT-T)]\,. \end{aligned} \tag{6.294}$$

So

$$h(t) = [g(t)-g(t-T)] \tag{6.297}$$

and

$$H(j\omega) = (1-e^{-j\omega T})G(j\omega)\,. \tag{6.298}$$

Note that $H(j\omega)=0$ for all $\omega = m2\pi/T$, so the Nyquist criterion is not satisfied for any $G(j\omega)$. Furthermore,

$$P(j\omega) = (1-e^{-j\omega T})G(j\omega)F(j\omega) \tag{6.299}$$

does not satisfy the Nyquist criterion for any $G(j\omega)$ and $F(j\omega)$ that are finite for all ω. (It turns out that ISI can be eliminated using a receive filter that has infinite gain at DC, but this filter is not stable.)

6-5. The only zero excess-bandwidth pulse satisfying the Nyquist criterion is (6.16). But since the pulse falls off as $1/t$, the worst case transmitted symbol sequence will result in infinite intersymbol interference for any sampling phase other than the ideal phase (where the intersymbol interference is zero).

Consider binary PAM signaling with a zero excess-bandwidth raised-cosine pulse shape, which is an ordinary sinc pulse. We can show that if the timing phase is off from the ideal by any amount, the data cannot be recovered. The pulse shape is given by

$$p_0(t) = \frac{\sin(\pi t/T)}{\pi t/T} \tag{6.300}$$

and the PAM signal by

$$R(t) = \sum_{m=-\infty}^{\infty} A_m p_0(t - mT) = \sum_{m=-\infty}^{\infty} A_m \frac{\sin(\frac{\pi}{T}(t - mT))}{\frac{\pi}{T}(t - mT)} . \tag{6.301}$$

Sampling with exactly the correct timing phase, we get for any integer n

$$R(nT) = A_n . \tag{6.302}$$

To see what happens if the timing phase is slightly off, we rewrite the signal using trigonometric properties of the sine function,

$$R(t) = \frac{T}{\pi}\sin(\frac{\pi}{T}t) \sum_{m=-\infty}^{\infty} A_m \frac{(-1)^m}{(t - mT)} . \tag{6.303}$$

For any nonzero ε, if we sample at $t = \varepsilon$ instead of $t = 0$ we get

$$R(\varepsilon) = \frac{T}{\pi}\sin(\frac{\pi}{T}\varepsilon) \sum_{m=-\infty}^{\infty} A_m \frac{(-1)^m}{(\varepsilon - mT)} . \tag{6.304}$$

For small ε this is

$$R(\varepsilon) \simeq \varepsilon \sum_{m=-\infty}^{\infty} A_m \frac{(-1)^m}{\varepsilon - mT} \simeq A_0 + \sum_{m \neq 0} A_m \frac{(-1)^m}{-mT} . \tag{6.305}$$

This is far from the desired value A_0, and with the unfortunate outcome $A_m = (-1)^m$, the sample is not even finite for any nonzero ε. Since the interference from neighboring symbols may not even be finite for any arbitrarily small error in the timing phase, the width of the eye is zero. Consequently, binary antipodal excess bandwidth *must* be larger than zero.

6-6. Decreasing K also decreases the signal power so the SNR is unchanged. Furthermore, if we compensate by transmitting more power from the transmitter, then arbitrarily large power is required from the transmitter as K gets arbitrarily small. Arbitrary transmit power is not feasible.

6-7.

(a)

$$\mathrm{E}[|A_k|^2] = R_A(0) = \frac{T}{2\pi}\int_{-\pi/T}^{+\pi/T} S_A(e^{j\omega T})d\omega = 1 . \tag{6.306}$$

(b) Using the results of appendix 3-A, let the transmit signal be

$$Z(t) = \sum_{m=-\infty}^{\infty} A_m g(t + \Theta - kT) \tag{6.307}$$

and

$$S_Z(j\omega) = \frac{1}{T}|G(j\omega)|^2 S_A(e^{j\omega T}) = 1 , \tag{6.308}$$

so the power spectrum in independent of T.

(c) From (6.35),

$$F(j\omega) = \sqrt{T}\,\mathrm{rect}(\omega, \pi/T) . \tag{6.309}$$

The pulse satisfies the Nyquist criterion.

(d) From (6.41)

$$\sigma^2 = \frac{N_0}{2\pi}\int_{-\infty}^{\infty} \left| \sqrt{T}\,\mathrm{rect}(\omega, \pi/T) \right|^2 d\omega = N_0 . \tag{6.310}$$

Also, $p(t)$ satisfies the Nyquist criterion, which implies it is properly normalized,

$$p(0) = \frac{1}{2\pi}\int_{-\infty}^{\infty} P(j\omega)d\omega = 1 \tag{6.311}$$

so

$$SNR = \frac{1}{N_0}. \tag{6.312}$$

(e) The noise power can be gotten from (6.41),

$$\begin{aligned}\sigma^2 &= \frac{1}{2\pi}\int_{-\infty}^{\infty} N_0 \left| \frac{P(j\omega)}{\sqrt{T}} \right|^2 d\omega \\ &= \frac{N_0}{\pi T}\int_0^{2\pi/T} (T - \omega\frac{T^2}{2\pi})^2 d\omega = N_0\frac{2}{3}.\end{aligned} \tag{6.313}$$

The SNR is therefore

$$SNR = \frac{3}{2N_0} \tag{6.314}$$

which is better than in part b even though the receive filter bandwidth is greater!

6-8.

(a) Yes this pulse satisfies the Nyquist criterion. So does Re{ $p(t)$ }.

(b) From appendix 3-A we get

$$S_Q(j\omega) = \frac{\sigma_A^2}{T}|P(j\omega)|^2 \tag{6.315}$$

which is sketched below.

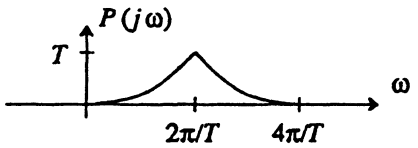

(c) Let

$$X(j\omega) = T\sqrt{2}\,\mathrm{rect}(\omega,\pi/2T) \tag{6.316}$$

and

$$Y(j\omega) = \frac{1}{2\pi}X(j\omega)*X(j\omega) \tag{6.317}$$

and note that

$$P(j\omega) = Y(j\omega - j\pi/T). \tag{6.318}$$

In the time-domain, from appendix 2-A,

$$y(t) = [x(t)]^2 \tag{6.319}$$

and also from appendix 2-A,

$$x(t) = \frac{\sqrt{2}}{2}\cdot\frac{\sin(t\pi/2T)}{t\pi/2T}. \tag{6.320}$$

Hence

$$p(t) = e^{jt\pi/T}\left[\frac{\sqrt{2}}{2}\cdot\frac{\sin(t\pi/2T)}{t\pi/2T}\right]^2. \tag{6.321}$$

6-9.

(a) The power of the received signal as a function of α is given by (6.285) multiplied by σ_A^2. The noise power is the same thing multiplied by N_0. The SNR is therefore σ_A^2/N_0, independent of α.

(b) The receive filter is an ideal LPF

$$F(j\omega)=\begin{cases}1; & |\omega|<\pi(1+\alpha)/T\\ 0; & \text{otherwise}\end{cases}. \tag{6.322}$$

The noise power after the receive filter is therefore $N_0(1+\alpha)/T$. The signal power is given by (6.285) multiplied by σ_A^2. The SNR is the ratio of the two, not a pretty sight.

(c) This can be found using techniques similar to those in problem 6-2.

6-10.

(a) 64 kb/s are required, so with binary antipodal signaling this is 64,000 symbols per second, so the minimum bandwidth is 32 kHz.

(b) 64 kHz.

(c) 32 kHz.

(d) 16 kHz.

6-11.

(a) The frequency response of the baseband equivalent channel is:

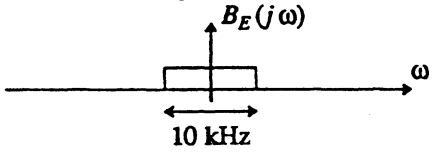

and the impulse response is a corresponding sinc function.

(b) The answers are respectively 20 kb/s, 6667 b/s, 20 kb/s, and 40 kb/s. In the latter case, the receive filter should be properly designed to meet the Nyquist criterion.

(c) A reasonable transmit filter is $g(t)=\delta(t)$. There is no point in using a bandlimited transmit filter since the channel will bandlimit the signal. Using this transmit filter, the receive filter should be an ideal lowpass filter just like the baseband equivalent channel. This minimizes the noise that gets through to the slicer and properly forms $p(t)$.

6-12. Since the passband channel is the same as a baseband channel, the only difference being the complex data symbols, the criterion is the same. The required bandwidth is twice as great, since the spectrum is two-sided, or in other words a bandwidth of $2\pi/T$ is required for a symbol spacing of T. Although the bandwidth is twice as great, the symbol rate referenced to *real-valued* symbols is also twice as great, so the bandwidth efficiency is the same.

6-13. From appendix 2-A it is clear that $H(j\omega)X(j\omega)=Y(j\omega)$ in either case.

6-14.

(a) From appendix 2-A, the Fourier transform of $\mathrm{Re}\{z(t)\}$ is $Z_e(j\omega)$ and the Fourier transform of $j\,\mathrm{Im}\{z(t)\}$ is $Z_o(j\omega)$. Hence the Fourier transform of $\mathrm{Im}\{z(t)\}$ is $-jZ_o(j\omega)$. So we need to show that

$$H(j\omega)Z_e(j\omega)=-jZ_o(j\omega). \tag{6.323}$$

Note that since $z(t)$ is analytic, $Z(j\omega)=0$ for $\omega<0$ so

$$Z_e(j\omega)=0.5[Z(j\omega)+Z^*(-j\omega)]=\begin{cases}0.5Z(j\omega); & \omega>0\\ 0.5Z^*(-j\omega); & \omega<0\end{cases}. \tag{6.324}$$

Hence

$$H(j\omega)Z_e(j\omega)=-j0.5[Z(j\omega)-Z^*(-j\omega)]=-jZ_o(j\omega), \tag{6.325}$$

which is the desired result.

(b) We need to show that

$$-Z_e(j\omega) = H(j\omega)[-jZ_o(j\omega)]. \tag{6.326}$$

This follows similarly.

6-15. Define

$$z(t) = H(jt) = H(j\omega)|_{\omega=t}. \tag{6.327}$$

From the duality property in appendix 2-A

$$Z(j\omega) = 2\pi h(-\omega). \tag{6.328}$$

Note that $Z(j\omega) = 0$ for $\omega < 0$, so $z(t)$ is analytic. From problem 6-14,

$$\mathrm{Im}\{z(t)\} = \frac{1}{\pi t} * \mathrm{Re}\{z(t)\} \tag{6.329}$$

so

$$\mathrm{Im}\{H(jt)\} = \frac{1}{\pi t} * \mathrm{Re}\{H(jt)\}. \tag{6.330}$$

Formally replace t with ω and the result follows.

6-16. Using appendix 2-A

$$\mathrm{DTFT}[\mathrm{Re}\{z_k\}] = Z_e(e^{j\omega T}) = 0.5[Z(e^{j\omega T}) + Z^*(e^{-j\omega T})]. \tag{6.331}$$

Hence

$$\begin{aligned} Z_e(e^{j\omega T})H(e^{j\omega T}) &= 0.5Z(e^{j\omega T})H(e^{j\omega T}) + 0.5Z^*(e^{-j\omega T})H(e^{j\omega T}) \\ &= -0.5jZ(e^{j\omega T}) + 0.5jZ^*(e^{-j\omega T}) \\ &= -jZ_o(e^{j\omega T}). \end{aligned} \tag{6.332}$$

The inverse discrete-time Fourier transform is $\mathrm{Im}\{z_k\}$ (from appendix 2-A).

6-17.

(a) This follows from problem 6-16 and the observation that the signal is bandlimited.

(b)

$$h_k = 2g_k \sin(\omega_c kT). \tag{6.333}$$

This is the desired filter because using the discrete-time Fourier transform of $\sin(\omega_c kT)$ from appendix 2-A we get

$$\begin{aligned} H(j\omega) &= \frac{1}{j}\int_{-\pi/T}^{\pi/T} G(e^{j\Omega T})[\delta(\omega - \Omega - \omega_c) - \delta(\omega - \Omega + \omega_c)]d\Omega \\ &= \frac{1}{j}[G(e^{j(\omega-\omega_c)T}) - G(e^{j(\omega+\omega_c)T})]. \end{aligned} \tag{6.334}$$

6-18. Use ROMs with N bit addresses, two outputs, each with $2^{\lceil N/2 \rceil}$ bits.

6-19.

$$\begin{aligned} \int_{-\infty}^{\infty} g_0(t)g_1(t)dt &= \int_0^T \sin(\omega_0 t)\sin(\omega_1 t)dt \\ &= \frac{1}{2}\int_0^T \Big[\cos((\omega_0 - \omega_1)t) + \cos((\omega_0 + \omega_1)t)\Big]\,dt\,. \end{aligned} \tag{6.335}$$

Under both set of assumptions, the integral evaluates to zero.

6-20. Write the pulses from (6.149) as

$$\begin{aligned} g_0(t) &= \pm \sin((\omega_c + \omega_d)t)w(t) \\ g_1(t) &= \pm \sin((\omega_c - \omega_d)t)w(t) \end{aligned} \tag{6.336}$$

where

$$\omega_d = \frac{\omega_0 - \omega_1}{2} \tag{6.337}$$

is the peak deviation. Then

$$\begin{aligned} \int_0^T g_0(t)g_1(t)dt &= \pm \frac{1}{2}\int_0^T \cos(2\omega_d t)dt \pm \frac{1}{2}\int_0^T \cos(2\omega_c t)dt \\ &= \frac{1}{4\omega_d}\sin(2\omega_d T). \end{aligned} \tag{6.338}$$

The signals are orthogonal if and only if this is zero, which occurs if and only if

$$2\omega_d T = K\pi \tag{6.339}$$

for some integer K. The minimum (non-zero) frequency spacing therefore occurs when

$$2\omega_d T = \pi \tag{6.340}$$

or

$$\omega_d = \frac{\pi}{2T}. \tag{6.341}$$

This is the frequency spacing (6.148) of MSK signals.

6-21. For MSK, the frequency separation should be $\omega_i - \omega_{i-1} = \pi/T$, or $f_i - f_{i-1} = 1/2T = 0.5$ MHz. So the desired frequencies are $f_1 = 10.5$ MHz, $f_2 = 11.0$ MHz, etc.

6-22.

(a) From (6.152), using trigonometric identities,

$$X(t) = \sum_{m=-\infty}^{\infty} \left[\sin(\omega_c t + b_k \frac{\pi t}{2T})\cos(\phi_k) + \cos(\omega_c t + b_k \frac{\pi t}{2T})\sin(\phi_k) \right] w(t - kT). \tag{6.342}$$

Since $\sin(\phi_k) = 0$ this becomes, using more trigonometric identities

$$X(t) = \sum_{m=-\infty}^{\infty} \left[\sin(\omega_c t)\cos(b_k \frac{\pi t}{2T}) + \cos(\omega_c t)\sin(b_k \frac{\pi t}{2T}) \right] \cos(\phi_k)w(t - kT). \tag{6.343}$$

From the symmetry of the cosine we get

$$\cos(b_k \frac{\pi t}{2T}) = \cos(\frac{\pi t}{2T}) \tag{6.344}$$

and from the anti-symmetry of the sine we get

$$\sin(b_k \frac{\pi t}{2T}) = b_k \sin(\frac{\pi t}{2T}), \tag{6.345}$$

from which the result follows.

(b) Notice that $b_{k-1} - b_k$ is always either zero or ± 2 so if k is even then from (6.153)

$$\phi_k = \phi_{k-1} + K2\pi \tag{6.346}$$

where K is an integer. Hence

$$Q_k = \cos(\phi_k) = Q_{k-1} = \cos(\phi_{k-1}). \tag{6.347}$$

If k is odd then examining (6.153) we see that if $b_k = b_{k-1}$ then $I_k = I_{k-1}$. Furthermore, if $b_k = -b_{k-1}$ then

$$\phi_k = \phi_{k-1} \pm \pi k \tag{6.348}$$

and since k is off $\cos(\phi_k) = -\cos(\phi_{k-1})$ and again $I_k = I_{k-1}$.

(c) Write the first summation of (6.226)

$$\cos(\omega_c t) \sum_{k\,\text{even}} I_k \sin(\frac{\pi t}{2T})[w(t-kT) - w(t-kT-T)] \tag{6.349}$$

using the fact that for k even $I_k = I_{k+1}$. Then notice that for k even

$$\sin(\frac{\pi}{2T}(t-kT)) = (-1)^{k/2}\sin(\frac{\pi t}{2T}) \tag{6.350}$$

so

$$\sin(\frac{\pi t}{2T}) = \sin(\frac{\pi}{2T}(t-kT))(-1)^{k/2}. \tag{6.351}$$

Hence the first summation of (6.226) is

$$\cos(\omega_c t) \sum_{k\,\text{even}} I_k (-1)^{k/2} p(t-kT). \tag{6.352}$$

The second summation follows similarly.

6-23. The real part of the output of the phase splitter is

$$\frac{A}{\sqrt{2}}\cos(\omega_c t) \tag{6.353}$$

while the imaginary part is

$$\frac{A}{\sqrt{2}}\sin(\omega_c t), \tag{6.354}$$

where we have used problem 6-13. The magnitude squared of the complex output is therefore $A^2/2$.

6-24. Each of 128 subchannels (one per pulse) must carry a bit rate of 19,200/128 or 150 bits per second. Using 4-PSK, we can transmit 2 bits per symbol, so the symbol rate should be 75 symbols/second. Hence, T is 1/75 seconds or about 13msec.

6-25.

(a) This follows because the DTFT of a linear combination of pulses is the linear combination of the DTFT of the pulses.

(b)

$$\begin{aligned} G_n(e^{j\omega T'}) &= \sum_{k=0}^{N-1} g_k^{(n)} e^{-j\omega T' k} \\ &= \sum_{k=0}^{N-1} e^{j2\pi nk/N} e^{-j\omega Tk/N} \\ &= \sum_{k=0}^{N-1} e^{jk(2\pi n - \omega T)/N} \\ &= \frac{1 - e^{j(2\pi n - \omega T)}}{1 - e^{j(2\pi n - \omega T)/N}}. \end{aligned} \tag{6.355}$$

where we have used the given identity for the last equality. We can now factor out half-angle terms in the numerator and denominator to get the required result.

6-26. Observe that E[Z(t)] has zero mean, since $E[\cos(\omega_c t + \Theta)] = 0$. To find its autocorrelation function, use the trigonometric identity

$$\cos(a)\cos(b) = 0.5\cos(a-b) + 0.5\cos(a+b) \tag{6.356}$$

to get

$$\begin{aligned} R_Z(\tau) &= 2E[\cos(\omega_c(t+\tau)+\Theta)\cos(\omega_c t + \Theta)S(t+\tau)S^*(t)] \\ &= E[\cos(\omega_c\tau) + \cos(\omega_c(2t+\tau)+2\Theta)]R_S(\tau) \\ &= \cos(\omega_c\tau)R_S(\tau)\ . \end{aligned} \tag{6.357}$$

We have used the easily shown fact that

$$E[\cos(\omega_c(2t+\tau)+2\Theta)] = 0. \tag{6.358}$$

The power spectrum is then given by

$$S_Z(j\omega) = 0.5[S_S(j\omega_c - j\omega) + S_S(-j\omega_c - j\omega)]\ . \tag{6.359}$$

For example, given the same complex-valued baseband power spectrum shown below,

the power spectrum of $Z(t)$ is shown below:

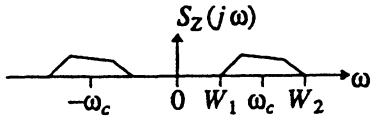

6-27. We can write

$$X(t) = \sqrt{2}\mathrm{Re}\{Z(t)\} = \frac{\sqrt{2}}{2}[Z(t) + Z^*(t)] \tag{6.360}$$

where

$$Z(t) = S(t)e^{j(\omega_c t + \Theta)}. \tag{6.361}$$

Showing that the expected value is independent of time is easy using

$$E[X(t)] = \sqrt{2}\mathrm{Re}\{E[S(t)]E[e^{j(\omega_c t + \Theta)}]\}\ . \tag{6.362}$$

The second expectation is easily shown to be zero by directly computing it (the expectation is over Θ, which has a uniform p.d.f., so we simply need to integrate over $[0,2\pi]$). The autocorrelation can be written

$$E[X(t_1)X^*(t_2)] = \frac{1}{2}E[Z(t_1)Z(t_2)Z(t_1)Z^*(t_2)Z^*(t_1)Z(t_2)Z^*(t_1)Z^*(t_2)]\ , \tag{6.363}$$

where the first term,

$$E[Z(t_1)Z(t_2)] = E[S(t_1)S(t_2)]E[e^{j(\omega_c(t_1+t_2)+2\Theta)}]\ . \tag{6.364}$$

can also easily be shown to be zero by directly computing the expectation over Θ of the complex exponential. The fourth term $E[Z^*(t_1)Z^*(t_2)]$ will similarly turn out to be zero. The second term is

$$E[Z(t_1)Z^*(t_2)] = E[S(t_1)S^*(t_2)]e^{j\omega_c(t_1-t_2)}\ . \tag{6.365}$$

The exponential is now a deterministic function of $t_1 - t_2$, as is $E[S(t_1)S^*(t_2)]$, the autocorrelation of $S(t)$, because $S(t)$ is WSS. The third term will similarly prove to be a function of $t_1 - t_2$, so $X(t)$ is WSS.

6-28. We need to check the conditions of exercise 6-14 to see if they are satisfied. Since the Hilbert transform is an all-pass filter, $S_{\hat{Y}}(j\omega) = S_Y(j\omega)$, and hence $R_{\hat{Y}}(\tau) = R_Y(\tau)$. Further, since

$$S_{\hat{Y}Y}(j\omega) = -j\,\mathrm{sgn}(\omega) S_Y(j\omega) \ , \tag{6.366}$$

we have that

$$R_{\hat{Y}Y}(\tau) = \hat{R}_Y(\tau) \ . \tag{6.367}$$

Since $S_{\hat{Y}Y}(\tau)$ is imaginary-valued, it follows that $R_{\hat{Y}Y}(-\tau) = -R_{\hat{Y}Y}(\tau)$ is an odd function. Thus the conditions for $X(t)$ to be WSS are satisfied. Letting $S(t) = Y(t) + j\,\hat{Y}(t)$, it follows from exercise 6-18 that

$$\begin{aligned} R_S(\tau) &= 2R_Y(\tau) - 2j\,R_{\hat{Y}Y}(\tau) \\ &= 2R_Y(\tau) + 2j\,R_{\hat{Y}Y}(\tau) \\ &= 2R_Y(\tau) + 2j\,\hat{R}_Y(\tau) \ . \end{aligned} \tag{6.368}$$

Hence

$$S_S(j\omega) = \begin{cases} 4S_Y(j\omega) \ , & \omega \geq 0 \\ 0 \ , & \omega < 0 \end{cases} \ . \tag{6.369}$$

The power spectrum of $X(t)$ is then given by (6.195).

6-29. The sketches are shown in figure 6-60. Define

$$s_n(t) = \frac{1}{2\sqrt{T}} \left[\frac{\sin(\pi t/2T)}{\pi t/2T} \right] \cos((n + \tfrac{1}{2})\frac{\pi}{T} t) \tag{6.370}$$

Then

$$h_0(t) = s_1(t) + s_3(t) \tag{6.371}$$

$$h_1(t) = s_1(t) - s_3(t) \tag{6.372}$$

$$h_2(t) = s_2(t) + s_0(t) \tag{6.373}$$

$$h_3(t) = s_2(t) - s_0(t) \tag{6.374}$$

The bandwidth efficiency is the same as that of the pulses in figure 6-38.

6-30.

(a) This is just a matter of multiplying it out.

(b) Let $\mathrm{H}(\omega) = \sqrt{\frac{T}{3}}\mathrm{D}(\omega)$.

(c) If we choose $M_1 = 0$ and $M_2 = 2$ in (6.199), we get the pulses with Fourier transforms shown in figure 6-61. From this, we see that each pulse consists of three parts. Each part is a sinc pulse modulated by $e^{-j2\pi mt/T}$ for $m = 0$, 1, and 2, and scaled by a complex value that depends on n. For $n = 0$, 1, and 2, we can write

$$h_n(t) = \frac{sinc\,(\pi t/T)}{\sqrt{3T}} \left[1 + e^{-j2\pi(\frac{t}{T} + \frac{n}{3})} + e^{-j4\pi(\frac{t}{T} + \frac{n}{3})} \right] \ , \tag{6.375}$$

where $sinc\,(x) = \sin(x)/x$.

(d) The time domain pulses are not real. To use these pulses for orthogonal multipulse over a real channel, we need to modulate them, forming the real-valued passband equivalent pulses

$$\hat{h}_n(t) = \sqrt{2}\mathrm{Re}\{ e^{j\omega_c t} h_n(t) \} \tag{6.376}$$

for some $\omega_c \geq \pi/T$. The bandwidth of such a signal is twice that of figure 6-38, or N/T Hz, making the spectral efficiency of orthogonal multipulse

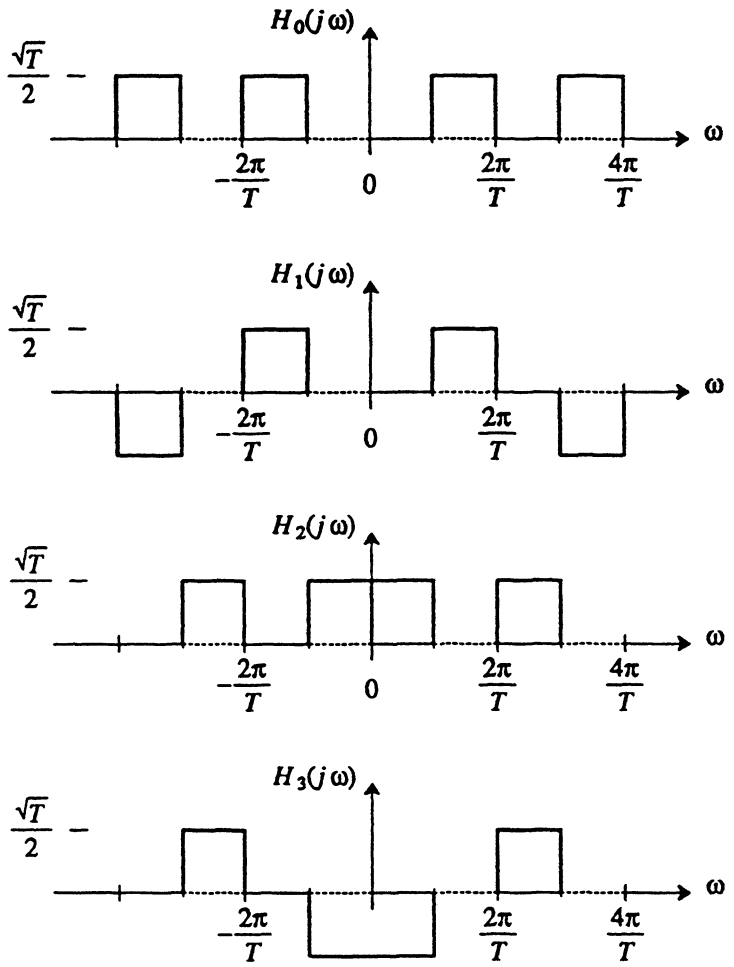

Figure 6-60. The Fourier transform for the orthonormal pulses in problem 6-29. The value of $H_n(j\omega)$ in the dashed regions of the ω axis is determined by the requirement for conjugate symmetry, while the value in the solid regions is determined by $\mathbf{H}(\omega)$.

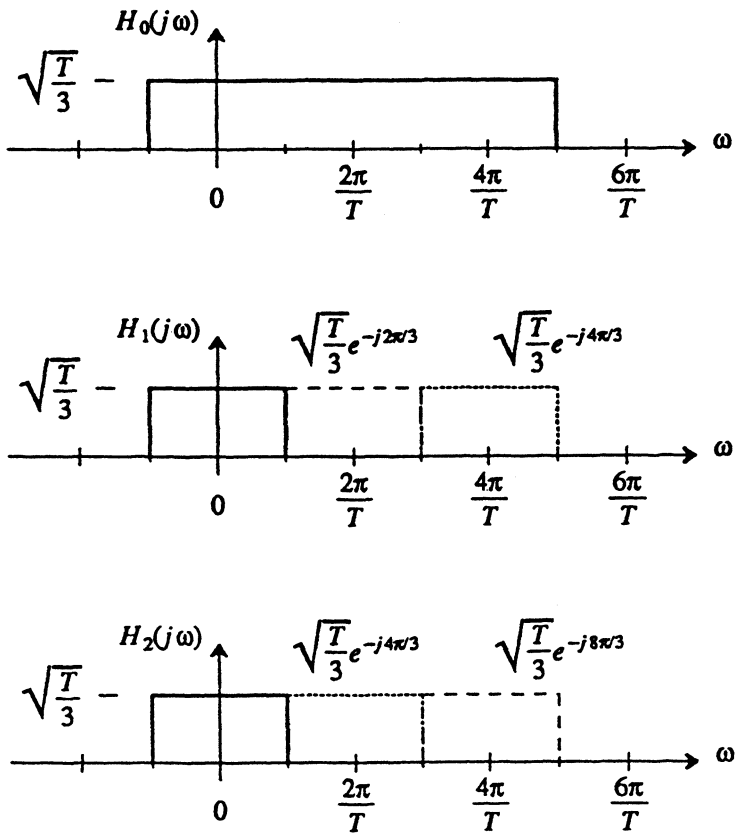

Figure 6-61. The Fourier transforms of three orthogonal multipulse pulses. Complex values are plotted as magnitudes but labeled with the actual complex value.

$$\nu = \frac{\log_2(N)}{N} = \log_2 \frac{(3)}{3} \approx 0.528 . \tag{6.377}$$

With combined PAM and multipulse, instead of transmitting $\log_2(3)$ bits per symbol we can transmit $\log_2(M)$ on each of N simultaneously transmitted pulses, so

$$\nu = \frac{N \log_2(M)}{N} = \log_2(M) . \tag{6.378}$$

This is equivalent to passband PAM with the same alphabet size, and since symbols can be complex, is equivalent to baseband PAM and to PAM plus multipulse using figure 6-38. The pulses are not practical because of the gradual rolloff of the sinc function, or equivalently, because of the abrupt transitions in the frequency domain.

CHAPTER 7: SOLUTIONS TO PROBLEMS

7-1. The conditions of the problem are satisfied if

$$\|\mathbf{Y}-\mathbf{S}_j\|^2 \le \|\mathbf{Y}-\mathbf{S}_i\|^2 \tag{7.88}$$

and substituting for Y, this becomes

$$\|\mathbf{E}+\mathbf{S}_i-\mathbf{S}_j\|^2 \le \|\mathbf{E}\|^2 . \tag{7.89}$$

Multiplying out the left side, we get

$$\|\mathbf{E}\|^2 + d_{ij}^2 - 2\mathrm{Re}\{\langle \mathbf{E}, \mathbf{S}_j-\mathbf{S}_i\rangle\} \le \|\mathbf{E}\|^2 , \tag{7.90}$$

and dividing by d_{ij},

$$\mathrm{Re}\{\langle \mathbf{E}, \frac{\mathbf{S}_j-\mathbf{S}_i}{d_{ij}}\rangle\} \ge \tfrac{1}{2}d_{ij} . \tag{7.91}$$

This is the result promised, since $(\mathbf{S}_j-\mathbf{S}_i)/d_{ij}$ is a unit vector in the direction of $(\mathbf{S}_j-\mathbf{S}_i)$.

7-2.

(a)

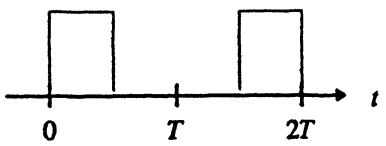

(b)

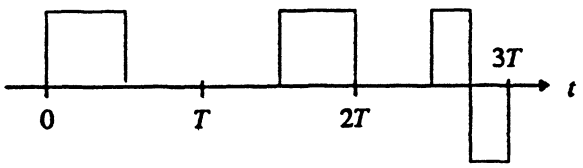

7-3.

(a)

$$\rho_h^*(-k) = \int_{-\infty}^{\infty} h^*(t)h(t+kT)\,dt = \int_{-\infty}^{\infty} h(u)h^*(u-kT)\,du , \tag{7.92}$$

where the change of variables $u = t + kT$ has been made.

(b)

$$S_h^*(e^{j\omega T}) = \sum_k \rho_h^*(k)e^{j\omega kT} = \sum_k \rho_h^*(-k)e^{-j\omega kT} = S_h(e^{j\omega T}) \tag{7.93}$$

7-4. Dividing the folded spectrum Z-transform into positive and negative time,

$$S_h(z) = \sum_{k=0}^{\infty} \rho_h(k) z^{-k} + \sum_{k=-\infty}^{0} \rho_h(k) z^{-k} - \rho_h(0) . \tag{7.94}$$

The second summation can be written

$$\sum_{k=0}^{\infty} \rho_h(-k) z^k = \sum_{k=0}^{\infty} \rho_h^*(k) z^k = S_{h,+}^*(1/z^*) . \tag{7.95}$$

7-5.

(a)

$$\begin{aligned} \rho_h(k) &= \int_{-\infty}^{\infty} \sum_{m=0}^{K} f_m h_0(t - mT) \cdot \sum_{n=0}^{K} f_n^* h_0^*(t - nT - kT)\, dt \\ &= \sigma_0^2 \sum_{m=0}^{K} f_m f_{m-k}^* . \end{aligned} \tag{7.96}$$

(b)

$$\sigma_k^2 = \sigma_0^2 \sum_{k=0}^{K} |f_k|^2 . \tag{7.97}$$

7-6. The receiver can consider three received symbols at a time. The detection of these symbols goes as follows: For each of 16 possibilities, generate the corresponding set of three tertiary symbols by table lookup. Calculate the Euclidean distance between u_k and these three symbols, in three-dimensional Euclidean space. Choose the four bits corresponding to the minimum Euclidean distance.

7-7. For this case, $S_h(z) = \sigma_k^2$, and hence we get that $A_k^2 = \sigma_k^2$, $G_h(z) = 1$. The criterion of (7.61) becomes

$$\min_{\{a_k,\, 1 \le k \le K\}} \left[\sum_{k=-\infty}^{0} |w_k|^2 + \sum_{k=1}^{K} |w_k - a_k|^2 + \sum_{k=K+1}^{\infty} |w_k|^2 \right] . \tag{7.98}$$

Clearly, the first and third sums do not affect the minimization, and the middle sum is equivalent to figure 7-10.

7-8.

(a) $\mathbf{X} \in M_h$ must be of the form

$$x(t) = \sum_{k=1}^{K} x_k h(t - kT) \tag{7.99}$$

which has energy

$$\|\mathbf{X}\|^2 = \sum_{k=1}^{\infty} \sum_{l=1}^{\infty} x_k x_l^* \rho_h(l - k) . \tag{7.100}$$

If $x(t)$ is input to the filter, the discrete-time output will be

$$w_k = x_k * g_{h,k} = \sum_{m=1}^{K} x_m g_{h,k-m} , \tag{7.101}$$

which has energy

$$\begin{aligned} \sum_{k=1}^{\infty} \Big| \sum_{m=1}^{K} x_m g_{h,k-m} \Big|^2 &= \sum_{k=1}^{\infty} \sum_{m=1}^{K} \sum_{n=1}^{K} x_m x_n^* g_{h,k-m} g_{h,k-n}^* \\ &= \sum_{m=1}^{K} \sum_{n=1}^{K} x_m x_n^* \sum_{k=1}^{\infty} g_{h,k-m} g_{h,k-n}^* = \sum_{m=1}^{K} \sum_{n=1}^{K} x_m x_n^* \rho_h(n-m) . \end{aligned} \tag{7.102}$$

(b) Using the property of the projection that $\mathbf{Y} - \mathbf{Y}_h$ is orthogonal to the subspace M_h.

$$\mathbf{Y} - \mathbf{X}_i = \mathbf{Y} - \mathbf{Y}_k + \mathbf{Y}_k - \mathbf{X}_i \tag{7.103}$$

and $\mathbf{Y} - \mathbf{Y}_k$ is orthogonal to $\mathbf{Y}_k - \mathbf{X}_i$, since the later is a vector in M_k. Hence,

$$\| \mathbf{Y} - \mathbf{X}_i \|^2 = \| \mathbf{Y} - \mathbf{Y}_k \|^2 + \| \mathbf{Y}_k - \mathbf{X}_i \|^2 \tag{7.104}$$

and since $\| \mathbf{Y} - \mathbf{Y}_k \|^2$ is a constant it cannot affect the minimization.

(c) This signal is orthogonal to M_k, and hence the sampled matched filter response to it will be zero.

(d) Since

$$\mathbf{Y} - \mathbf{X}_i = \mathbf{Y} - \mathbf{Y}_k + \mathbf{Y}_k - \mathbf{X}_i \,, \tag{7.105}$$

and further the filter response to $\mathbf{Y} - \mathbf{Y}_k$ is zero, the response to $\mathbf{Y} - \mathbf{X}_i$ is the same as the response to $\mathbf{Y}_k - \mathbf{X}_i$. The latter input is a vector in M_k, and hence

$$\| \mathbf{Y}_k - \mathbf{X}_i \|^2 = \sum_{k=1}^{\infty} | w_{y,k} - w_{i,k} |^2 . \tag{7.106}$$

(e) If the known input signal corresponds to data symbol sequence a_k, the output is $a_k * g_{k,k}$. The minimum-distance receiver calculates the distance between this and w_k, the response of the filter to $y(t)$.

7-9. The allpass filter has transfer function

$$H_{\text{allpass}}(z) = \frac{d^* - z^{-1}}{1 - dz^{-1}} \,, \quad |d| < 1 \,. \tag{7.107}$$

(a) The precursor equalizer filter is

$$\frac{(1 - c^* z)(d^* - z^{-1})}{1 - dz^{-1}} \tag{7.108}$$

and the channel model filter is

$$\frac{d^* - z^{-1}}{(1 - cz^{-1})(1 - dz^{-1})} \,. \tag{7.109}$$

(b) The zero location of the upper-path filter is outside the unit circle, since it is maximum-phase. In order to cancel this zero, the pole of the allpass filter would have to be outside the unit circle, which would make it anti-causal.

(c) The filter transfer function can be expanded in partial fractions as

$$\frac{a}{1 - cz^{-1}} + \frac{b}{1 - dz^{-1}} \tag{7.110}$$

which has impulse response

$$ac^k u_k + bd^k u_k \tag{7.111}$$

where

$$a = \frac{cd^* - 1}{c - d} \,, \quad b = \frac{|d|^2 - d^2}{d - c} \,. \tag{7.112}$$

7-10.

(a) The precursor equalizer filter is

$$\frac{d^* - z^{-1}}{(1 - c^* z)(1 - dz^{-1})} \tag{7.113}$$

and the channel-model filter is

$$\frac{(1 - cz^{-1})(d^* - z^{-1})}{1 - dz^{-1}} \,. \tag{7.114}$$

(b) The pole location of the precursor equalizer filter is outside the unit circle, since it is maximum-phase. In order to cancel this pole, the zero of the allpass filter would have to be outside the unit circle, which is

acceptable because the allpass filter is then causal. The precursor equalizer filter then has transfer function

$$-\frac{z^{-1}}{1-cz^{-1}}, \tag{7.115}$$

which is causal, and the channel-model filter transfer function is $c^* - z^{-1}$.

(c) The filter transfer function can be expanded in partial fractions as

$$A_k^2 \frac{d^* - (cd^* + 1)z^{-1} + cz^{-2}}{1 - dz^{-1}} \tag{7.116}$$

which has impulse response

$$A_k^2(d^* d^k u_k - (cd^* + 1)d^{k-1}u_{k-1} + cd^{k-2}u_{k-2}. \tag{7.117}$$

(d) The impulse response is FIR,

$$c^*\delta_k - \delta_{k-1}. \tag{7.118}$$

7-11.

(a) If the data symbols have magnitude unity, then the minimum distance between them is $d_{\min} = \sqrt{2}$.

(b) $d_{\min}$ is σ_k times the minimum distance between data symbols, and hence $\sqrt{2}\sigma_k$.

(c)

$$d_{\min}^2 = \sigma_k^2 + \sigma_k^2, \; d_{\min} = \sqrt{2}\sigma_k \tag{7.119}$$

(d) The distance is

$$d^2 = |\varepsilon_1|^2 + |\varepsilon_2|^2 + 2\alpha \cdot \mathrm{Re}\{\varepsilon_1 \varepsilon_2^*\}. \tag{7.120}$$

Clearly we want to make the third term as large negative as we can. Since the ε can be have a phase that is any multiple of $\pi/4$, clearly the third term is minimized if ε_1 and ε_2 are antipodal; that is, they have opposite phase. Also, the ε can have magnitude either $\sqrt{2}$ or 2. Thus, there are three cases to consider:

$$d_{\min}^2 = 4 + 4 - 2\alpha \cdot 2 \cdot 2 \tag{7.121}$$

$$d_{\min}^2 = 4 + 2 - 2\alpha \cdot \sqrt{2} \cdot 2 \tag{7.122}$$

$$d_{\min}^2 = 2 + 2 - 2\alpha \cdot \sqrt{2} \cdot \sqrt{2} \tag{7.123}$$

It is easy to verify that the third case is always the smallest for all $0 \le \alpha < 1$, and hence

$$d_{\min} = 2 \cdot \sqrt{1 - \alpha}. \tag{7.124}$$

Note that the minimum distance goes to zero as $\alpha \to 1$.

7-12. Let us bound the energy of $s(t)$ in the interval $[KT, \infty)$,

$$\begin{aligned} \int_{KT}^{\infty} s^2(t)\,dt &= \int_{KT}^{\infty} \left[\sum_{k=0}^{K-1} \sum_{n=1}^{N} A_{k,n} h_n(t - kT) \right]^2 dt \\ &\le \sum_{k=0}^{K-1} \sum_{n=1}^{N} A_{k,n}^2 \int_{KT}^{\infty} h_n^2(t - kT)\,dt \\ &\le \sum_{k=0}^{K-1} \sum_{n=1}^{N} A_{k,n}^2 \frac{\alpha}{(KT - kT)^2}. \end{aligned} \tag{7.125}$$

If the data symbols are drawn from a finite constellation, we can assume that $\sum_{n=1}^{N} A_{k,n}^2$ is bounded, say by C_1. The remaining sum, $\sum_{k=0}^{K-1} 1/(KT - kT)^2$ is also bounded, since the series is convergent, say by C_2. Hence, the energy outside $[0, KT]$ is bounded by a constant $\alpha C_1 C_2$, independent of K, and the fraction of the energy outside $[KT, \infty]$ goes to zero since the energy of $s(t)$ is increasing with K.

CHAPTER 8: SOLUTIONS TO PROBLEMS

8-1.

(a) Writing it as

$$\sqrt{2}f(t)e^{j\omega_c t} = f_a(t) + j\hat{f}_a(t) \ , \tag{8.210}$$

since the analytic bandpass filter impulse response is analytic, the imaginary part $\hat{f}_a(t)$ must be the Hilbert transform of the real part $f_a(t)$.

(b)

$$f_a(t) = \mathrm{Re}\{\sqrt{2}f(t)e^{j\omega_c t}\} = \sqrt{2}\mathrm{Re}\{f(t)\}\cos(\omega_c t) - \sqrt{2}\,\mathrm{Im}\{f(t)\}\sin(\omega_c t) \tag{8.211}$$

$$\hat{f}_a(t) = \mathrm{Im}\{\sqrt{2}f(t)e^{j\omega_c t}\} = \sqrt{2}\mathrm{Re}\{f(t)\}\sin(\omega_c t) + \sqrt{2}\,\mathrm{Im}\{f(t)\}\cos(\omega_c t) \tag{8.212}$$

(c)

$$\mathrm{Var}\{M_R(t)\} = N_0\int_{-\infty}^{\infty} f_a^2(t)\,dt \ , \ \ \mathrm{Var}\{M_I(t)\} = N_0\int_{-\infty}^{\infty} \hat{f}_a^2(t)\,dt \ , \tag{8.213}$$

$$E[M_R(t)M_I(t)] = N_0\int_{-\infty}^{\infty} f_a(t)\hat{f}_a(t)\,dt \ . \tag{8.214}$$

(d) Since $f_a(t)$ and $\hat{f}_a(t)$ have the same energy, the real and imaginary parts of $M(t)$ have equal variance, equal to $N_0\int_{-\infty}^{\infty} f_a^2(t)\,dt$. The energy of $f_a(t)$ and $\hat{f}_a(t)$ are equal since the Hilbert transform is a phase only (allpass) filtering. We need to relate the energy in $f_a(t)$ to the energy in $f(t)$. This follows easily from the relationship

$$2\int_{-\infty}^{\infty} |f(t)|^2\,dt = \int_{-\infty}^{\infty} f_a^2(t)\,dt + \int_{-\infty}^{\infty} \hat{f}_a^2(t)\,dt \ , \tag{8.215}$$

and since the two terms on the right side are equal, we get the power of the complex noise

$$E[M_R^2(t)] = E[M_I^2(t)] = \sigma^2 \ , \ \ E[|M(t)|^2] = 2\sigma^2 \tag{8.216}$$

where

$$\sigma^2 = N_0\int_{-\infty}^{\infty} |f(t)|^2\,dt = \frac{N_0}{2\pi}\int_{-\infty}^{\infty} |F(j\omega)|^2\,d\omega \ . \tag{8.217}$$

This establishes that samples of the real and imaginary parts of the complex noise have equal variance. We can also easily show that they are uncorrelated, and hence independent, since a function and its Hilbert transform are orthogonal. The latter fact follows directly from Parseval's relation,

$$\int_{-\infty}^{\infty} f_a(t)\hat{f}_a(t)\,dt = \frac{1}{2\pi}\int_{-\infty}^{\infty} |F_a(j\omega)|^2(j\,\mathrm{sgn}\omega)\,d\omega = 0 \tag{8.218}$$

since the integrand is an odd function of frequency.

(e) Since the real and imaginary parts of $Z(t)$ are obviously just linear combinations of the real and imaginary parts of $M(t)$, they are also jointly Gaussian. We know that

$$E[M^2] = E[(M^*)^2] = 0 \,, \tag{8.219}$$

and thus

$$E[(\mathrm{Re}\{Z(t)\})^2] = E[(\mathrm{Im}\{Z(t)\})^2] = \sigma^2 \,, \tag{8.220}$$

$$E[\mathrm{Re}\{Z(t)\}\mathrm{Im}\{Z(t)\}] = 0 \,. \tag{8.221}$$

Considering just one case,

$$(\mathrm{Re}\{Z(t)\})^2 = \tfrac{1}{4}\left[M^2(t)e^{-j2\omega_c t} + 2|M(t)|^2 + ((M^*(t))^2 e^{+j2\omega_c t} \right] \tag{8.222}$$

and the result follows immediately since the expectation of the first and third terms is zero. Similarly,

$$\mathrm{Re}\{Z(t)\}\mathrm{Im}\{Z(t)\} = \frac{1}{4j}(M^2(t)e^{-j2\omega_c t} - (M^*(t))^2 e^{+j2\omega_c t}) \tag{8.223}$$

which immediately has zero expected value. The statistics of $Z(t)$ are identical to those of $M(t)$, and the demodulator has no effect on the *statistics* of one sample of the noise.

8-3.

$$Q(2) = 0.027 \qquad Q^2(2) \approx 0.00073 \tag{8.224}$$

The second is much smaller.

$$Q(4) \approx 3.35\times10^{-5} \qquad Q^2(4) \approx 1.12\times10^{-9} \tag{8.225}$$

The approximation in (8.62) is clearly valid for these cases.

8-4. The first probability is $Q(\sqrt{2}/0.5)$ which is roughly 2.6×10^{-3}. The second probability is $Q(2/0.5)$ which is roughly 3.4×10^{-5}, two orders of magnitude lower!

8-5. The probability of error for the four innermost points (which have probability 1/4) is

$$1 - (1 - 2Q(d/2\sigma))(1 - 2Q(d/2\sigma)) = 4Q(d/2\sigma) - 4Q^2(d/2\sigma) \,. \tag{8.226}$$

The probability of error for the eight intermediate points (which have probability 1/2) is

$$1 - (1 - 2Q(d/2\sigma))(1 - Q(d/2\sigma)) = 3Q(d/2\sigma) - 2Q^2(d/2\sigma) \,. \tag{8.227}$$

The probability of error for the eight intermediate points (which have probability 1/2) is

$$1 - (1 - Q(d/2\sigma))(1 - Q(d/2\sigma)) = 2Q(d/2\sigma) - Q^2(d/2\sigma) \,. \tag{8.228}$$

The result follows by adding these weighted by their probabilities.

8-6. Given the transmit power limitation we set

$$\mathrm{E}[|A_k|^2] = \sigma_A^2 = 1 \,. \tag{8.229}$$

The received pulse has Fourier transform

$$P(j\omega) = G(j\omega)B_E(j\omega)F(j\omega) = KG(j\omega) \,, \tag{8.230}$$

where $B_E(j\omega) = 1$ and $F(j\omega) = K\,\mathrm{rect}(\omega, 2\pi/T)$. The baseband equivalent discrete-time channel is

$$P(e^{j\omega T}) = \frac{K}{T}\sum_{m=-\infty}^{\infty} G(j(\omega - \frac{2\pi}{T}m)) = K \,. \tag{8.231}$$

We should select $K = 1$. Then the signal component at the slicer has power $\sigma_A^2 = 1$, and

$$\sigma^2 = 2N_0/T \,. \tag{8.232}$$

The SNR at the slicer is

$$SNR = \frac{\sigma_A^2}{2\sigma^2} = \frac{T}{4N_0} \,. \tag{8.233}$$

Now the probability of error is

$$3Q\left(\frac{\sqrt{T}}{2\sqrt{5N_0}}\right) - 2.25Q^2\left(\frac{\sqrt{T}}{2\sqrt{5N_0}}\right). \tag{8.234}$$

8-7.

(a) A suitable coder works as follows. Take one bit; if it is a one, transmit one of the inner points depending on the next bit. If it is a zero, transmit one of the outer points depending on the next two bits. An example bit mapping (which is a Gray code) is given in the following figure.

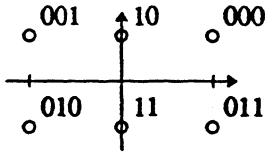

(b) Let C denote a correct decision and E a signal error. Then

$$\Pr[C \mid inner] = (1 - 2Q(b/2\sigma))(1 - Q(b/2\sigma)) \tag{8.235}$$

which implies that

$$\Pr[\text{symbol error} \mid inner] = 3Q(b/2\sigma) - 2Q^2(b/2\sigma). \tag{8.236}$$

Also

$$\Pr[C \mid outer] = (1 - Q(b/2\sigma))^2 \tag{8.237}$$

which implies that

$$\Pr[\text{symbol error} \mid outer] = 2Q(b/2\sigma) - Q^2(b/2\sigma). \tag{8.238}$$

Combining,

$$\begin{aligned}\Pr[\text{symbol error}] &= \tfrac{1}{2}[3Q(b/2\sigma) - 2Q^2(b/2\sigma)] + \tfrac{1}{2}[2Q(b/2\sigma) - Q^2(b/2\sigma)] \\ &= \frac{5}{2}Q(b/2\sigma) - \frac{3}{2}Q^2(b/2\sigma).\end{aligned} \tag{8.239}$$

(c) The power is

$$\begin{aligned}\mathrm{E}[A_k^2] &= \tfrac{1}{2}\left[\frac{d^2}{4}\right] + \tfrac{1}{2}\left[d^2 + \frac{d^2}{4}\right] \\ &= \frac{3}{4}d^2.\end{aligned} \tag{8.240}$$

(d)

$$\Pr[\text{symbol error}] = \frac{5}{2}Q(\sqrt{SNR/3}) - \frac{3}{2}Q^2(\sqrt{SNR/3}). \tag{8.241}$$

If $10\log_{10}(SNR) = 10$ then $SNR = 10$ so

$$\Pr[\text{symbol error}] = \frac{5}{2}Q(\sqrt{10/3}) - \frac{3}{2}Q^2(\sqrt{10/3}) \approx 0.10. \tag{8.242}$$

(e) The approximations are respectively,

$$\Pr[\text{symbol error}] \approx \frac{5}{2}Q(\sqrt{SNR/3}) \qquad \Pr[\text{symbol error}] \approx Q(\sqrt{SNR/3}). \tag{8.243}$$

The values when $SNR = 10dB$ are 0.10 and 0.041 respectively.

8-8.

(a) The decision regions are bounded by the planes formed by pairs of axes.

(b) The probability of error is

$$\Pr[\text{symbol error}] = 1 - (1 - Q(d/2\sigma))^M . \tag{8.244}$$

8-9. Since the distance between symbols is $d = a\sqrt{2}$,

$$\Pr[E_{ij}] = Q(a/\sigma\sqrt{2}) \tag{8.245}$$

so

$$\Pr[\text{symbol error}] = \Pr[\text{symbol error} \mid A_k = a_i] \le (M-1)Q(a/\sigma\sqrt{2}) \tag{8.246}$$

8-10.

(a) There are 4 symbols at distance $d = 2c$, 4 symbols at distance $d = 2\sqrt{2}c$, 2 symbols at distance $d = 4c$, 4 symbols at distance $d = 2\sqrt{5}c$, and 1 symbol at distance $d = 4\sqrt{2}c$, so from the union bound

$$\begin{aligned}\Pr[\text{symbol error} \mid A_k = c + jc] &\le 4Q(c/\sigma) + 4Q(\sqrt{2}c/\sigma) + 2Q(2c/\sigma) \\ &\quad + 4Q(\sqrt{5}c/\sigma) + Q(2\sqrt{2}c/\sigma) \\ &\approx 4Q(c/\sigma) .\end{aligned} \tag{8.247}$$

(b) There are 2 symbols at distance $d = 2$, 2 symbols at distance $d = \sqrt{5}$, 2 symbols at distance $d = 2\sqrt{2}$, 4 symbols at distance $d = \sqrt{17}$, 2 symbols at distance $d = 2\sqrt{5}$, 1 symbol at distance $d = 4\sqrt{2}$, and 2 symbol at distance $d = \sqrt{37}$, so from the union bound

$$\begin{aligned}\Pr[\text{symbol error} \mid A_k = 1 + j] &\le 2Q(1/\sigma) + 2Q(\sqrt{5}/2\sigma) + 2Q(\sqrt{2}/\sigma) + 4Q(\sqrt{17}/2\sigma) \\ &\quad + 2Q(\sqrt{5}/\sigma) + Q(2\sqrt{2}/\sigma) + 2Q(\sqrt{37}/2\sigma) \\ &\approx 2Q(1/\sigma) .\end{aligned} \tag{8.248}$$

(c) The noise components in the directions of the nearest neighbors are not orthogonal, and hence not independent.

(d) The average power in the 16-QAM constellation is $10c^2$ and in the V.29 constellation it is 13.5, so $c = \sqrt{1.35} \approx 1.16$. The approximate probabilities of error are $4Q(1.16/\sigma)$ for 16-QAM and $2Q(1/\sigma)$ for V.29, so assuming the SNR is high enough that the constant multipliers are not important, 16-QAM is about 1.3 dB better. There are good reasons, nonetheless, for using the V.29 constellation. In particular, it is less sensitive to phase jitter.

8-11. Taking a second pulse of the form of (8.113),

$$g(t) = \sum_{m=0}^{N-1} y_k \, h_c(t - mT_c) , \tag{8.249}$$

then the inner product of $h(t)$ and $g(t)$ is

$$\int_{-\infty}^{\infty} h(t) g^*(t) \, dt = \sigma_c^2 \sum_{m=0}^{N-1} x_m \, y_m^* . \tag{8.250}$$

Considering $\{x_m, 0 \le m \le N-1\}$ and $\{x_m, 0 \le m \le N-1\}$ as vectors $\mathbf{x}$ and $\mathbf{y}$ in N-dimensional Euclidean space, then the pulses $h(t0$ and $g(t)$ will be orthogonal when Euclidean vectors $\mathbf{x}$ and $\mathbf{y}$ are orthogonal. The number of pulses specified in this fashion that can be mutually orthogonal is $N = 2BT$, the dimensionality of the Euclidean space.

8-12. For every zero in $H(z)$ at location $z = c$, if $H(z)$ is to be allpass, we must have a pole at location $z = 1/c^*$, as shown in Section 2.5.3. Since FIR filters can only have poles at $z = 0$ or $z = \infty$, an allpass FIR can only have zeros at $z = \infty$ or $z = 0$. A filter with $L \geq 0$ poles at $z = 0$ and L zeros at $z = \infty$ has impulse response δ_{k-L}. If $L < 0$, then the poles are at $z = \infty$ and the zeros are at $z = 0$.

8-13. The received signal is $r(t) = \pm h(t) + J(t)$, and the matched filter output is a random variable

$$U = \int_0^T r(t)h(t)\,dt = \sum_{i=1}^{N}(S_i^2 + S_i J_i) \ . \tag{8.251}$$

(a) The signal component of U is $\sum_{i=1}^{N} S_i^2$ and the noise component is $\sum_{i=1}^{N} S_i J_i$.

(b) The mean-value of the signal is σ_h^2. The variance of the noise conditioned on knowledge of the signal is, since the J_i are independent,

$$\sum_{i=1}^{N} S_i^2 \mathrm{Var}\{J_i\} \ . \tag{8.252}$$

The variance of the noise is the expected value of this conditional variance, which is

$$\sum_{i=1}^{N} E[S_i^2]\mathrm{Var}\{J_i\} = \frac{\sigma_h^2}{N}\sum_{i=1}^{N}\mathrm{Var}\{J_i\} = \frac{\sigma_h^2 E_J}{N} \ . \tag{8.253}$$

The SNR is therefore

$$SNR = \frac{\sigma_h^2}{\sigma_h^2 E_J/N} = N\cdot\frac{\sigma_h^2}{E_J} \ . \tag{8.254}$$

The processing gain is therefore N independent of how the jammer distributes its energy.

8-14. For the passband channel of figure 8-6b the complex-baseband channel has bandwidth $B/2$, and hence the dimensionality of the signal subspace in time T is BT. The received vector C is now complex-valued, and the noise vector is complex-valued where the components are independent, have independent real and imaginary parts, each with variance $\sigma^2 = N_0$ (by circular symmetry of the noise). We can think of C as an $N = 2BT$ dimensional real-valued vector with independent noise components. The signal power constraint now applies directly to the resulting $2BT$-dimensional real-valued signal vector

$$E[\sum_{n=1}^{N} |S_n|^2] = E[\sum_{n=1}^{N} \mathrm{Re}\{S_n\}^2 + \mathrm{Im}\{S_n\}^2] = T P_S \ . \tag{8.255}$$

This establishes the equivalence of the baseband and passband cases.

8-15. From (8.137),

$$B_1\cdot\log_2(1 + SNR_1) = B_2\cdot\log_2(1 + SNR_2) \ , \tag{8.256}$$

or at high SNR,

$$SNR_1^{B_1} \approx SNR_2^{B_2} \ . \tag{8.257}$$

Taking, the logarithm, we can express the SNRs in dB, as

$$10\cdot\log_{10}SNR_1 \approx \frac{B_2}{B_1}\cdot 10\cdot\log_{10}SNR_2 \ . \tag{8.258}$$

Thus, for high SNR, to get the same channel capacity in half the bandwidth, the SNR (in dB) must be doubled, meaning that the SNR (not in dB) must be squared.

8-16. We have $M = 2$, and assuming the signal constellation is ± 1, $\sigma_A^2 = 1$ and $a_{\min} = 2$, and $\gamma_A = 1$. The spectral efficiency is $\nu = (\log_2 2)/BT = 1/BT$, and hence

$$\gamma_{SS} = \frac{2BT\,(1^{1/BT} - 1)}{3} = \frac{2}{3}\cdot BT\cdot(2^{1/BT} - 1) \ . \tag{8.259}$$

Asymptotically, as $BT \to \infty$, $\gamma_{SS} \to \frac{2}{3}\cdot\log_e 2 = 0.46$. Thus, the SNR gap to capacity is asymptotically

increased by $-10\cdot\log_{10}0.46 = 3.35$ dB.

8-17. Assume that the threshold used in the slicer is halfway between the two signal levels, or $(\Gamma_0+\Gamma_1)/2$. Using the results of problem 3-19, for one case the mean is Γ_0 and the threshold is $(\Gamma_0+\Gamma_1)/2$. For the other case, the mean is Γ_1 and the threshold is the same. Hence,

$$P_e < \tfrac{1}{2}\left[\frac{2\Gamma_0}{\Gamma_0+\Gamma_1}\right]^{(\Gamma_0+\Gamma_1)/2} e^{(\Gamma_1-\Gamma_0)/2} + \tfrac{1}{2}\left[\frac{2\Gamma_1}{\Gamma_0+\Gamma_1}\right]^{(\Gamma_0+\Gamma_1)/2} e^{-(\Gamma_1-\Gamma_0)/2}. \tag{8.260}$$

For example, when $\Gamma_0 = 0$ we can't make an error when zero is transmitted, and

$$P_e < \tfrac{1}{2}\left[\frac{2}{e}\right]^{\Gamma_1/2}. \tag{8.261}$$

8-18.

(a) Assuming 20 photons per bit, and interpreting the optical power as the optical power for a received one-bit, the power is

$$20\cdot h\nu\cdot 10^8 = 2.6\cdot 10^{-10} \text{ Watts}, \tag{8.262}$$

or -66 dBmW. The average optical power, assuming equally likely zero and one-bits, would be 3 dB lower.

(b) Assuming that $N(t)$ is the thermal noise voltage across the resistor, which is white with power spectrum $N_0 = 2kT_nR$, and letting $T = 10^{-8}$ be one symbol interval, the variance of the noise at the output of an ideal integrator will be

$$E\left[\int_0^T\int N(t)N(\tau)\,dt\,d\tau\right] = N_0T. \tag{8.263}$$

This is numerically $8\cdot 10^{-24}$ volt^2–sec^2. Similarly, the signal output of the integrator is the total charge per bit times the resistance, or RqN.

(c) If, for a received one-bit, the average current in the resistor is i, the power is i^2R, and we set this 100 times as big as the noise power in bandwidth B, or

$$i^2R = (rP)^2R = \frac{4kT_nRB}{R}\cdot 100 \tag{8.264}$$

where P is the optical power and $r = 1.21$ is the responsivity. Thus, we get the optical power as

$$P = \sqrt{\frac{4kT_nB\cdot 100}{1.21^2R}} = 3.3\cdot 10^{-8} \tag{8.265}$$

or -45 dBmW. This power is 21 dB higher than for part a.

(d) Let the number of photons in one bit time be N, and the average number of photons be $\bar{N}$. The optical power is equal to $\bar{N}h\nu$ times the bit rate (10^8), or $\bar{N} = 2500$.

(e) Similarly, the signal output of the integrator is the total charge per bit times the resistance, or $Rq\bar{N}$, and the variance of this signal is $R^2q^2\mathrm{Var}\{N\} = R^2q^2\bar{N}$, which evaluates to $6.4\cdot 10^{-25}$ volt^2–sec^2. Note that the thermal noise variance at the output of the integrator is 11 dB larger than the signal variance, and even though the error rate is very low, the thermal noise is still the dominant noise source. Of course in practice both of the noise variances, as well as the signal level, would be much larger due to the preamplifier, but this would not change the relative levels.

8-19.

(a) As in problem 8-18, the signal power is

$$P^2 = 10\cdot\frac{4kT_nB}{r^2R} \tag{8.266}$$

which evaluates to $P = 10^{-8}$ Watts, where $r = 1.21$ is the responsivity of the photodetector. This corresponds to -49.8 dBmW power. Let N be a random variable equal to the number of photons arriving during one bit time. Then the average number of photons per bit is

$$\bar{N} = \frac{P\lambda T}{Rc} = 790.6\,, \tag{8.267}$$

where $T = 10^{-8}$ is the baud interval. Now, at the output of the integrate and dump, the signal is shot noise with a random multiplier and with pulse shape

$$h(t) = \begin{cases} qR\,, & 0 \le t \le T \\ 0, & \text{otherwise} \end{cases} \tag{8.268}$$

and constant arrival rate $\bar{N}/T$. The mean of the signal is the convolution of $h(t)$ with the arrival rate, times the average avalanche multiplier, or $\bar{G}qR\bar{N}$. The variance of the signal is the convolution with $h^2(t)$ times $\bar{G}^2$, or

$$\bar{G}^2 q^2 R^2 \bar{N} = F_G \bar{G}^2 q^2 R^2 \bar{N} \tag{8.269}$$

$$F_G = k\bar{G} + (2 - \frac{1}{\bar{G}})(1-k)\,,\ k = 0.03\,. \tag{8.270}$$

Finally, the thermal noise variance at the output of the integrator is $N_0 T = 2kT_n RT$. The SNR is then

$$SNR = \frac{(\bar{G}qR\bar{N})^2}{F_G \bar{G}^2 q^2 R^2 \bar{N} + 2kT_n RT} \tag{8.271}$$

which evaluates to 19.5 (12.9 dB) at $\bar{G} = 1$, and peaks at 317.6 (25 dB) at $\bar{G} = 13$. If we change to $k = 0.97$, the peak SNR is at only $\bar{G} = 4$, and is 123.5 (20.9 dB).

(b) The maximum advantage due to avalanche gain is 12.1 dB for $k = 0.03$.

8-20. At the sampler the desired signal *amplitude* is $\pm 2AB = \pm 2\sqrt{1000}A^2$ while the undesired common term amplitude is $B^2 + A^2 = 1001A^2$. The power of the common term is 24dB stronger.

8-21. The probability of error for OOK if the received power is P when a "one" bit is transmitted is

$$P_e = 0.5e^{-P} \tag{8.272}$$

from (8.162). For homodyne it is bounded by

$$P_e \le 0.5e^{-2P} \tag{8.273}$$

from (8.178), which is at least 3 dB better (half the received power for the same performance).

8-22. For large a, a Poisson random variable with parameter a can be approximated as a Gaussian random variable with mean a and variance a (see Section 3.4). The input to the slicer therefore can be written

$$Q = \pm 2ABT + N \tag{8.274}$$

where each N is a zero mean Gaussian random variable with variance Λ. Assuming large B, $\Lambda \approx B^2 T$. Then an error occurs with probability

$$\begin{aligned} \Pr[error] &= Q(2ABT/\sqrt{\Lambda}) = Q(2A\sqrt{T}) \\ &\le e^{-2A^2T} = e^{-2M}\,, \end{aligned} \tag{8.275}$$

where the inequality follows from the Chernoff bound (3.43).

CHAPTER 9: SOLUTIONS TO PROBLEMS

9-1.

(a) Since $p < \frac{1}{2}$, the ML detector selects $\hat{a} = 0$ if $y = 0$ and $\hat{a} = 1$ if $y = 1$. That is, it chooses $\hat{a} = y$.

(b) An error occurs every time the channel flips a bit, which occurs with probability p.

(c) The posterior probabilities are

$$p_{Y|A}(0|\hat{a})p_A(\hat{a}) = \begin{cases} (1-p)q; & \hat{a}=0 \\ p(1-q); & \hat{a}=1 \end{cases}$$
$$p_{Y|A}(1|\hat{a})p_A(\hat{a}) = \begin{cases} pq; & \hat{a}=0 \\ (1-p)(1-q); & \hat{a}=1 \end{cases} \tag{9.176}$$

Using the numbers supplied we see that the MAP detector always selects $\hat{a} = 0$. An error occurs whenever $a = 1$ is transmitted, which occurs with probability $1 - q = 0.1$. This is lower than the probability of error in part b, which is $p = 0.2$.

(d) The MAP detector will maximize the probability $p_{Y|A}(y|a)p_A(a)$, which is given in the following table:

a	y	$p_{Y\|A}(y\|a)p_A(a)$
1	1	$(1-p)(1-q)$
1	0	$p(1-q)$
0	1	pq
0	0	$(1-p)q$

If we observe $y = 0$, then we will choose $\hat{a} = 0$ if $(1-p)q > p(1-q)$, or $q > p$. If we observe $y = 1$ we will choose $\hat{a} = 1$ if $(1-p)(1-q) > pq$, or $q < 1-p$. Hence we must divide the q axis into three regions as shown below:

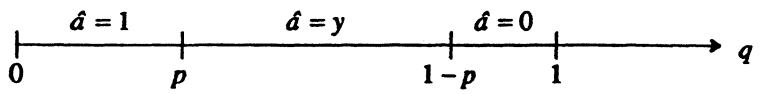

For very small q, the prior probability of $a = 0$ is small, so the MAP detector always chooses $\hat{a} = 1$. Similarly, for large q it always chooses $\hat{a} = 0$. In the mid-range of q, the MAP detector makes the same decision as the ML detector.

(e) The MAP detector will always select $\hat{a} = 0$ if $q > 1 - p$.

9-2. The MAP detector maximizes

$$p_{Y|\hat{s}}(y|\hat{s})p_{\hat{s}}(\hat{s}) = (1-p)^{M - W(\hat{s},y)} \cdot p^{W(\hat{s},y)} p_{\hat{s}}(\hat{s}) \ . \tag{9.177}$$

Taking the logarithm of this expression and discarding the constant term, the MAP detector equivalently minimizes

$$W(\hat{s},y) \log\left[\frac{1-p}{p}\right] - \log p_{\hat{s}}(\hat{s}) \ . \tag{9.178}$$

9-3. The values for $f_Y(y|\hat{x})p_X(\hat{x})$ are shown below for each possible $\hat{x}$ as a function of the observation y.

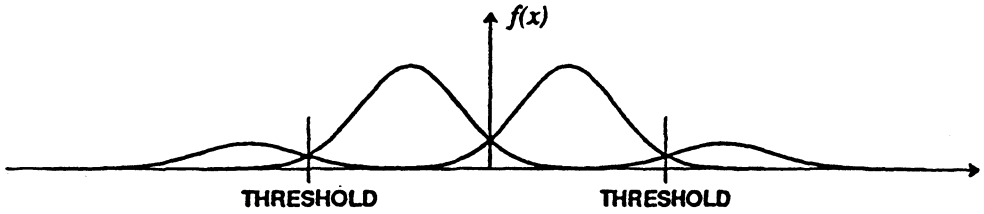

The decision regions are determined by three thresholds, the middle of which is zero. The other two can be found by finding the observation at which the receiver is indifferent between a decision +3 and a decision +1. That is the point y satisfying

$$|y-3|^2 - 2\sigma^2\ln(0.1) = |y-1|^2 - 2\sigma^2\ln(0.4). \tag{9.179}$$

Solving this yields

$$y = 2 + \tfrac{1}{2}\sigma^2\ln(4). \tag{9.180}$$

The thresholds are therefore at $\pm(2 + \frac{1}{2}\sigma^2\ln(4))$. If $\sigma^2 = 0.25$ the thresholds are at ± 2.17, so an observation of 2.1 yields a decision $\hat{x} = 1$.

9-4. Using techniques similar to those in problem 9-3, the final answer is

$$\frac{x_1+x_2}{2} + \frac{\sigma^2}{x_1-x_2}\ln\left[\frac{p_X(x_2)}{p_X(x_1)}\right]. \tag{9.181}$$

9-5.

(a)

$$\mathbf{s}_1 = [1,0,0],\ \mathbf{s}_2 = [0,1,0],\ \mathbf{s}_3 = [0,0,1]. \tag{9.182}$$

(b)

$$\mathbf{s}_1 = [100],\ \mathbf{s}_2 = [010],\ \mathbf{s}_3 = [001]. \tag{9.183}$$

(c)

$$\Pr[\text{ error } |\mathbf{s}_i \text{ transmitted }] \le 3Q(\sqrt{2}/2\sigma) \tag{9.184}$$

$$\Pr[\text{ error } |\mathbf{s}_i \text{ transmitted }] \le 3Q(2,p). \tag{9.185}$$

Note that in both cases $\Pr[\text{ error } |\mathbf{s}_i \text{ transmitted }]$ is independent of i, so

$$\Pr[\text{ error }] \le 3Q(\sqrt{2}/2\sigma) \tag{9.186}$$

$$\Pr[\text{ error }] \le 3Q(2,p). \tag{9.187}$$

9-6. The likelihood to be maximized is

$$L = f_{X_1,\ldots,X_N|\sigma^2}(x_1,\cdots,x_N|\hat{\sigma}^2)$$
$$= \left[\frac{1}{\hat{\sigma}\sqrt{2\pi}}\right]^N e^{-x_1^2/2\hat{\sigma}^2} e^{-x_2^2/2\hat{\sigma}^2}\cdots e^{-x_N^2/2\hat{\sigma}^2},$$

from independence. This can be rewritten

$$L = \left[\frac{1}{\hat{\sigma}\sqrt{2\pi}}\right]^N e^{-(x_1^2+\cdots+x_N^2)/2\hat{\sigma}^2}.$$

Taking the derivative with respect to $\hat{\sigma}$ we get

$$\frac{\partial L}{\partial \hat{\sigma}} = \left[\frac{1}{\hat{\sigma}\sqrt{2\pi}}\right]^N e^{-(x_1^2+\cdots+x_N^2)/2\hat{\sigma}^2}\left[\frac{1}{\hat{\sigma}^3}(x_1^2+\cdots+x_N^2)-\frac{N}{\hat{\sigma}}\right],$$

which is zero only when

$$\hat{\sigma}^2 = \frac{(x_1^2+\cdots+x_N^2)}{N}.$$

Thus, the ML estimator for the variance is the average of the squares of the observations.

9-7. By symmetry, we can condition the probability of error on any of the signals transmitted, and the result will be the same as the un-conditioned error probability. Hence assume that (1,1) is transmitted, in which case the error probability is

$$P_e = \Pr\{N_1 > 1\} + \Pr\{N_2 > 1\} - \Pr\{N_1 > 1, N_2 > 1\} = 2Q(\tfrac{1}{\sigma}) - Q^2(\tfrac{1}{\sigma}). \tag{9.188}$$

9-8.

(a) By symmetry, is clear that the error probability is the same whether (000000) or (111111) is transmitted, and similarly for (111000) or (000111). If (000000) is transmitted, a detection error occurs whenever two out of the first three bits are in error, or two out of the last three bits, or both. If there is one channel error, no detection error is ever made, and this occurs with probability $(1-p)^6$. If there are two channel errors, if one is in the first three bits and the other is in the second three bits, no error is made, and this occurs with probability $(3p(1-p)^2)^2$. However, if both errors are in the first three or second three bits, there is an error. If there are three channel errors, there must always be two errors in either the first three or the second three bits, and there is therefore always a detection error. Similarly, four or more channel errors will always result in a detection error. Thus,

$$P_e = 1 - [(1-p)^6 + 6p(1-p)^5 + (3p(1-p)^2)^2]. \tag{9.189}$$

It is easy to verify that when (111000) is transmitted, the error probability is the same.

(b) Since the minimum Hamming distance is three, the approximate error probability is

$$P_e \approx 2Q(1,p) = 2[3^2(1-p)+p^3]. \tag{9.190}$$

When $p = 0.1$, the error probability evaluates to $P_e = 0.05522$ and the approximation is 0.056.

9-9.

(a) In this case, $L = 1$ and $\|\mathbf{h}\|^2 = 1.25$, so the threshold test can be implemented as a slicer, and the system can be simplified as shown in figure 9-27.

(b) The probability of error of the discrete-time matched filter detector can be found using the techniques of Section 7.2. Using the vector model, there are two possible transmit vectors in problem 9-9, $\mathbf{s}_1 = [1,0.5]$ and $\mathbf{s}_2 = [0,0]$. The probability of error is

$$P_e = Q(d/2\sigma) = Q(\sqrt{1.25}/2\sigma). \tag{9.191}$$

If $\mathbf{s}_1$ and $\mathbf{s}_2$ are equally likely, the ML receiver is the MAP receiver, and this is the minimum probability of

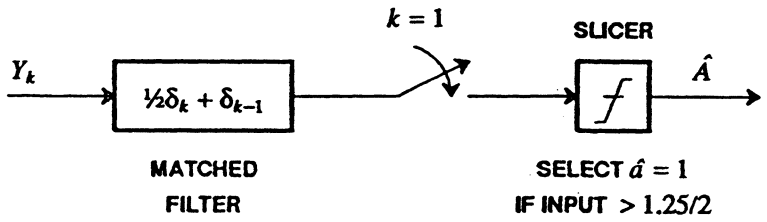

Figure 9-27. A representation of the receiver where the threshold test is represented as a slicer.

error.

9-10.

(a) The only difference from problem 9-9 is that the matched filter has causal impulse response

$$h_{M-k} = 0.1\delta_k - 0.5\delta_{k-1} + \delta_{k-2} \tag{9.192}$$

and the output is sampled at $k = 2$. The equivalent slicer threshold is at 1.26/2.

(b) The probability of error is

$$Q\left[\frac{\sqrt{1.26}}{2\sigma}\right] . \tag{9.193}$$

(c) The receiver is shown below:

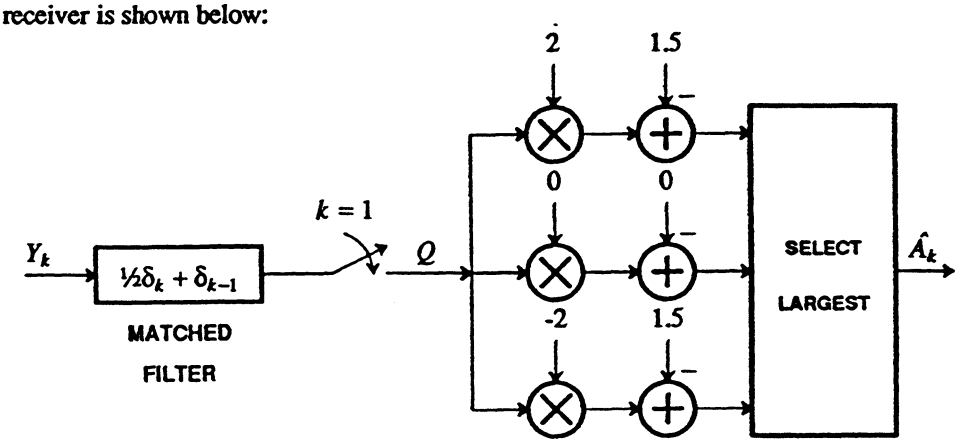

The receiver selects $\hat{a} = +1$ if $2q - 1.5 > 0$ and $2q - 1.5 > -2q - 1.5$, where q is the sampled output of the matched filter. These conditions together are $q > 0.75$. Similarly, the receiver selects $\hat{a} = -1$ is $q < -0.75$, and selects $\hat{a} = 0$ otherwise. Hence the slicer thresholds are at ± 0.75 as expected.

9-11.

(a) We have

$$\tilde{s}_1(t) = 0 \quad \tilde{s}_2(t) = h(t) \tag{9.194}$$

$$\|\tilde{S}_1\|^2 = 0 \quad \|\tilde{S}_2\|^2 = \rho_h(0) . \tag{9.195}$$

Defining

$$K_1 = 0, \quad K_2 = \left| \int_{-\infty}^{\infty} Y(t) e^{-j\omega_c t} h^*(t)\, dt \right| , \tag{9.196}$$

the ML detector chooses $\tilde{S}_1$ if

$$I_0\left(\frac{K_1}{\sigma^2}\right) = I_0(0) = 1 \; > \; e^{-\frac{\rho_h(0)}{2\sigma^2}} I_0\left(\frac{K_2}{\sigma^2}\right) . \tag{9.197}$$

Taking the logarithm of both sides will not change the inequality, so we get equivalently

$$\ln I_0\left(\frac{K_2}{\sigma^2}\right) < \frac{\rho_h(0)}{2\sigma^2} . \tag{9.198}$$

In view of the monotonicity of $\ln I_0(\cdot)$, the ML detector compares K_2 to some threshold v, where that threshold depends on the SNR. The receiver is the same as a passband PAM coherent receiver, consisting of a demodulator, matched filter, and sampler. The difference is that instead of comparing the complex-valued slicer input to the transmitted data symbols, we only evaluate the magnitude of this input (distance from the origin) and compare in effect to the magnitude of the data symbols.

(b) The data symbols must all have distinct radii in the signal constellation. Thus, for example, PSK would not work, but the ASK of this problem will work.

(c) When signal one is transmitted,

$$K_2 = |\langle Z, \tilde{S}_2 \rangle| \ , \tag{9.199}$$

where of course $\tilde{S}_2 = H$, the PAM pulse shape. The error probability in this case is

$$\Pr\{\text{error} \mid \tilde{S}_1 \text{ transmitted}\} = \Pr\{K_2 > v\} \ . \tag{9.200}$$

Similarly when signal two is transmitted,

$$K_2 = |e^{j\theta}\|\tilde{S}_2\|^2 + \langle Z, \tilde{S}_2 \rangle| \tag{9.201}$$

and the probability of error is

$$\Pr\{\text{error} \mid \tilde{S}_2 \text{ transmitted}\} = \Pr\{K_2 < v\} \ . \tag{9.202}$$

The get the overall probability of error we sum these two probabilities weighted by the prior probabilities of the two signals.

9-12.

(a) With respect to the signal, an isolated pulse before sampling has Fourier transform $H(j\omega)F^*(j\omega)$, and hence after sampling the discrete-time Fourier transform is

$$\frac{1}{T}\sum_m H(j(\omega + m\frac{2\pi}{T}))F^*(j(\omega + m\frac{2\pi}{T})) \ . \tag{9.203}$$

Note that the impulse response of the equivalent discrete-time channel is equivalent to the sampled isolated pulse response. Similarly, for the noise, after demodulation the noise has power spectrum $S_N(\omega + \omega_c)$, and at the output of the matched filter, before sampling, $2S_N(\omega + \omega_c)|F(j\omega)|^2$. After sampling, the spectrum is

$$\frac{2}{T}\sum_m S_N(\omega + \omega_c + m\frac{2\pi}{T})|F(j(\omega + m\frac{2\pi}{T}))|^2 \ . \tag{9.204}$$

(b) The discrete-time isolated pulse has Fourier transform

$$\frac{1}{T}\sum_m \frac{|H(j(\omega + m\frac{2\pi}{T}))|^2}{S_N(\omega + \omega_c + m\frac{2\pi}{T})} \ , \tag{9.205}$$

and the discrete-time noise has a power spectrum which is the same formula multiplied by two.

(c) When $S_N(\omega) = N_0$, the isolated pulse response is $S_h(e^{j\omega T})/N_0$ and the noise power spectrum is $2S_h(e^{j\omega T})/N_0$. If we scale the signal size by N_0, the noise spectrum is scaled by N_0^2, and we get the same answer as in the text.

9-13. Doing a factorization of the folded spectrum,

$$S_h(z) = A_h^2 \cdot G(z)G^*(1/z^*) \tag{9.206}$$

for some constant A_h^2. Assume that the received pulse is of the form

$$h(t) = \sum_{m=-\infty}^{\infty} h_m g(t - mT) \tag{9.207}$$

for some pulse $g(t)$ for which $g(t)$ and $g(t - mT)$ are mutually orthogonal for $m \neq 0$ (for example, "sinc" pulses in the case of zero excess bandwidth). Then,

$$\rho_h(z) = \int_{-\infty}^{\infty} \sum_{m=-\infty}^{\infty} h_m g(t - mT) \sum_{l=-\infty}^{\infty} h_l^* g^*(t - lT - kT) \tag{9.208}$$

and after minor manipulation,

$$\rho_h(k) = \rho_g(0) \sum_{m=-\infty}^{\infty} h_m h_{m-k}^* \ . \tag{9.209}$$

Taking the Z-transform, we get

$$S_k(z) = \rho_g(0)H(z)H^*(1/z^*) . \tag{9.210}$$

Comparing (9.206) and (9.210), we conclude that

$$H(z) = \sqrt{\frac{K}{\rho_g(0)}}G(z) \tag{9.211}$$

will suffice, or $h_k = g_k$ within a constant.

9-14. The conditional probability density is

$$p(x_1 \cdots x_N \mid s_1 \cdots s_N) = \prod_{k=1}^{N} e^{-\alpha s_k} \frac{(\alpha s_k)^{x_k}}{x_k!} \tag{9.212}$$

and hence the log-likelihood function is

$$-\log_e p(x_1 \cdots x_N \mid s_1 \cdots s_N) = \sum_{k=1}^{N} (\alpha s_k - x_k \log_e \alpha s_k + \log_e x_k!) . \tag{9.213}$$

The last term is independent of the signal, as is the $x_k \log_e \alpha$ term, so the simplified branch metric is $(\alpha s_k - x_k \log_e s_k)$.

9-15. The log-likelihood function is given by the following table, where the last column specifies the branch metric:

x	y	$\Pr\{y \mid x\}$	$-\log \Pr\{y \mid x\}$
0	0	$1-p$	$-\log(1-p)$
0	1	p	$-\log(p)$
1	2	0	$-\infty$
1	0	0	$-\infty$
1	1	p	$-\log(p)$
1	2	$1-p$	$-\log(1-p)$

9-16.

(a) The ML detector can operate independently on each observation. It will perform a threshold test with the threshold set at 0.5. The decision is $\hat{x}_k = \{1,1,1,0\}$.

(b) The outputs associated with each transition are shown in figure 9-17. We can find the transition weights by just subtracting those outputs from the observations and squaring. The result is shown in the following figure.

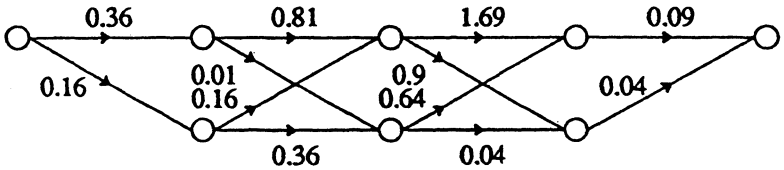

Performing the Viterbi algorithm, the surviving paths and their path metrics after each observation are shown in the following figure.

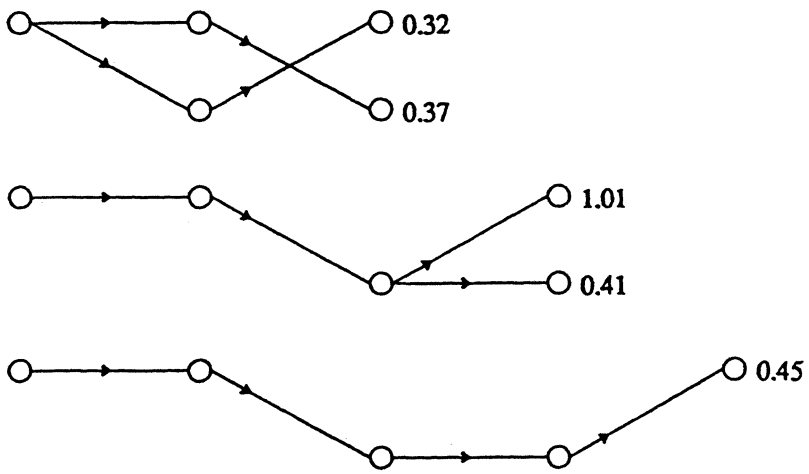

The decision is $\hat{x}_k = \{0,1,1,0\}$, which is different from the decision in part (a). The knowledge of the ISI is useful.

9-17.

(a) The probability of error in the comparable system free of ISI is $Q(1/2\sigma')$, where σ'^2 is the noise in this system. The two systems have the same probability of error when

$$\frac{\sqrt{1.25}}{2\sigma} = \frac{1}{2\sigma'}, \tag{9.214}$$

or $\sigma' = 0.8944\sigma$. This implies that σ' is about 1 dB smaller than σ, so the system with ISI has about 1 dB more noise margin than the system without ISI.

(b) In example 9-25, S_k takes on the values 0.0, 0.5, 1.0 and 1.5 with equal probability. So its power is

$$E[|S_k|^2] = 0.8750. \tag{9.215}$$

The power in the modified system in part (a) is

$$E[|S'_k|^2] = 0.5. \tag{9.216}$$

So let $K = \sqrt{\frac{0.8750}{0.5}} = 1.32$.

(c) The probability of error in the new normalized system is

$$Q(1.32/2\sigma') \tag{9.217}$$

which will be the same as the probability of error in the ISI system when

$$\frac{1.32}{2\sigma'} = \frac{\sqrt{1.25}}{2\sigma} \tag{9.218}$$

or $\sigma' = 1.183\sigma$. The new normalized system has about 1.46 dB better noise margin than the system with ISI.

9-18.

(a) The shift register model and state transition diagram are shown in the following figure:

(a)

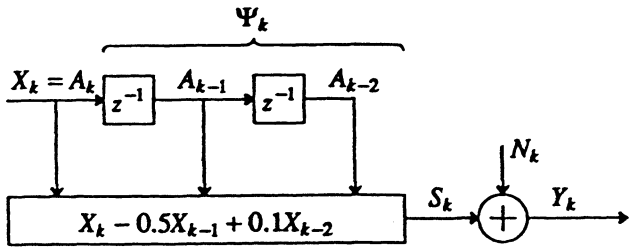

(b)

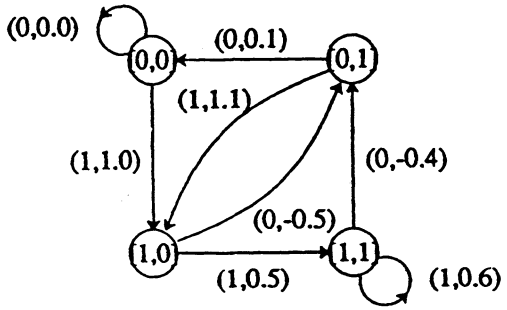

(b) The trellis is shown in the following figure:

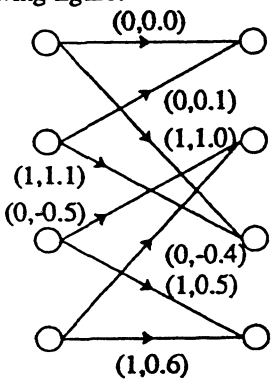

(c)

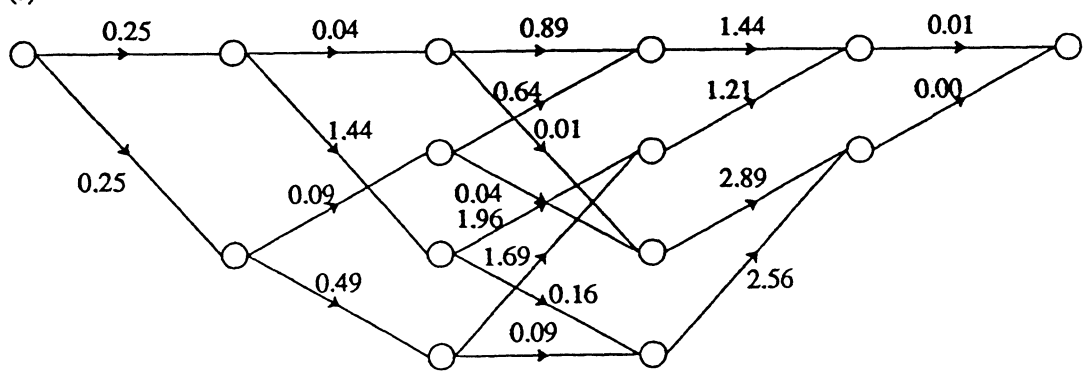

(d)

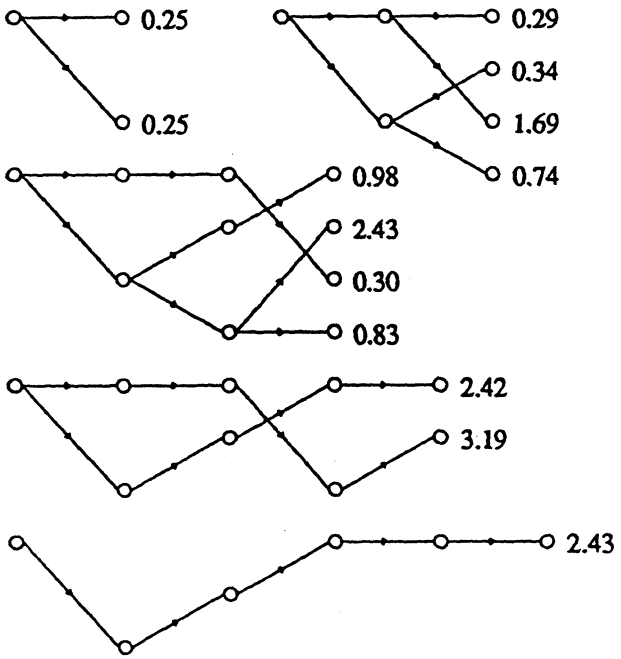

(e)

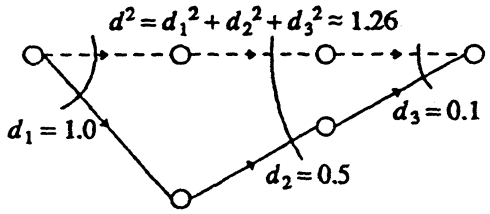

9-19.

(a) The state is $(\varepsilon_{k-1}, \varepsilon_{k-2})$, and the branch metric is

$$|\varepsilon_k + g_1\varepsilon_{k-1} + g_2\varepsilon_{k-2}|^2 . \tag{9.219}$$

The trellis diagram, not labeled with the branch metrics, is shown below:

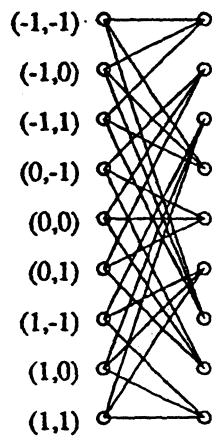

(b) A finite set of error events which do not pass through the same state or its negative twice is shown below:

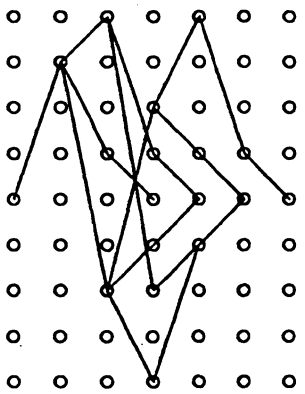

(c) Shown below are the single-error error event, and another error event corresponding to two symbol errors:

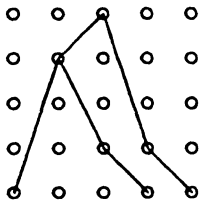

The shorter path has path metric (distance-squared) $(1 + g_1^2 + g_2^2)$ while the longer path has metric

$$1 + (1 + g_1)^2 + (g_1 + g_2)^2 + g_2^2 \tag{9.220}$$

and hence will have a smaller metric if $g_1 \approx 1$ and $g_2 \approx -g_1$. For example, if $g_1 = 1$ and $g_2 = -1$, the minimum distance is $\sqrt{2}$.

9-20.

The metric in this case is $(\varepsilon_k + d\varepsilon_{k-1} + d\varepsilon_{k-2})^2$, and the trellis diagram is pictured in figure 9-28. A set of five paths guaranteed to include the minimum distance path is pictured in figure 9-29. The path metrics for these paths are:

$$\text{Path 1: } 1 + (1 + d)^2 + 4d^2 + d^2 \quad \text{Path 2: } 1 + (1 + d)^2 + (1 - 2d)^2 + d^2 \tag{9.221}$$

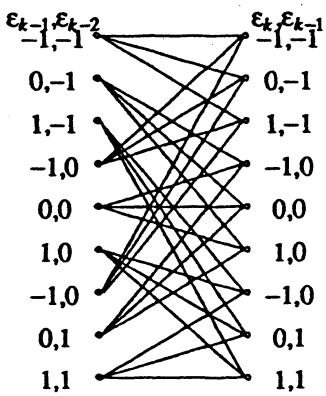

Figure 9-28. Trellis diagram for a four-state ISI channel.

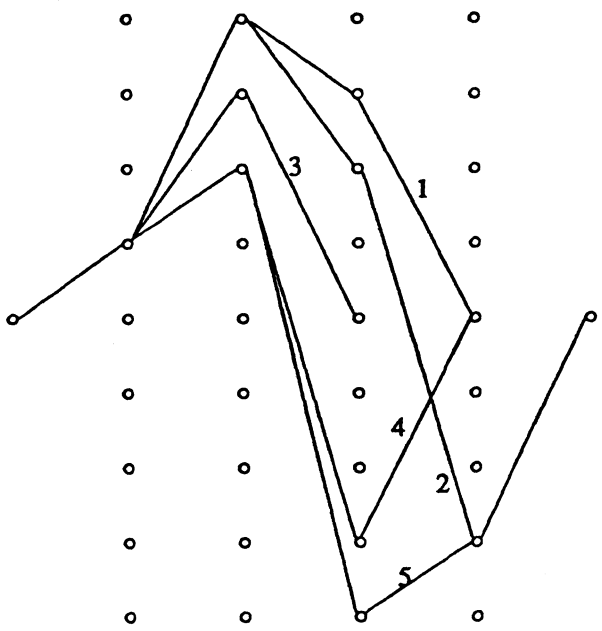

Figure 9-29. A set of candidate minimum-distance paths for the trellis of figure 9-28.

$$\text{Path 3: } 1+d^2+d^2 \quad \text{Path 4: } 1+(1-d)^2+d^2 \quad \text{Path 5: } 1+(1-d)^2+1+4d^2+d^2 \tag{9.222}$$

The metric for paths 1 and 2 are always bigger than path 3, and similarly the metric for path 5 is always bigger than path 4. When $0 \le d \le \frac{1}{2}$, the path 3 metric is smaller than path 4. Thus, the answer is

$$g_{\min}^2 = \begin{cases} 1+2d^2, & 0 \le d \le \frac{1}{2} \\ 1+d^2+(1-d)^2, & \frac{1}{2} \le d \le 1 \end{cases} . \tag{9.223}$$

9-21. The trellis diagram and the two error events at a minimum distance $\sqrt{2}$ are shown in figure 9-30. As in example 9-38, there is an infinite set of error events at this minimum distance, where the only difference is that each error event corresponds to a sequence of alternating data symbols. The error probability estimates are the same. The intuitive explanation is that the output of the channel is zero during sequences of alternating data symbols. It is therefore difficult to distinguish the two sequences of alternating symbols which are the complement of each other.

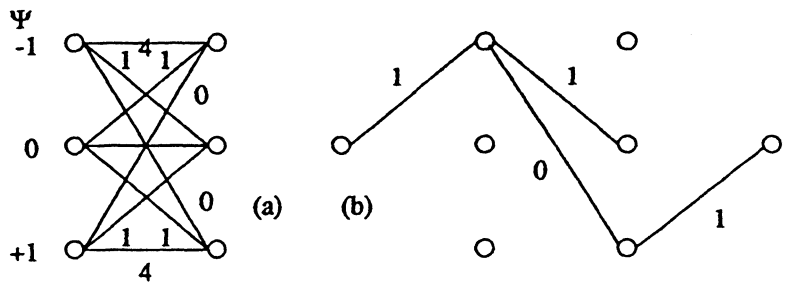

Figure 9-30. A trellis diagram and two corresponding events at the minimum distance of $\sqrt{2}$.

9-22.

(a) The logarithm of the moment generation function is, from (3.137),

$$\Psi_i(v) = \int (\lambda_i(t) + \lambda_{dark})\left[e^{vf(-t)} - 1\right] dt \tag{9.224}$$

and hence the Chernov bound is

$$P_e \le \exp\left\{ \tfrac{1}{2}\left(\int (\lambda_1(t) + \lambda_{dark})[e^{vf(-t)} - 1] + (\lambda_2(t) + \lambda_{dark})[e^{-vf(-t)} - 1]\right) dt \right\}. \tag{9.225}$$

(b) By the method of variations, we substitute $f + \varepsilon \Delta f$ for f, differentiate w.r.t. ε, set $\varepsilon = 0$, and set the result to zero. The result is

$$f(-t) = \frac{\log(\lambda_2(t) + \lambda_{dark}) - \log(\lambda_1(t) + \lambda_{dark})}{2}, \tag{9.226}$$

which says that we correlate the shot noise against the logarithm of the known intensity.

(c) Substituting into the Chernov bound from b., we get

$$P_e \le \exp\left\{ \int (\lambda_1(t) + \lambda_{dark})^{1/2} (\lambda_2(t) + \lambda_{dark})^{1/2} dt - \frac{E_1 + E_2}{2} \right\} \tag{9.227}$$

where E_i is the energy corresponding to the intensity,

$$E_i = \int (\lambda_i(t) + \lambda_{dark})\, dt. \tag{9.228}$$

9-23. First equate the two representations of $f_l(t)$, (9.116) and (9.48),

$$f_l(t) = \sum_{k=1}^{N} F_{l,k}\, \psi_k(t) = \sum_{i=1}^{\infty} \frac{s_{l,i}}{\sigma_i} \phi_i(t). \tag{9.229}$$

Now form the inner product of both sides with $\phi_m(t)$,

$$\sum_{k=1}^{N} F_{l,k} \int_0^T \psi_k(t)\, \phi_m^*(t)\, dt = \sum_{i=1}^{\infty} \frac{s_{l,i}}{\sigma_i} \int_0^T \phi_i(t)\, \phi_m^*(t)\, dt \tag{9.230}$$

and applying (9.118) we get

$$\sum_k F_{l,k}\, \psi_{k,m} = \frac{s_{l,m}}{\sigma_m}. \tag{9.231}$$

Finally, substituting (9.231) into (9.46),

$$\begin{aligned} V_l &= \sum_{i=1}^{\infty} Y_i \cdot \frac{s_{l,i}^*}{\sigma_i^2} \\ &= \sum_{i=1}^{\infty} \frac{Y_i}{\sigma_i} \sum_{k=1}^{N} F_{l,k}\, \psi_{k,i}^* = \sum_{k=1}^{N} F_{l,k}^* \sum_{i=1}^{\infty} \frac{Y_i}{\sigma_i} \cdot \psi_{k,i}^* \\ &= \sum_{k=1}^{N} f_{l,k}^*\, U_k. \end{aligned} \tag{9.232}$$

CHAPTER 10: SOLUTIONS TO PROBLEMS

10-1. The trellis and three error events are sketched below:

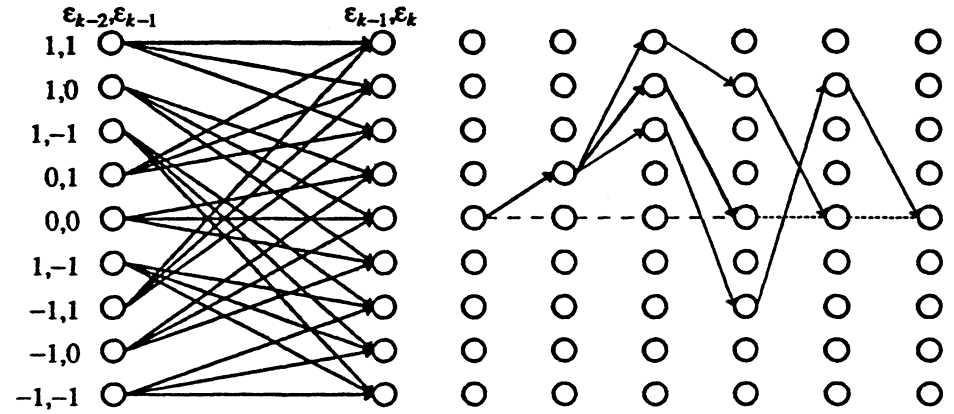

The error event with the dark lines is the one requested in (b), and the two events in light lines are those requested in (c). (The answer to (c) is not unique.)

10-2. Let J be the order of the FIR filter $G_h(z)$. We will show that the inequality (10.27) is strict for every error event. To do this, we need to show that at least one of the terms thrown away ($m \geq 2$) is non-zero, for any error event. Assume L is the length of a given error event ($\varepsilon_L \neq 0$ and $\varepsilon_k = 0$ for $k > L$), and consider the $m = J+L$ term,

$$\left| \sum_{k=1}^{L} \varepsilon_k g_{hJ+L-k} \right|^2 = |\varepsilon_L g_{hJ}|^2 > 0 . \tag{10.187}$$

Thus, the inequality is strict for each and every error event, which implies that it is strict for the minimum-distance error event.

10-3. Since

$$|H|^{-2} = (1 - cz^{-1})(1 - c^* z) , \tag{10.188}$$

the coefficient of z^0 is $1 + |c|^2$ independent of whether the channel is minimum-phase or maximum-phase. For $|c| < 1$, the geometric mean is clearly unity, since (10.188) is in the form of a minimum-phase spectral factorization. When $|c| > 1$, we can write (10.188) in the form

$$|H|^{-2} = |c|^2 (1 - (c^*)^{-1} z^{-1})(1 - c^{-1} z) , \tag{10.189}$$

and thus the geometric mean is $|c|^2$.

10-4.

(a) $(1 - cz^{-1})$

(b)

$$\varepsilon^2_{\text{LE-ZF}} = A_z^2 < |H|^{-2} >_A = A_z^2 (1 + |c|^2) \tag{10.190}$$

from problem 10-3.

(c) When $c = 0$ there is no noise enhancement. As $|c| \to 1$ the noise enhancement approaches 3 dB. For $|c| > 1$ the noise enhancement gets even larger because the channel transfer function gets smaller.

(d) The maximum-phase case will not arise in practice, because the channel impulse response would be both IIR and anticausal.

10-5. For the minimum-phase case, multiply the transfer function by $\sqrt{1-|c|^2}$ to normalize it, and thus

$$\mathcal{E}^2_{\text{LE-ZF}} = A_x^2 \cdot \frac{1+|c|^2}{1-|c|^2} . \tag{10.191}$$

For the maximum-phase case, the normalization constant can be determined by

$$H(z) = \frac{z}{c\,(1-c^{-1}z)} = \frac{1}{c}\sum_{k=0}^{\infty} c^{-k} z^{k+1} , \tag{10.192}$$

and the energy is $1/(|c|^2-1)$ so that the normalization constant becomes $\sqrt{|c|^2-1}$, and

$$\mathcal{E}^2_{\text{LE-ZF}} = A_x^2 \cdot \frac{|c|^2+1}{|c|^2-1} . \tag{10.193}$$

The solution is quite different from problem 10-4, since the noise enhancement approaches infinity as $|c| \to 1$ and goes away as $|c|$ gets large. This is to be expected, since as $|c| \to 1$ the channel transfer function on the unit circle goes to zero at all frequencies except the pole location, and as $|c|$ gets large the channel approaches a negative unit delay, which is easily equalized without noise enhancement by a unit delay.

10-6.

(a) From problem 10-3, the geometric mean is unity and hence $\mathcal{E}^2_{\text{DFE-ZF}} = A_x^2$. No precursor equalizer is required, and the postcursor equalizer is

$$H(z) - 1 = \frac{cz^{-1}}{1-cz^{-1}} . \tag{10.194}$$

(b) From problem 10-3, the geometric mean is $|c|^2$, and hence $\mathcal{E}^2_{\text{DFE-ZF}} = A_x^2 |c|^2$. Writing H in monic form,

$$H(z) = \frac{-c^{-1}z}{1-c^{-1}z} \tag{10.195}$$

we get $r = 1$, $H_0 = -c^{-1}$, and $H_{\max} = 1/(1-c^{-1}z)$. The precursor equalizer is

$$C(z)E(z) = -c\frac{1-(c^*)^{-1}z^{-1}}{1-c^{-1}z} \tag{10.196}$$

and the postcursor equalizer is $E(z) - 1 = -(c^*)^{-1}z^{-1}$

(c) In the maximum-phase case the precursor equalizer is IIR and anticausal, and hence not practical to implement. However, the MSE gets smaller because the equalizer utilizes the large delayed sample for decision making. The MSE of the LE-ZF is always larger than the LE-ZF, by a factor of $1 + |c|^2$ for $|c| < 1$ and by a factor of $(1 + |c|^2)/|c|^2$ for $|c| > 1$. This difference is largest (about 3 dB) in the region of $|c| \approx 1$.

10-7. In the minimum-phase case the normalization constant is $\sqrt{1-|c|^2}$, and

$$\mathcal{E}^2_{\text{DFE-ZF}} = \frac{A_x^2}{1-|c|^2} . \tag{10.197}$$

In the maximum-phase case the normalization constant is $\sqrt{|c|^2-1}$ and

$$\mathcal{E}^2_{\text{DFE-ZF}} = A_x^2 \cdot \frac{|c|^2}{|c|^2-1} . \tag{10.198}$$

As for the LE-ZF, the MSE blows up as the pole approaches the unit circle. The DFE-ZF can tolerate zeros on the unit circle, but not poles. Likewise, the noise enhancement goes away as $|c| \to \infty$ because the equalizer bases its decision on the larger delayed sample, which is asymptotically unity in the normalized case.

10-8. The formula for the MSE follow readily. The spectral factorization of (10.81) approaches, as $S_Z \to 0$,

$$S_Y \to S_A HH^* \tag{10.199}$$

$$S_Y \to |H_0|^2 A_a^2 G_a G_a^* H_{min} H_{max}^* H_{min}^* H_{max} \tag{10.200}$$

$$A_y^2 \to |H_0|^2 \sigma_A^2 \tag{10.201}$$

$$G_y \to G_a H_{min} H_{max}^* \tag{10.202}$$

and finally

$$CE \to \frac{1}{H_0} \frac{H_{max}^*}{H_{max}} \cdot G_z^{-1} \tag{10.203}$$

which is the DFE-ZF precursor equalizer.

10-9.

(a) When the excess bandwidth is less than 200%, we get the following picture:

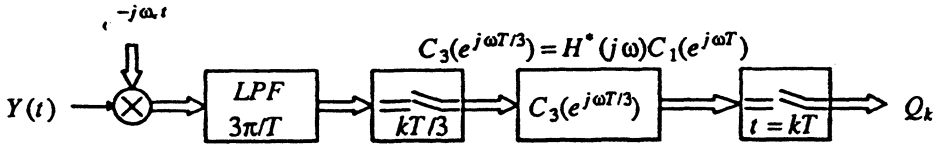

(b)

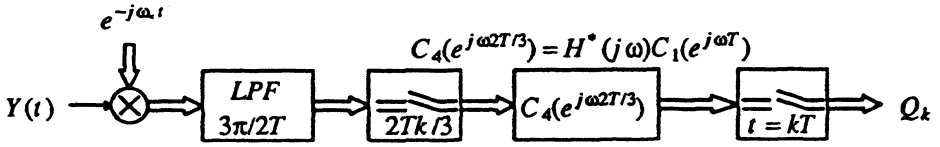

10-10. The picture is as follows:

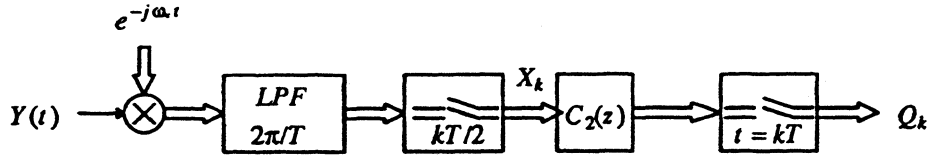

The output is

$$Q_k = \sum_{m=-\infty}^{\infty} c_m X_{2k-m} \,. \tag{10.204}$$

10-11. Given a baseband transmit spectrum S_X, the transmit power constraint of (10.114) is

$$\frac{P_S}{2} = |F| \cdot \langle S_X \rangle_{A,F} \,, \tag{10.205}$$

where $S_x = L - S_N/|H|^2$ for $f \in F$, and hence we get a relation for L,

$$\frac{P_S}{2} = |F| \cdot (L - \langle S_N/|H|^2 \rangle_{A,F}) \,. \tag{10.206}$$

Substituting this into (10.112), if the integral is restricted to $f \in F$,

$$2^{C/|F|} = \langle 1 + S_X |H|^2/S_N \rangle_{G,F} = \frac{L}{\langle S_N/|H|^2 \rangle_{G,F}}$$
$$= \frac{P_S/2 \cdot |F| + \langle S_N/|H|^2 \rangle_{A,F}}{\langle S_N/|H|^2 \rangle_{G,F}}. \tag{10.207}$$

Finally,

$$C = |F| \cdot \log_2 \left[\frac{P_S/2 \cdot |F| + \langle S_N/|H|^2 \rangle_{A,F}}{\langle S_N/|H|^2 \rangle_{G,F}} \right]. \tag{10.209}$$

10-12. The pulse at the output of the receive filter has Fourier transform $T \cdot G(j2\pi f)H(j2\pi f)F(j2\pi f)$ and the noise has power spectrum $T \cdot S_N(j2\pi f)|F(j2\pi f)|^2$. After sampling, the isolated pulse has Fourier transform

$$H(e^{j2\pi fT}) = \sum_m G(j2\pi(f + m/T))H(j2\pi(f + m/T))F(j2\pi(f + m/T)), \tag{10.210}$$

and the noise has power spectrum

$$S_N(e^{j2\pi fT}) = \sum_m S_N(j2\pi(f + m/T))|F(j2\pi(f + m/T))|^2, \tag{10.211}$$

(a) The capacity is given by (10.119) with these values of $H(e^{j2\pi fT})$ and $S_N(e^{j2\pi fT})$.

(b) For this case, $F = G^*H^*$, and thus

$$H(e^{j2\pi fT}) = \sum_m |G(j2\pi(f + m/T))|^2 \cdot |H(j2\pi(f + m/T))|^2, \tag{10.212}$$

and

$$S_N(e^{j2\pi fT}) = \sum_m S_N(j2\pi(f + m/T))|G(j2\pi(f + m/T))|^2 \cdot |H(j2\pi(f + m/T))|^2. \tag{10.213}$$

Note that when the noise is white, $H(e^{j2\pi fT})$ and $S_N(e^{j2\pi fT})$ have the same shape; that is, they are equal within a multiplicative constant N_0. Thus,

$$\frac{S_N(e^{j2\pi fT})}{|H(e^{j2\pi fT})|^2} = \frac{N_0}{|H(e^{j2\pi fT})|}. \tag{10.214}$$

(c) First, the discrete-time system has to be able to generate the water-pouring spectrum. A sufficient condition for this is the following: If F is the water-pouring band, which must be symmetric about $f = 0$, then the sampling rate is twice $|F|/2$, or $1/T > |F|$, and the transmit filter is ideally bandlimited to half the sampling rate and non-zero over this bandwidth. (This is not a necessary condition, because if F is a "generalized Nyquist interval" with respect to sampling rate $1/T$, then the water-pouring spectrum can be generated by an appropriate transmit filter. A generalized Nyquist interval has the property that for each $|f| \le 1/2T$, $f + m/T \in F$ for precisely one value of m.) Second, the receive filter must prevent aliasing and allow all frequencies within the water-pouring band to pass. A sufficient condition for this is that it be an ideal LPF bandlimited to $1/2T$ Hz. (Again this is not a necessary condition. If the water-pouring band is a generalized Nyquist interval with respect to sampling rate $1/T$ then the receive filter that is ideally bandlimited to this water-pouring band will do.)

(d) For this case, if the transmit filter and sampling rate meet the criteria of (c), then the receive filter will automatically be OK. The fact that the receive filter is not flat within the generalized Nyquist interval will not be a problem, since this transfer function can always be reversed with an equalizer filter in a reversible fashion.

(e) The precursor equalizer is a reversible operation, and thus will not affect the capacity.

10-13. For the baseband case, we get $S_N = N_0$ and $H = 1$, and thus from (10.120), $S_X = L - N_0$. From the power constraint, $P_S = (L - N_0)/T$ or $S_X = P_S T$. Substituting into (10.119),

$$C = \frac{1}{2T} \cdot \log_2(1 + P_S T/N_0) = B \cdot \log_2(1 + P_S/2N_0 B), \tag{10.215}$$

since in this case the sampling rate is $1/T = 2B$.

In the passband case, we have $S_Z = 2N_0$ and $H = 1$, and thus from (10.124) $S_X = 2L - N_0$, and the power constraint of (10.122) becomes $P_S = (2L - 2N_0)/T$. Substituting into (10.123),

$$C = \frac{1}{T} \cdot \log_2(1 + P_S T/2N_0) = B \cdot \log_2(1 + P_S/2N_0 B), \tag{10.216}$$

since the sampling rate is $1/T = B$ in this case.

10-14.

(a) At the output of the channel, the noise spectrum is S_Z and hence the total noise power is $|F| \cdot \langle S_Z \rangle_{A,F}$. If the channel input signal has power spectrum S_X, confined to water-pouring band F, then the total signal power at the channel output is $|F| \cdot \langle S_X |H|^2 \rangle_{A,F}$. This is easily related back to the transmit signal power P_S through the water-pouring spectrum since for $f \in F$,

$$S_X |H|^2 = |H|^2 \cdot \left(\frac{P_S}{|F|} + \langle S_Z/|H|^2 \rangle_{A,F}\right) - S_Z, \tag{10.217}$$

and from this the channel-output SNR is

$$\begin{aligned} SNR_{out} &= \frac{|F| \cdot \langle S_X |H|^2 \rangle_{A,F}}{|F| \cdot \langle S_Z \rangle_{A,F}} \\ &= \langle |H|^2 \rangle_{A,F} (P_S/|F| + \langle S_Z/|H|^2 \rangle_{A,F}) \cdot \frac{\langle |H|^2 \rangle_{A,F}}{\langle S_Z \rangle_{A,F}} - 1. \end{aligned} \tag{10.218}$$

(b)

$$SNR_{norm} = \frac{(SNR_{out} + 1) \cdot \langle S_Z \rangle_{A,F} / \langle |H|^2 \rangle_{A,F} - \langle S_Z/|H|^2 \rangle_{A,F}}{2^{vB_s/|F|} \cdot \langle S_Z/|H|^2 \rangle_{G,F} - \langle S_Z/|H|^2 \rangle_{A,F}}. \tag{10.219}$$

10-15. We require that $\langle |G|^2 \rangle_A = P_S T/\sigma_A^2$. The effect of the transmit filter is to change the channel from H to GH, and hence the MSE at the output of the DFE-ZF to

$$\varepsilon^2_{DFE-ZF} = \langle S_Z/|GH|^2 \rangle_G = \frac{\langle S_Z/|H|^2 \rangle_G}{\langle |G|^2 \rangle_G}. \tag{10.220}$$

Using the geometric mean inequality $\langle |G|^2 \rangle_G \le \langle |G|^2 \rangle_A = P_S T/\sigma_A^2$, we get $\varepsilon^2_{DFE-ZF} \ge \langle S_Z/|H|^2 \rangle_G \sigma_A^2/P_S T$ with equality if and only if $G = \sqrt{P_S T}/\sigma_A$.

10-16. We have that $\langle S_A \rangle_A = \sigma_A^2$ and constraint $\langle S_A |G|^2 \rangle_A = P_S \cdot T$.

(a) Expliciting calculating the MSE,

$$\begin{aligned} \langle S_Z/|GH|^2 \rangle_G &= \langle S_A S_Z/S_A |G|^2 |H|^2 \rangle_G = \frac{\langle S_Z/|H|^2 \rangle_G \langle S_A \rangle_G}{\langle S_A |G|^2 \rangle_G} \\ &\ge \langle S_Z/|H|^2 \rangle_G \cdot \frac{\langle S_A \rangle_G}{P_S T}. \end{aligned} \tag{10.221}$$

Thus, the MSE is bounded below by a quantity that can be achieved when $S_A |G|^2$ is a constant, namely $\sqrt{P_S T}$.

(b) $\varepsilon^2_{DFE-ZF} = \langle S_Z/|H|^2 \rangle_G \langle S_A \rangle_G / P_S T$.

(c) Since $\langle S_A \rangle_G \le \langle S_A \rangle_A = \sigma_A^2$, we get that, when the transmit filter is optimized,

$$\varepsilon^2_{DFE-ZF} \le \langle S_Z/|H|^2 \rangle_G \cdot \frac{\sigma_A^2}{P_S T}. \tag{10.222}$$

The right side of (10.222) is the MSE for the white symbol case, established in problem 10-15.

10-17. The derivation for the error probability assumed Gaussian noise at the slicer. For the DFE-MSE, the slicer error includes residual ISI, and hence is not Gaussian. It would be surprising to find the SNR gap to capacity shrunk by the presence of ISI, so it is likely that if the effect of ISI at the slicer were taken into account we would find ISI to be beneficial.

CHAPTER 11: SOLUTIONS TO PROBLEMS

11-1. For a predictor with coefficient vector $\mathbf{f}$, the error is given by

$$\begin{aligned} E[|E_k|^2] &= E[|R_k - \mathbf{f}'\mathbf{r}_k|^2] \\ &= E[|R_k|^2] - 2\mathrm{Re}\{\mathbf{f}^{*\prime} E[R_k \mathbf{r}_k^{*}]\} + \mathbf{f}^{*\prime} E[\mathbf{r}_k^{*}\mathbf{r}_k'] \mathbf{f} \\ &= \phi_0 - 2\mathrm{Re}\{\mathbf{f}^{*\prime}\alpha\} + \mathbf{f}^{*\prime}\Phi\mathbf{f} \end{aligned} \tag{11.166}$$

where

$$\alpha = E[R_k \mathbf{r}_k^{*}] = [\phi_1 \phi_2 \ldots \phi_n]' \tag{11.167}$$

$$\Phi = E[\mathbf{r}_k^{*}\mathbf{r}_k'], \tag{11.168}$$

the same as before, by wide-sense stationarity. The solution is the same as the the equalizer, with the new definition of α.

11-2. The orthogonality principle of (11.26) implies that

$$\begin{aligned} \mathbf{0} &= E[E_k \mathbf{r}_k^{*}] \\ &= E[(A_k - \mathbf{c}'\mathbf{r}_k)\mathbf{r}_k^{*}] \\ &= \alpha - \Phi\mathbf{c} \end{aligned} \tag{11.169}$$

where the last equality follows since $\mathbf{c}'\mathbf{r}_k$ is a scaler and therefore

$$E[(\mathbf{c}'\mathbf{r}_k)\mathbf{r}_k^{*}] = E[\mathbf{r}_k^{*}\mathbf{r}_k']\mathbf{c}. \tag{11.170}$$

11-3.

$$\begin{aligned} E[E_k \mathbf{r}_k^{*}] &= E[(R_k - \mathbf{f}_{opt}'\mathbf{r}_k)\mathbf{r}_k^{*}] \\ &= E[R_k \mathbf{r}_k^{*}] - E[\mathbf{r}_k^{*}\mathbf{r}_k'] \mathbf{f}_{opt} \\ &= \alpha - \Phi\mathbf{f}_{opt} \\ &= \mathbf{0}. \end{aligned} \tag{11.171}$$

11-4.

(a) This follows from the definition of matrix multiplication since the i,j element of Φ is $\phi_{i-j} = \phi_{j-i}$.

(b) As $L \to \infty$,

$$\sum_{i=-\infty}^{\infty} \phi_{j-i} v_i = \lambda v_j \ , \ -\infty < j < \infty \ . \tag{11.172}$$

Since this is a convolution sum, the Fourier Transform gives:

$$S(e^{j\omega})V(e^{j\omega}) = \lambda V(e^{j\omega}) \tag{11.173}$$

(c) Either $V(e^{j\omega}) = 0$ or $\lambda = S(e^{j\omega})$. Since $S(e^{j\omega})$ is single valued, $\lambda = S(e^{j\omega})$ can occur at only one ω_0 since λ is a constant. Hence $V(e^{j\omega})$ will be zero at other ω. $V(e^{j\omega}) = \delta(\omega-\omega_0)$ will be an eigenvector, or $v_i = e^{j\omega_0 i}$ (a complex exponential).

(d) As $L \to \infty$ the eigenvalues are by this argument the values of the function $S(e^{j\omega})$.

11-5.

(a) Taking the Fourier transform of the autocorrelation function ϕ_k, the power spectrum is

$$\begin{aligned} S(e^{j\omega}) &= \sum_k \alpha^{|k|} e^{-j\omega k} \\ &= \frac{1-\alpha^2}{(1-\alpha e^{j\omega})(1-\alpha e^{-j\omega})} \\ &= \frac{1-\alpha^2}{1-2\alpha\cos(\omega)+\alpha^2} \end{aligned} \tag{11.174}$$

(b) Assume $0 < \alpha < 1$. Then the minimum of the power spectrum is at $\cos(\omega) = -1$, and

$$\lambda_{min} \to \frac{1-\alpha}{1+\alpha} \tag{11.177}$$

Similarly the maximum is at $\cos(\omega) = +1$, and

$$\lambda_{max} \to \frac{1+\alpha}{1-\alpha} \tag{11.178}$$

(c) For $N = 2$, the autocorrelation matrix is

$$\Phi = \begin{bmatrix} 1 & \alpha \\ \alpha & 1 \end{bmatrix} \tag{11.179}$$

and setting the determinant of $\lambda I - \Phi$ equal to zero, we get eigenvalues $\lambda_1 = 1-\alpha$ and $\lambda_2 = 1+\alpha$.

(d) As $N \to \infty$ we get that

$$\frac{\lambda_{max}}{\lambda_{min}} = \left[\frac{1+\alpha}{1-\alpha}\right]^2 \tag{11.180}$$

and for $N = 2$,

$$\frac{\lambda_{max}}{\lambda_{min}} = \left[\frac{1+\alpha}{1-\alpha}\right] \tag{11.181}$$

For $\alpha \approx 1$ these values are the same.

(e) As $N \to \infty$,

$$\beta_{opt} = \frac{1-\alpha^2}{1+\alpha^2} \tag{11.182}$$

and the dominant mode of convergence is proportional to

$$\left[\frac{2\alpha}{1+\alpha^2}\right]^k. \tag{11.183}$$

As $\alpha \to 1$, the input samples become perfectly correlated and the convergence of the MSEG algorithm slows.

11-6. The error vector is given by (11.32),

$$\begin{aligned} \mathbf{q}_j &= \left[\mathbf{I} - \beta\Phi\right]^j \mathbf{q}_0 \\ &= \sum_{i=1}^{n} \left[1 - \beta\lambda_i\right]^j \mathbf{v}_i \mathbf{v}_i^{*\prime} \mathbf{q}_0 \\ &= \sum_{i=1}^{n} \gamma_{i,j} \mathbf{v}_i \end{aligned} \tag{11.184}$$

where

$$\gamma_{i,j} = \left[1 - \beta\lambda_i\right]^j \mathbf{v}_i^{*\prime} \mathbf{q}_0 \tag{11.187}$$

The component of the error in the direction of each eigenvector $\mathbf{v}_i$ is $\gamma_{i,j}$, and decreases exponentially as $\left[1 - \beta\lambda_i\right]^j$. The component of the initial error in the direction of $\mathbf{v}_i$ is $\mathbf{v}_i^{*\prime}\mathbf{q}_0$, the component of the initial error in the direction of $\mathbf{v}_i$.

11-7. From problem 11-6,

$$\mathbf{q}_j^{*\prime} \mathbf{v}_l = \sum_{i=0}^{n} \gamma_{i,j} \mathbf{v}_i^{*\prime} \mathbf{v}_l = \gamma_{l,j} \tag{11.188}$$

or

$$\begin{aligned} E\left[E_k^2\right] - E\left[E_k^2\right]_{\min} &= \sum_{i=1}^{n} \lambda_i \left[\mathbf{q}_j^{*\prime} \mathbf{v}_i\right]^2 = \sum_{i=1}^{n} \lambda_i \gamma_{i,j}^2 \\ &= \sum_{i=1}^{n} \lambda_i \left[1 - \beta\lambda_i\right]^{2j} \left[\mathbf{v}_i^{*\prime} \mathbf{q}_0\right]^2 \end{aligned} \tag{11.189}$$

which decreases exponentially with n modes as $\left[1 - \beta\lambda_i\right]^{2j}$

11-8.

(a) Assume the dominant mode is $i, \lambda_i, \mathbf{v}_i$. From problem 11-7, the excess MSE for this mode is

$$\lambda_i (1 - \beta\lambda_i)^{2j} (\mathbf{v}_i^{*\prime} \mathbf{q}_0)^2, \tag{11.191}$$

and taking $10\log_{10}$ of this we get

$$\gamma_1 - j\,\gamma_2 \tag{11.192}$$

where

$$\gamma_1 = 10 \log_{10} (\lambda_i (\mathbf{v}_i^{*\prime} \mathbf{q}_0)^2) \tag{11.193}$$

$$\gamma_2 = -20 \log_{10} (1 - \beta\lambda_i) \tag{11.194}$$

Note that the excess MSE measured in dB decreases linearly with time. Hence the speed of convergence is often measured in dB/sec. or some equivalent units.

(b) From figure 11-4, when β is small the dominant mode corresponds to $\lambda_{\min}$, so that

$$\begin{aligned}\gamma_1 &= 10\log_{10}(\mathbf{v}_i^{*\prime}\mathbf{q}_0)^2 + 10\log_{10}\lambda_{\min} \\ \gamma_2 &= -20\log_{10}(1-\beta\lambda_{\min}) \\ &= \frac{-20\log_e(1-\beta\lambda_{\min})}{\log_e(10)} \\ &= \frac{20\beta\lambda_{\min}}{\log_e(10)}\end{aligned} \tag{11.195}$$

As β increases, the speed of convergence increases in direct proportion.

11-9. The MSE is

$$E[Y_k - \hat{Y}_k]^2 = E[Y_k - aY_{k-1} - b]^2 \tag{11.199}$$

and setting the derivative w.r.t. a and b to zero,

$$0 = \phi_1 - a\phi_0 - b\mu = \mu - a\mu - b\ . \tag{11.200}$$

Solving for a and b we get the stated results.

11-10.

(a) Doing a partial fraction expansion, we get

$$\Phi(z) = \frac{A}{1-\alpha^2}\left[\frac{1}{1-\alpha z} + \frac{\alpha}{z-\alpha}\right] \tag{11.201}$$

and expanding each term, the first corresponding to positive time and the second to negative, we get

$$\phi_k = \frac{A}{1-\alpha^2}\alpha^{|k|}\ . \tag{11.202}$$

(b) Putting Y_k thru a filter $(1 - \alpha z^{-1})$ results in a white signal. This filter is in the form of a predictor, and hence is the optimal predictor of infinite order. Hence the optimal predictor of any order one or higher has all-zero tap coefficients except for $f_1 = \alpha$.

11-11.

(a) From (11.38), we know that

$$\mathbf{q}_{j+1} = \sum_{i=1}^{n}(1-\beta_{j+1}\lambda_i)(\mathbf{v}_i^{*\prime}\mathbf{q}_j)\,\mathbf{v}_i\ . \tag{11.203}$$

Using this result and the assumption that the eigenvectors are orthonormal, we can prove the stated result by induction.

(b) We force the error to zero after N iterations by choosing

$$\beta_j = \frac{1}{\lambda_j},\ 1 \le j \le N. \tag{11.204}$$

The product term then always contains a term $1 - \beta_l\lambda_l = 0$ for every i.

11-12. Note: The problem should state that R_k is a real-valued and zero-mean process.

(a)

$$E[\sigma_k^2] = (1-\alpha)\sum_{j=0}^{\infty}\alpha^j\sigma^2 = \sigma^2\ . \tag{11.205}$$

(b) A key fact is that when X is a Gaussian zero-mean random variable, $E[X^3] = 0$ and $E[X^4] = 3\sigma^4$, which can be derived from the moment-generating function (Section 3.1). Then calculating the variance,

$$\mathrm{Var}[\sigma_k^2] = E[(\sigma_k^2)^2] - (\sigma^2)^2\ . \tag{11.206}$$

The first term can be calculated directly,

$$(1-\alpha)^2 \sum_{m=0}^{\infty}\sum_{n=0}^{\infty} \alpha^{m+n} E[R_{k-m}^2 R_{k-n}^2]$$
$$= (1-\alpha)^2 \left[\sum_{m=0}^{\infty} \alpha^{2m} E[R_{k-m}^4] + \sum_{m=0}^{\infty}\sum_{n=0}^{\infty} \alpha^{m+n} (\sigma^2)^2 - \sum_{m=0}^{\infty} \alpha^{2m} (\sigma^2)^2 \right] \tag{11.207}$$

where the third term subtracts off terms that were included twice in the first and second terms. Using the result for the fourth moment, we get

$$\mathrm{Var}[\sigma_k^2] = 2\sigma^4 \frac{1-\alpha}{1+\alpha} \tag{11.208}$$

where this variance approaches zero as $\alpha \to 1$ and $2\sigma^4$ as $\alpha \to 0$. It is of course desirable to have an α near unity because of the long time constant, since this results in a lot of averaging. The price we pay is a long convergence time, or poor tracking capability.

11-13. In figure 10-18c, let the samples at the LPF output be R_k, so that this implies that

$$Q_k = \sum_{m=-N}^{N} c_m R_{2k-m} \quad E_k = A_k - Q_k \tag{11.209}$$

For simplicity, doing the real-valued case,

$$\frac{\partial}{\partial c_j} E_k^2 = 2E_k R_{2k-j} \,. \tag{11.210}$$

Then analogous to (11.54),

$$[\mathbf{c}_{k+1}]_j = [\mathbf{c}_k]_j - \beta E_k R_{2k-j} \,. \tag{11.211}$$

For each increment of k, the delay line storing R_k shifts two positions.

11-14.

(a) Φ is replaced by $(\Phi + \sigma^2\mathbf{I})$, and it is simple to verify that the eigenvalues of this matrix are $(\lambda_i + \sigma^2)$, with the same eigenvectors.

(b) The new eigenvalue spread is $(\lambda_{max} + \sigma^2)/(\lambda_{min} + \sigma^2)$, which is smaller than before.

(c) From exercise 11-7,

$$(\phi + \sigma^2\mathbf{I})^{-1} = \sum_{i=1}^{N} \frac{1}{\lambda_k + \sigma^2} \mathbf{v}_i \mathbf{v}_i^{*\prime} \tag{11.212}$$

and hence

$$(\mathbf{c} - \Phi^{-1}\alpha) = \sum_{i=1}^{N} \frac{\sigma^2}{\lambda_i(\lambda_i + \sigma^2)} (\mathbf{v}_i^{*\prime}\alpha)\mathbf{v}_i \tag{11.213}$$

and the excess MSE is

$$(\mathbf{c} - \Phi^{-1}\alpha)^{*\prime} \Phi (\mathbf{c} - \Phi^{-1}\alpha) = \sigma^4 \sum_{i=1}^{N} \frac{|\mathbf{v}_i^{*\prime}\alpha|^2}{\lambda_i(\lambda_i + \sigma^2)} \tag{11.214}$$

which is the same result as problem 11-15. For small σ^2 the increase in MSE is approximately proportional to $(\sigma^2/\lambda_i)^2$ for the i-th mode.

11-15. Adding $\mu \|\mathbf{c}\|^2$ to (11.8),

$$E[E_k^2] = E[|A_k|^2] - 2\mathrm{Re}\{\mathbf{c}^{*\prime}\alpha\} + \mathbf{c}^{*\prime}(\Phi + \mu\mathbf{I})\,\mathbf{c} \,. \tag{11.215}$$

Hence the solution is the same as before with Φ replaced by $(\Phi+\mu\mathbf{I})$, or

$$\mathbf{c}_\mu = (\Phi + \mu\mathbf{I})^{-1}\alpha \,. \tag{11.216}$$

The eigenvalues of $(\Phi+\mu\mathbf{I})$ are $\mathbf{v}_i$ and the eigenvalues $(\lambda_i+\mu)$, where $\mathbf{v}_i$ and λ_i are the eigenvectors and eigenvalues of Φ. The eigenvectors and eigenvalues of $(\Phi+\mu\mathbf{I})^{-1}$ are $\mathbf{v}_i$ and $1/(\lambda_i+\mu)$ and hence

$$(\Phi+\mu I)^{-1} = \sum_{i=1}^{n} \frac{1}{\lambda_i+\mu} v_i v_i^{*\prime} \tag{11.217}$$

and

$$c_\mu - c_{opt} = \sum_{i=1}^{n} \left(\frac{1}{\lambda_i+\mu} - \frac{1}{\lambda_i}\right) v_i v_i^{*\prime} \alpha. \tag{11.218}$$

The excess mse is given by (11.42),

$$E[E_k^2(T)] - E[E_k^2(T)]_{min} = \sum_{i=1}^{n} \lambda_i [(c_\mu - c_{opt})^{*\prime} v_i]^2 = \sum_{i=1}^{n} \lambda_i \left[\frac{\mu v_i^{*\prime} \alpha}{\lambda_i} (\lambda_i+\mu)\right]^2 \tag{11.219}$$

The excess mse of the ith mode increases as

$$\left(\frac{\mu}{\lambda_i+\mu}\right)^2 \tag{11.220}$$

which has derivative

$$\frac{\partial}{\partial \mu}\left(\frac{\mu}{\lambda_i+\mu}\right)^2 = \frac{2\mu\lambda_i}{(\lambda_i+\mu)^3} \tag{11.221}$$

and since this derivative is zero at $\mu = 0$, the excess mse increases very slowly with μ.

11-16.

(a)

$$\nabla_c \mu \|c\|^2 = 2\mu c \tag{11.222}$$

so that the gradient algorithm is

$$c_{i+1} = (1 - \beta\mu)c_i + \beta(\alpha - \Phi c_i) \tag{11.223}$$

(b) The eigenvalues of $(\Phi - \mu I)$ are $(\lambda_i+\mu)$, so replace λ_{min} by $(\lambda_{min}+\mu)$ and λ_{max} by $(\lambda_{max}+\mu)$. The algorithm is stable if

$$0 < \beta < \frac{2}{\lambda_{max}+\mu}. \tag{11.224}$$

(c)

$$\beta_{opt} = \frac{2}{\lambda_{min}+\lambda_{max}+2\mu} \tag{11.225}$$

(d) The eigenvalue spread is now

$$\frac{\lambda_{max}+\mu}{\lambda_{min}+\mu} \approx \frac{\lambda_{max}}{\lambda_{min}+\mu} \tag{11.226}$$

which can be reduced dramatically by $\mu > 0$ when λ_{min} is very small.

(e) They apply to the speed of convergence of the average trajectory and the asymptotic excess mse caused by the algorithms converging to c_μ rather than c_{opt}. The second term in (11.226) biases the solution in the direction of keeping the coefficients small. The SG algorithm corresponding to minimizing (11.226) is

$$c_{k+1} = (1 - \beta\mu)c_k + \beta E_k p_k^*, \tag{11.227}$$

where $\mu = 0$ corresponds to the previous algorithm without leakage (11.53). The operation of this algorithm is evident, since the coefficient vector is multiplied by a constant slightly less than unity at each step before adding in the correction term. When the corrections are small, as when the coefficient vector is wandering in the direction of a eigenvector corresponding to a small eigenvalue, this leakage decreases the size of the vector over time.

11-17. The lowest frequency in the passband signal is

$$1800 - 1200 \cdot 1.1 = 480 \text{ Hz} \tag{11.228}$$

and the highest frequency is

$$1800 + 1200 \cdot 1.1 = 3120 \text{ Hz}. \tag{11.229}$$

(a) The baseband case is shown below:

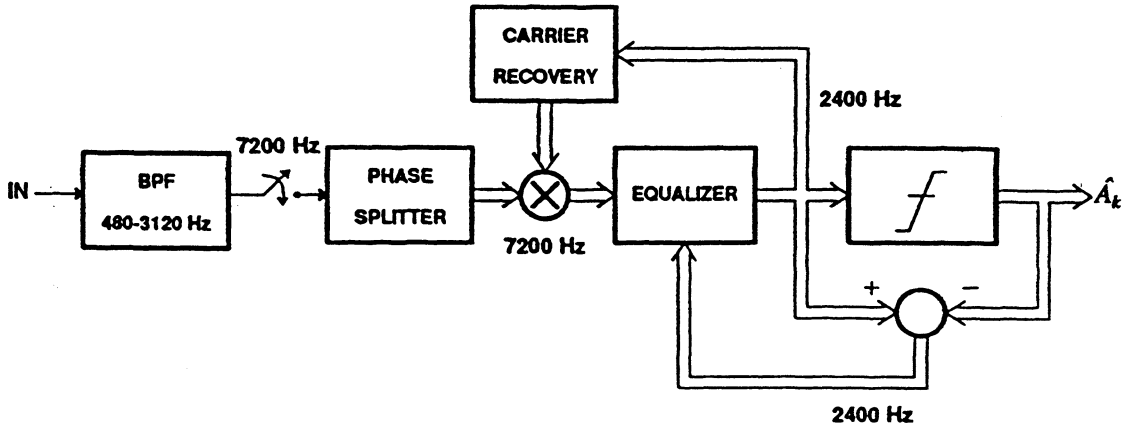

The BPF rejects all frequencies other than the signal bandwidth. The sampling rate at the front end of 7200 Hz is greater than twice the highest frequency of the passband signal. Following demodulation, a sampling rate of 4800 Hz would be adequate since the highest signal frequency is 1320 Hz; however, it is not convenient to decimate by a factor of two-thirds (perhaps a 9600-4800 decimation would be more appropriate, but this does not meet the specifications of the problem statement). The fractionally spaced equalizer can generate a signal at the slicer input at the symbol rate, a decimation factor of three.

(b) The passband case is shown below:

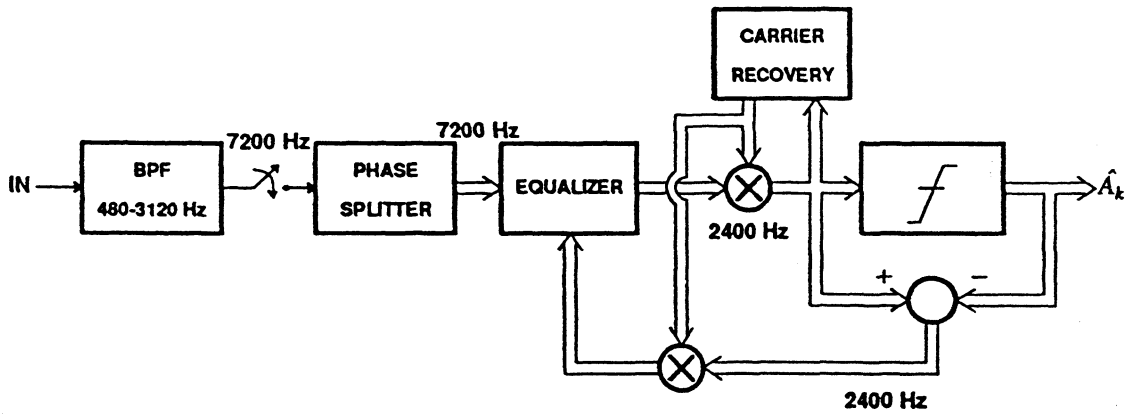

You might expect that the equalizer output had to be sampled at 7200 Hz also, but after demodulation a rate of 2400 is adequate. Since demodulation followed by decimation is equivalent to decimation followed by demodulation, in fact the equalizer output can be decimated to the symbol rate.

(c) This case is shown below:

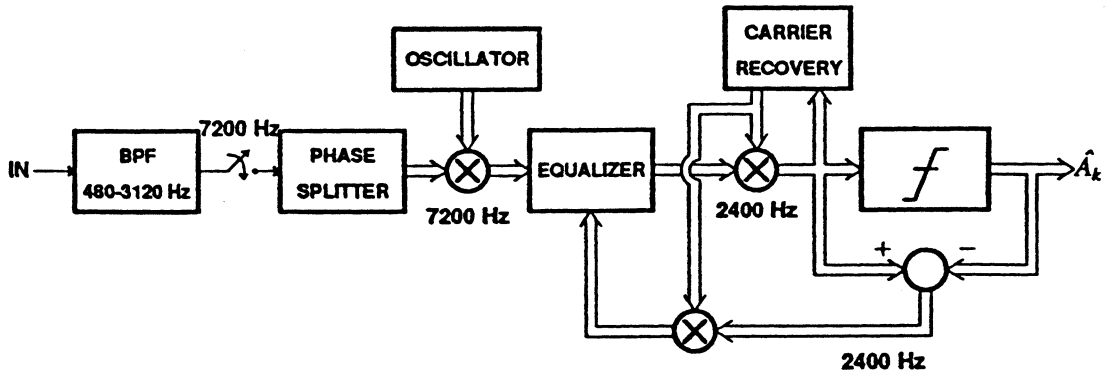

This case is similar, except for the reasoning. The equalizer input could again have a sampling rate of 4800, although this is not convenient. The 2400 Hz sampling rate at equalizer output is adequate for the same reason as in the baseband case (no funny business as in the passband case).

The passband equalizer case seems superior since the sampling rates are the same, but only one complex multiply for demodulation is required rather than two.

11-18. The block diagram is shown below:

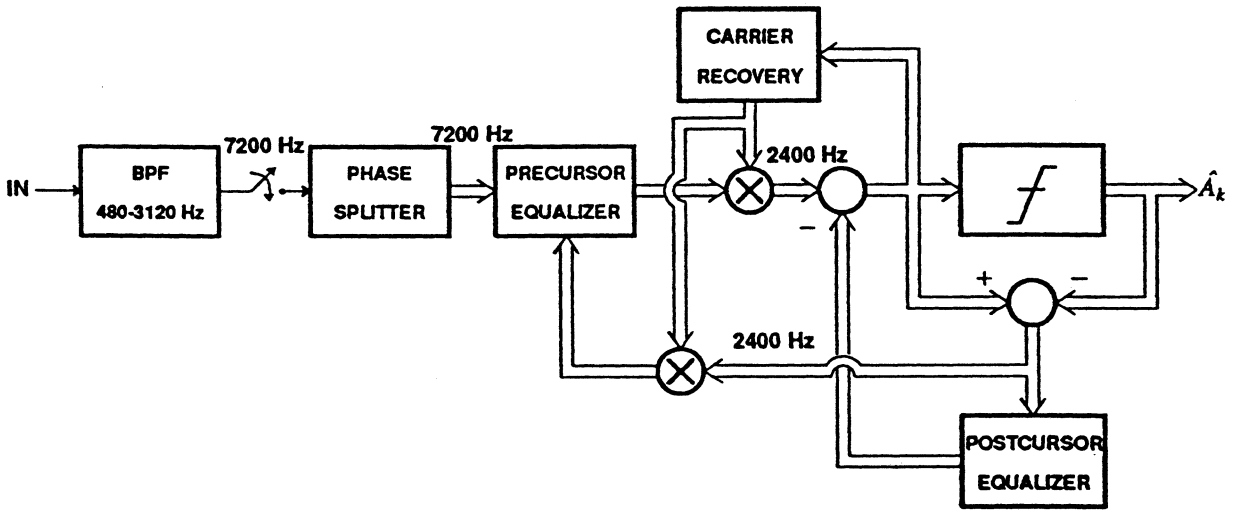

The postcursor equalizer and carrier recovery circuits work in the non-rotated domain along with the slicer. The slicer error is used directly in the postcursor equalizer and is rotated before being input to the precursor equalizer.

CHAPTER 12: SOLUTIONS TO PROBLEMS

12-1.

(a) The relation between input and output is

$$y(t) = \frac{x(t)}{2} - \frac{1}{2\tau}\int_{-\infty}^{t} x(u)e^{-\frac{(t-u)}{\tau}}\,du \tag{12.122}$$

where $\tau = 2RC$ is the time constant of the circuit. The first term in (12.122) represents the desired data signal attenuated by the voltage divider. The second term represents an undesirable ISI, consisting of an exponentially weighted average into the past.

(b) The output ISI becomes

$$X_k = \frac{T}{\tau}\sum_{m=-\infty}^{k-1} A_m e^{-(k-m)T/\tau} \tag{12.123}$$

12-2.

(a) We get a maximum ISI of $\frac{T}{\tau}\frac{\rho}{1-\rho}$ times the maximum data symbol.

(b) We get

$$\frac{T}{\tau} = 2\pi\cdot 0.01 = 0.0628 \tag{12.124}$$

$$\rho = e^{-0.0628} = 0.939\,. \tag{12.125}$$

The maximum ISI is therefore 0.97 times the maximum data symbol. While this worst-case is very unlikely, nevertheless this situation is unacceptable!

12-3. Performing a similar integral to exercise 12-1, we get this time

$$(x^4 - 2x^3 + 2x - 1) \tag{12.126}$$

for $x = e^{-\frac{\pi\beta}{2}}$. Letting $\beta = .033$, we get an intersymbol interference of 2.6×10^{-4}, much smaller than for the biphase case.

12-4.

(a) If an equalized pulse has Fourier transform $G(j\omega)$, then since the transmitted biphase pulse has zero area, so must the equalized pulse, and $G(0) = 0$. In order for the equalized pulse to satisfy the Nyquist criterion, we must have $G(j2\pi/T) \neq 0$ in order for the folded spectrum to be constant. This implies that the pulse bandwidth must be at least as great as the symbol rate $2\pi/T$, or a minimum of 100% excess bandwidth.

(b) The bandwidth of the equalized pulse is less than $3\pi/T$, and it is easily verified that two aliases will fold over into the frequency band $[0,\pi/T]$ in the folded spectrum. Thus, we must have that

$$G(j(\omega + \frac{2\pi}{T})) + G(j\omega) + G(j(\omega - \frac{2\pi}{T})) \tag{12.127}$$

is a constant over the band $[0,\pi/T]$.

(c) The minimum bandwidth pulse has bandwidth $2\pi/T$. We can find a zero-area Nyquist pulse with this bandwidth by starting with the pulse

$$h(t) = \text{sinc}(\frac{2\pi}{T}t) \tag{12.128}$$

which has bandwidth $2\pi/T$ and satisfies the Nyquist criterion since it has zero crossings at multiples of $T/2$, but has non-zero area. Then we note that

$$g(t) = h(t) - h(t - \frac{T}{2}) \tag{12.129}$$

will have the same bandwidth, will also satisfy the Nyquist criterion (zero crossings at multiples of T), and has zero area. Hence this pulse meets all the requirements. In fact, the pulse that meets the requirements is unique, so this is it.

(d) Yes, since they have a zero at d.c., the only way the folded spectrum can be constant is if the pulse has energy at the symbol rate $2\pi/T$.

12-5. Assume the same pulse shape in both cases, the signal power is the same in both cases, and that we transmit levels ± 1 for binary antipodal and $0, \pm\rho$ for the twinned binary code. First we find the ρ for which the average power is the same. For both codes, since the pulses are orthogonal, the average power is proportional to $E[A_k^2]$. For the antipodal code this value is unity regardless of p. For the twinned binary code, assuming for the moment that $\rho = 1$,

$$\begin{aligned} E[A_k^2] &= E[(B_k - B_{k-1})^2] \\ &= E[B_k^2] + E[B_{k-1}^2] - 2E[B_k]E[B_{k-1}] \\ &= p + p - 2p^2 = 2p(1-p). \end{aligned} \tag{12.130}$$

For arbitrary ρ we must multiply this quantity by ρ^2. Setting the powers equal, we get

$$\rho^2 = \frac{1}{2p(1-p)} . \tag{12.131}$$

For the binary antipodal code the noise must be unity in magnitude to cause in error, and for the twinned binary code it must be $\rho/2$. Thus, the relative immunity expressed in dB is

$$20\log_{10}(\frac{\rho}{2}) = -10\log_{10}(p(1-p)) - 9 . \tag{12.132}$$

(a) When $p = \frac{1}{2}$ the immunity becomes -3 dB, implying that the antipodal code is better by 3 dB.

(b) The twinned binary code has better immunity when p is near zero or unity, because in this case a large number of data symbols are zero and the level spacing can be large for a given average power. In particular, it is better when

$$10\log_{10}(p(1-p)) < -9 \tag{12.133}$$

or $p < .148$ or $p > .853$.

12-6. Using binary antipodal signaling with the pulse shape shown below will result in the same transmitted signal as with a twinned binary code with an RZ transmitted pulse:

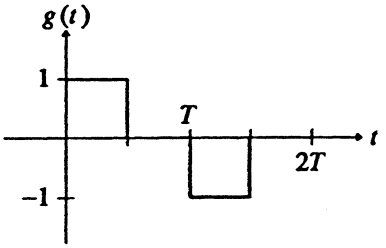

12-7. The receiver structure shown below will work, where the binary slicer (decision level at zero) output assumes the values ±1:

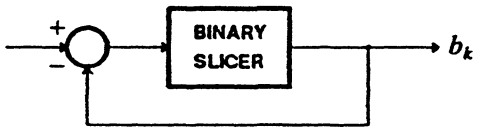

The signal values in the absence of noise at the slicer input assume the values ±½, and hence are the same distance apart as for the ternary slicer in figure 12-3. Hence, the SNR will be the same. Note that we do not have to normalize signal powers since the transmitted signal is identically the same in both cases.

12-8.

The twinned binary and AMI codes can be represented by trellis diagrams as shown in figure 12-21. Note that for twinned binary, if we observe $a_k = 0$, then the decoded output b_k depends on the previous state, and hence the decoder is not memoryless. For AMI, an observation of $a_k = 0$ uniquely specifies that $b_k = 0$, and observations $a_k = \pm 1$ uniquely specify $b_k = 1$, independent of the past state. Hence, in AMI the decoder is memoryless.

For twinned binary, at the slicer, $Q_k = B_k - B_{k-1} + N_k$. The minimum distance is $\sqrt{2}$, and the probability of error is approximately $4Q(\sqrt{2}/2\sigma)$. Without the VA, the received levels are 0 (probability ½) and ±1 (probability ¼). The error probability is thus

$$P_e = \frac{1}{4}Q(\frac{½}{\sigma}) + \frac{1}{4}Q(\frac{½}{\sigma}) + \frac{1}{2}\cdot 2\cdot Q(\frac{½}{\sigma}) = \frac{3}{2}Q(\frac{1}{2\sigma}) \ . \qquad (12.134)$$

This analysis ignores the error propagation, which results since the 0 level will be observed for $b_{k-1} = b_k$ for either $b_k = 0$ or $b_k = 1$. Hence the actual error probability, taking into account this error propagation, will be slightly worse. Thus, the VA is at least 3 dB better at high SNR.

12-9. Comparing the trellis diagrams in figure 12-21a and figure 12-21b, with respect to the observation a_k they are identical. Thus, the minimum distance is the same and the VA will perform the same in twinned binary and AMI. However, the error probability is slightly different for AMI without the VA because there is no error propagation. Thus, the error probability is the same as that calculated in problem 10-7, and in this case it is exact.

12-10.

(a) A bipolar violation consists of two "+" or two "-" symbols in a row with any number of intervening "0" symbols.

(b) We can count the number of bipolar violations, and the error rate should be proportional to this.

(c) When a single ternary slicing error is made the number of bit errors and bipolar violations that result are listed in the following table:

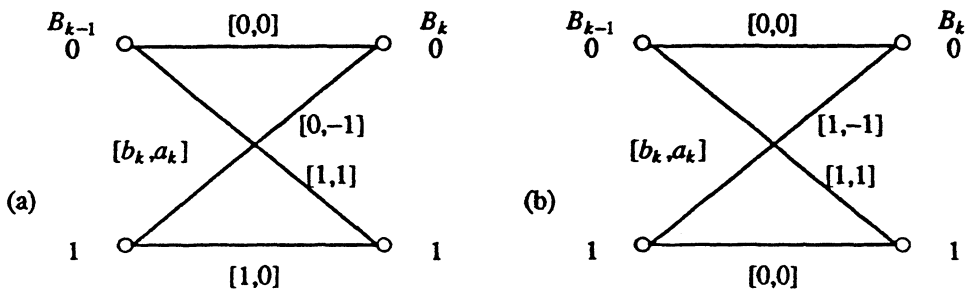

Figure 12-21. Trellis diagram representing two line coders. a. Twinned binary, and b. AMI.

Ternary Level		# Bit Errors	# Bipolar Violations
Actual	Detected		
+	0	1	1
+	-	0	2
0	+	1	1
0	-	1	1
-	+	0	2
-	0	1	1

Making the assumption that errors are infrequent and hence do not interact in funny ways, this table accurately reflects the relationship between bit error rate and rate of bipolar violations. We see that the rate of bipolar violations is higher. However, the slicer errors that result in two bipolar violations and no bit errors are much less probable than those that cause a single bipolar violation. Therefore, we conclude that the rate of bipolar violations is very similar to the rate of bit errors.

12-11.

(a) In accordance with this notation, an AMI signal would consist of only "0"'s and "B"'s.

(b) The sequence "BVBV" is d.c. balanced. The price we pay is a larger RDS. The example has a RDS in the range [−2,2], which is larger than AMI.

12-12.

(a) Long sequences of zeros are avoided, so that timing recovery circuits can function better.

(b) At the decoder, we can recognize this block of symbols since it violates the AMI constraints in a prescribed way, and substitute the "000000" decoded block of bits.

(c) This codeword always has zero-disparity, where the *disparity* of the codeword or block is defined as the digital sum of just that block. Hence the RDS at the end of the block is equal to the RDS at the beginning plus the disparity, or for this case is the same as AMI. However, at the end of the third symbol in the block, the RDS is in the range $-1 \le RDS \le +2$, and hence the DSV is three. We have therefore paid a penalty for the guaranteed timing energy in terms of a larger RDS and DSV.

12-13. The largest block consisting of one "V" and starting with a "V" has disparity zero (since it consists of an even number of non-zero symbols alternating in sign), and hence we can ensure that the RDS at the end of this block is zero. The RDS within the block alternates between +1 and 0 if it starts with V = + and alternates between -1 and 0 if it starts with V = -.

12-14.

(a) We could substitute "BVBV" for each block of four input "zeros".

(b) The disparity of the block is zero, so the RDS at the end of the block is in the range $0 \le RDS \le 1$. The RDS at the end of the second symbol is in the range of $-1 \le RDS \le 2$ and hence the DSV is three.

(c) The RDS properties are the same, and there will be more timing energy. However, the crosstalk and RFI will be increased. If the timing energy of B6ZS is adequate, then it will be preferable because of the improved crosstalk/RFI properties.

12-15.

(a) We want to substitute for blocks of three "zeros". The only non-zero blocks of three ternary digits with zero disparity have no bipolar violations, and hence would not be recognizable at the receiving terminal.

(b) This code is not unique, but choose the following code: If the RDS at the beginning of a block of three "zeros" is −1, then transmit "+0+". If the RDS is 0 or 1, transmit "00+". The reader can verify that the RDS at the end of this block is always in the range $-1 \le RDS \le +1$. Furthermore, the RDS within the block is in the same range. The DSV is therefore two, which is better than B6ZS.

12-16. The decoder can monitor the RDS and ensure that it falls in the range $-3 \le RDS \le 2$ at the end of each block. Any violation of this range indicates a ternary slicing error. Note however, that a ternary slicing error will cause a permanent offset in the RDS at the decoder. Thus, when the RDS at the decoder falls outside the allowable range, the RDS must be reset to the nearest value within the range. A more refined strategy would monitor the ternary blocks and detect any illegal combinations. For example, a block with disparity "+3" must always be followed by a block with negative disparity.

12-17. For AMI, the one's density is zero since any number of consecutive zeros are allowed.

For the remaining line codes, the one's density is listed in the table below:

n	B6ZS	HDB3	4B3T
1	0	0	0
2	0	0	0
3	0	0	0
4	0	1/4	0
5	0	1/5	1/5
6	1/6	1/6	1/6
7	2/7	1/7	1/7
8	2/8	2/8	2/8
9	2/9	2/9	2/9

The table can be extended to longer block sizes.

12-18. The code is not unique, but here is one such code:

Input Block	Output Block		
	Mode A	Mode B	
000	+-++	-+--	±2
001	-+++	+---	±2
010	-+-+	-+-+	0
011	-++-	-++-	0
100	+---	+---	0
101	+-+-	+-+-	0
110	+++-	--+	±2
111	++-+	--+-	±2

Mode A is used whenever RDS = 0 at the start of the block and Mode B is used when RDS = 2. The reader can verify that the RDS within the block never gets out of the range $-1 \le \text{RDS} \le +3$ for a DSV of four. The key to the design of this code is that we have not used two of the zero-disparity blocks, "--++" and "++--", which would otherwise carry the RDS to −2 and +4.

12-19. Use a filter $F_{\text{zero}}(z) = 1 + z^{-1}$. From the spectral factorization, $F_{\min}(z)$ is still a first-order filter with one pole, and the pole location β is still real-valued. Hence σ_X^2 is unchanged. However,

$$\sigma_Y^2 = E[|X_k + X_{k-1}|^2] = \sigma_X^2 \cdot (1 + \rho), \tag{12.135}$$

and hence

$$\sigma_Y^2 = 2\sigma_U^2 / (1 - \beta). \tag{12.136}$$

Clearly in this case we want $-1 < \beta \le 0$, which makes sense since this places the pole near the zero. The frequency response is just the mirror image of example 12-15, and the tradeoff between σ_X^2 and σ_Y^2 is the same.

12-20. Let the slicer output be $\hat{a}_k$, so that the postcoder output is

$$c_k = \hat{a}_k + c_{k-1} = c_0 + \sum_{i=1}^{k} \hat{a}_k . \tag{12.137}$$

It is evident that if one of the $\hat{a}_k$ is in error, then c_k is forever in error. Of course, if c_k goes outside of its allowable range, we can arrange to notice this, and perhaps correct the condition. For example, the Viterbi algorithm can be used for this purpose.

12-21.

(a) This pulse has samples ($\cdots$,0,0,1,2,1,0,0, $\cdots$) and therefore is a pulse approximately three symbol intervals wide. This pulse has two zeros at half the symbol rate, and therefore has relatively little high frequency content, as manifested by its width in the time domain.

(b) The intersymbol interference is

$$v_k = 2c_{k-1} + c_{k-2} \tag{12.138}$$

and since this assumes the values {+−1,+−3}, there must be five received levels. Therefore consulting figure 12-14 for the five-level case, we can develop the following table specifying the precoder:

c_{k-2}	c_k	v_k	b_k	c_k
-1	-1	-3	0	-1
-1	-1	-3	1	+1
-1	+1	+1	0	-1
-1	+1	+1	1	+1
+1	-1	-1	0	+1
+1	-1	-1	1	-1
+1	+1	+3	0	+1
+1	+1	+3	1	-1

Turning this into a logic truth table, we get:

c_{k-2}	c_k	b_k	c_k
0	0	0	0
0	0	1	1
0	1	0	0
0	1	1	1
1	0	0	1
1	0	1	0
1	1	0	1
1	1	1	0

We note that the output data symbol a_k is in fact independent of the last symbol c_{k-1}, so therefore the precoder need only use c_{k-2} and the current input bit b_k. A Boolean expression representing the truth table is

$$c_k = \bar{a}_{k-2} \cdot b_k + c_{k-2} \cdot \bar{b}_k \ . \tag{12.139}$$

(c) There are five received levels, and the following mapping is implemented between slicer output and information bit (from figure 12-14):

Slicer output	b_k
-4	0
-2	1
0	0
+2	1
+4	0

12-22. The precoders for dicode and duobinary PR are respectively

$$c_{k+1} = c_k \oplus b_{k+1} \quad c_{k+1} = c_k \oplus b_{k+1} \oplus 1 \ . \tag{12.140}$$

We can see that duobinary reverses the effect of dicode: in dicode, a "one" input causes the state to reverse, whereas in duobinary, a "one" input causes the state to be the same. Thus, the state diagrams for the two precoders will be the same, except that b_k is replaced by its complement in duobinary. There are therefore two differences: First, in duobinary the precoder output power spectrum is the same as dicode with p replaced by $(1-p)$. Second, the filter $F(D)$ is $(1+D)$ rather than $(1-D)$. Thus, we can write immediately, making these modifications to (12.20),

$$S_A(e^{j\omega T}) = 2p(1-p)\frac{1+\cos \omega T}{1+(2p-1)^2-2(2p-1)\cos \omega T} \ . \tag{12.141}$$

The case of modified duobinary is a little more complicated. Two dicode PR sequences of data symbols, which we can assume are uncorrelated, are interleaved. Calling this sequence X_k, and calling one of the interleaved sequences A_k,

$$R_X(m) = E[X_k X_{k+m}] = \begin{cases} 0, & m \text{ odd} \\ R_A(\frac{m}{2}), & m \text{ even} \end{cases} \tag{12.142}$$

and taking the Z-transform,

$$S_X(z) = \sum_{m=-\infty}^{\infty} R_X(m) z^{-m} = \sum_{r=-\infty}^{\infty} R_A(r) z^{-2r} = S_A(z^2) . \tag{12.143}$$

Thus, frequency is scaled by a factor of two, and the zero in the spectrum of dicode at d.c. (and hence the symbol rate) becomes a zero at the half symbol rate. In (12.20), ω is simply replaced by 2ω.

12-23.

(a) The equalizer in the receiver is

$$\frac{1}{1+\rho D} = 1 - \rho D + \rho^2 D^2 - \cdots \tag{12.144}$$

and therefore the noise variance at the slicer input is

$$\sigma^2(1 + \rho^2 + \rho^4 + \cdots) = \frac{\sigma^2}{1-\rho^2} . \tag{12.145}$$

The SNR is therefore $4(1-\rho^2)/\sigma^2$. Since both peak and average powers are unity, $SNR_{PEAK} = SNR_{AVG} = 4(1-\rho^2)E/\sigma^2$.

(b) The same equalizer is now put in the transmitter, so it has no effect on the slicer input noise, and therefore the SNR is $4/\sigma^2$. However, the peak transmitted signal is changed from unity to

$$1 + \rho + \rho^2 + \cdots = \frac{1}{1-\rho} . \tag{12.146}$$

and the average transmitted signal is changed to

$$1 + \rho^2 + \rho^4 + \cdots = \frac{1}{1-\rho^2} . \tag{12.147}$$

Hence,

$$SNR_{PEAK} = 4(1-\rho)^2 E/\sigma^2 , \tag{12.148}$$

or worse than the LE-ZF by a factor of $(1+\rho)/(1-\rho)$. The lesson is that transmitter equalization doesn't makes sense unless an increase in peak transmitted signal comes for free. Similarly,

$$SNR_{AVG} = 4(1-\rho^2)E/\sigma^2 , \tag{12.149}$$

the same as binary antipodal.

(c) In the receiver we implement an equalizer

$$\frac{1+D}{1+\rho D} = \frac{1}{\rho} + (1 - \frac{1}{\rho})\frac{1}{1+\rho D} = 1 + \frac{1-\rho}{\rho}(\rho D - \rho^2 D^2 + \rho^3 D^3 - \cdots) . \tag{12.150}$$

The noise variance at the slicer input is thus

$$\sigma^2(1 + (\frac{1-\rho}{\rho})^2(\rho^2 + \rho^4 + \cdots)) = \frac{2\sigma^2}{1+\rho} \tag{12.151}$$

and the SNR is $2(1+\rho)/\sigma^2$. The peak and average signal powers are both unity, so

$$SNR_{PEAK} = SNR_{AVG} = 2(1+\rho)E/\sigma^2 . \tag{12.152}$$

This is better than the LE-ZF by a factor of $1/2(1-\rho)$, yielding the conclusion again that duobinary has better noise immunity for this channel than conventional Nyquist signaling when $\rho > \frac{1}{2}$ because it is better matched to the channel.

(d) We put the same equalizer in the transmitter, so the SNR is the same, $4/\sigma^2$. But the peak transmitted signal is

$$1+\frac{1-\rho}{\rho}(\rho+\rho^2+\rho^3\cdots)=2 \tag{12.153}$$

and the average transmitted power is

$$1+(\frac{1-\rho}{\rho})^2(\rho^2+\rho^4+\cdots)=\frac{2}{1+\rho}\ . \tag{12.154}$$

Hence,

$$SNR_{PEAK}=\frac{E}{\sigma^2} \tag{12.155}$$

$$SNR_{AVG}=\frac{2(1+\rho)E}{\sigma^2}\ . \tag{12.156}$$

Thus we conclude again that equalization in the receiver is preferable unless the peak transmitted signal doesn't matter.

12-24. If we take the slicer output signal, and pass it through a filter $1/F(D)$, in the absence of errors the output will be a binary antipodal signal with values ± 1. Many possible errors will result in other values. For dicode PR, the filter $1/(1-D)$ is equivalent to calculating the RDS of the sequence, and checking that it is in the set $\{0,\pm 1\}$. This is of course equivalent to checking for bipolar violations. In the case of duobinary, the filter $1/(1-D)$ is equivalent to multiplying by alternating ± 1 and then forming the RDS.

12-25. Let the input symbols b_k lie in the M-ary set $\{0,1,\cdots,M-1\}$, and let c_k be the precoded symbol, assumed to fall in the same set. For the moment, assume that c_k is transmitted through the filter $F(D)$ to yield the transmitted symbols a_k (we will modify this in a moment). Then we get

$$a_k=c_k+\sum_{j=1}^{N} f_j c_{k-j}\ . \tag{12.157}$$

Let the precoder be specified as

$$c_k=(b_k-\sum_{j=1}^{N} f_j c_{k-j}) \text{ modulo } M \tag{12.158}$$

where the "modulo M" operator results in an integer in the interval $[0,M-1]$. Then we get the transmitted symbol

$$a_k=\sum_{j=1}^{N} f_j c_{k-j}+(b_k-\sum_{j=1}^{N} f_j c_{k-j}) \bmod M \tag{12.159}$$

The receiver then slices the reception into the nearest integer, and then reduces the result modulo M. In the absence of noise, the result is

$$\begin{aligned} a_k \bmod M &= [\sum_{j=1}^{N} f_j c_{k-j}+(b_k-\sum_{j=1}^{N} f_j c_{k-j}) \bmod M] \bmod M \\ &= [\sum_{j=1}^{N} f_j c_{k-j}+b_k-\sum_{j=1}^{N} f_j c_{k-j}] \bmod M = b_k \bmod M = b_k\ . \end{aligned} \tag{12.160}$$

The only problem with this approach is that c_k has a non-zero mean. This can be removed by replacing it by $(2c_k-(M-1))$, which lies in the range $[-(M-1),(M-1)]$. The output of the filter $F(D)$ will then be replaced by $2a_k-(M-1)F(1)$, and in the receiver we can simply add $(M-1)F(1)$ and multiply by 0.5 prior to the application of the modulo operation. As an example of this, for dicode, $F(1)=0$, and we get the following table specifying the precoding, $F(D)$ filtering, and noiseless decoding:

b_k	c_{k-1}	$2c_{k-1}-1$	c_k	$2c_k-1$	a_k	$\frac{a_k}{2}$	$\frac{a_k}{2} \bmod 2$
0	0	-1	0	-1	0	0	0
0	1	1	1	1	0	0	0
1	0	-1	1	1	2	1	1
1	1	1	0	-1	-2	-1	1

Similarly, for duobinary, $F(1) = 2$, and we get:

b_k	c_{k-1}	$2c_{k-1}-1$	c_k	$2c_k-1$	a_k	$\frac{a_k+2}{2}$	$\frac{a_k+2}{2} \bmod 2$
0	0	-1	0	-1	-2	0	0
0	1	1	1	1	2	2	0
1	0	-1	1	1	0	1	1
1	1	1	0	-1	0	1	1

Note that in both cases, the original input b_k is recovered by the noiseless and memoryless decoding operation in the last column.

12-26.

(a) The trellis is shown in figure 12-22

(b) From (6.150), note that the MSK signal within any pulse interval is

$$g_i(t) = c\sin(\omega_c + b\frac{\pi t}{2T}) \tag{12.161}$$

where $b = \pm 1$ and $c = \pm 1$. Upward-tending branches in figure 12-17 correspond to $b = +1$ and downward-tending branches correspond to $b = -1$. The value of c is dependent on the starting position of the branch in figure 12-17. The squared distance between any two branches going in opposite directions in figure 12-17 is

$$d^2 = \int_0^T [\sin(\omega_c + \pi t/2T) - \sin(\omega_c - \pi t/2T)]^2 dt = 2E \tag{12.162}$$

where E is the energy in one pulse. By contrast any two *distinct* (modulo 2π) *parallel* branches have squared distance $4E$. By inspection, therefore, being careful to associate branches in figure 12-17 with branches in figure 12-22, we see that the minimum-distance error event is the one of length two, with squared distance $4E$.

(c) The squared distance of $4E$ is 3 dB better than the squared distance $2E$ in figure 6-46.

12-27. Take as input the maximal-length sequence itself, and invert every other bit. Then the scrambled bit stream will be alternating zero-one.

12-28. The polynomial has octal entry "13" which corresponds to binary "1011". Hence the polynomial is

$$h(D) = 1 \oplus D \oplus D^3 \tag{12.163}$$

and the difference equation is

$$x_k = x_{k-1} \oplus x_{k-3}\,. \tag{12.164}$$

The sequence of states is given in the following table:

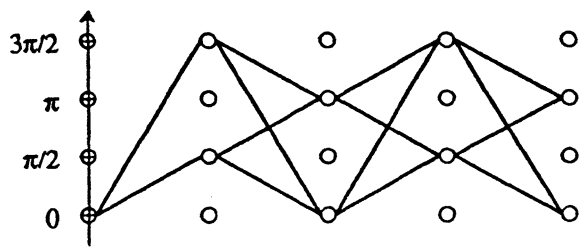

Figure 12-22. A finite planar trellis for the MSK signal.

x_k	x_{k-1}	x_{k-2}	x_{k-3}
1	0	0	1
1	1	0	0
1	1	1	0
0	1	1	1
1	0	1	1
0	1	0	1
0	0	1	0
1	0	0	1

Note that the period is seven, indicating a maximal-length sequence.

12-29. For this case the characteristic polynomial is

$$h(D) = 1 \oplus D \oplus D^4 \tag{12.165}$$

and the difference equation is

$$x_k = x_{k-1} \oplus x_{k-4} . \tag{12.166}$$

The sequence of states is given below:

x_k	x_{k-1}	x_{k-2}	x_{k-3}	x_{k-4}
1	0	0	0	1
1	1	0	0	0
1	1	1	0	0
1	1	1	1	0
0	1	1	1	1
1	0	1	1	1
0	1	0	1	1
1	0	1	0	1
1	1	0	1	0
0	1	1	0	1
0	0	1	1	0
1	0	0	1	1
0	1	0	0	1
0	0	1	0	0
0	0	0	1	0

CHAPTER 13: SOLUTIONS TO PROBLEMS

13-1. We use the approximation

$$Q(y) \approx \frac{1}{\sqrt{2\pi}y} e^{-y^2/2} \tag{13.128}$$

By successive approximation we find that

$$Q(y) \approx 10^{-5} \quad \text{when } y \approx 4.27 \tag{13.129}$$

and

$$Q(y) \approx 10^{-7} \quad \text{when } y \approx 5.20. \tag{13.130}$$

(A programmable calculator or a computer is useful here.) So the uncoded system achieves a probability of error of 10^{-5} when

$$a/\sigma_u \approx 4.27 \tag{13.131}$$

and a probability of error of 10^{-7} when

$$a/\sigma_u \approx 5.20 \tag{13.132}$$

For the coded system the probability of error will be at least 10^{-5} when

$$0.5Q\left[\frac{a\sqrt{4/3}}{\sigma_u}\right] \approx 10^{-5} \tag{13.133}$$

which by successive approximation occurs when

$$a/\sigma_u \approx 3.57. \tag{13.134}$$

Comparing this to (13.131) we find that the coding advantage in signal level is at best

$$20\log(5.20/3.57) \approx 1.56dB. \tag{13.135}$$

The best case coding advantage at 10^{-7} can be found the same way, using (13.132) instead of (13.131). The worst case coding advantages are also found the same way, but using (13.20) rather than (13.19).

13-2.

(a) There are only two codewords $00\cdots0$ and $11\cdots1$, which have distance n, so $d_{H,min} = n$.

(b) The (7,4) Hamming code has $d_{H,min} = 3$, and is rate 4/7 code. A minimum distance of $d_{H,min} = 3$ in a repetition code requires $n = 3$, which has rate 1/3, considerably worse than 4/7.

13-3.

(a) For all $\mathbf{c} \in C$, $\mathbf{cH}' = \mathbf{0}$. The product $\mathbf{cH}'$ is a linear combination of rows of $\mathbf{H}'$, or columns of $\mathbf{H}$. Hence the minimum number of columns of $\mathbf{H}$ that can be added to produce $\mathbf{0}$ is

$$\min_{\substack{\mathbf{c}\in C \\ \mathbf{c}\neq\mathbf{0}}} w_H(\mathbf{c}) \tag{13.136}$$

which equals $d_{H,min}$.

(b) From part (a), no linear combination of $d_{H,min} - 1$ or fewer columns of $\mathbf{H}$ can be zero, so $\mathbf{H}$ has rank $d_{H,min} - 1$. Since $\mathbf{H}$ has dimension $n \times (n-k)$, its rank cannot be larger than $n-k$, so

$$d_{H,min} - 1 \le n - k \tag{13.137}$$

from which the result follows.

13-4.

(a) Reverse the order of the first three columns.

(b)

$$\mathbf{H} = \begin{bmatrix} 1 & 0 & 1 & 1 & 0 & 0 & 0 \\ 1 & 1 & 1 & 0 & 1 & 0 & 0 \\ 0 & 1 & 1 & 0 & 0 & 1 & 0 \\ 1 & 1 & 0 & 0 & 0 & 0 & 1 \end{bmatrix}, \tag{13.138}$$

(c) In each case the most likely error pattern is the one with the smallest Hamming weight.

s	$\hat{\mathbf{e}}$	s	$\hat{\mathbf{e}}$
0000	000 0000	1000	000 1000
0001	000 0001	1001	000 1001
0010	000 0010	1010	000 1010
0011	000 0011	1011	000 1011
0100	000 0100	1100	100 0001
0101	000 0101	1101	100 0000
0110	000 0110	1110	001 0000
0111	010 0000	1111	100 0010

For those entries with two or three one bits in $\hat{\mathbf{e}}$, the choices for $\hat{\mathbf{e}}$ shown may not be unique. Syndromes for which this is this case correspond to errors that cannot be reliably corrected, but can be detected.

(d) This code equivalent to the dual of the (7,4) Hamming code.

(e) $d_{H,min} = 4$, so only one bit error can be reliably corrected.

(f) $\mathbf{c} = 1010011$.

13-5.

(a) In this case, $m = n - k = 4$, and the parity-check matrix has as columns all possible 4-bit patterns except the all zero pattern. To get it into systematic form, simply arrange the columns so that the last four columns form an identity matrix. The first 11 columns can appear in any order. The generator matrix can be gotten by comparing (13.39) with (13.34).

(b) The parity-check matrix is

$$\mathbf{H} = \begin{bmatrix} 000000011111111 \\ 000111100001111 \\ 011001100110011 \\ 101010101010101 \end{bmatrix}. \tag{13.139}$$

From (13.43), if $\mathbf{e}$ is all zero except for a 1 in position i, then $\mathbf{e}\mathbf{H}^T$ will be the transpose of the i^{Th} column of $\mathbf{H}$, which in (13.139) is a binary representation of i.

13-6. Following example 13-12,

$$d_{E,min} = 2a\sqrt{3} \tag{13.140}$$

and

$$\sigma_c = \sqrt{\frac{15}{11}}\sigma_u, \tag{13.141}$$

so the power advantage at high SNR is

$$10\log\frac{33}{15} \approx 3.42\,dB\ . \tag{13.142}$$

13-7. The coded system has 15/4 times the symbol rate of the uncoded system so the noise variance at the receiver is 15/4 times higher,

$$\sigma_c^2 = \frac{15}{4}\sigma_u^2 . \tag{13.143}$$

The minimum Hamming distance between codewords is 8 so the Euclidean distance is

$$d_{E,min} = 4a\sqrt{2} \tag{13.144}$$

from (13.7), where the alphabet is $\pm a$. Hence the probability of error for the coded system is approximately

$$Q\left[\frac{d}{2\sigma_c}\right] = Q\left[\frac{2a\sqrt{2}}{\sigma_u\sqrt{15/4}}\right] \tag{13.145}$$

compared to

$$Q\left[\frac{d}{2\sigma_u}\right] = Q\left[\frac{a}{\sigma_u}\right] \tag{13.146}$$

for the uncoded system, which means a power advantage of about

$$20\log\left[\frac{2\sqrt{2}}{\sqrt{15/4}}\right] = 10\log\left[\frac{32}{15}\right] \approx 3.29\,dB\ , \tag{13.147}$$

for the soft decoder.

13-8.

(a) The system is described by the following equations

$$C^{(1)}(D) = B^{(1)}(D) \oplus B^{(2)}(D)(D \oplus D^2) \tag{13.148}$$

$$C^{(2)}(D) = B^{(1)}(D)D \oplus B^{(2)}(D)(1 \oplus D^2) \tag{13.149}$$

$$C^{(3)}(D) = B^{(2)}(D)D\ . \tag{13.150}$$

These equations can be manipulated to get

$$0 = C^{(1)}(D)D^2 \oplus C^{(2)}(D)D \oplus C^{(3)}(D)(1 \oplus D^3) \tag{13.151}$$

which means that the parity-check matrix is

$$\mathbf{H}(D) = [D^2,\ D,\ 1 \oplus D^3]\ . \tag{13.152}$$

(b) A similar technique can be used to derive the parity-check matrix, showing that it is the same.

13-9. The condition $B_k = 0$ for $k < 0$ implies that the starting state is the (0,0) state. The condition $B_k = 0$ for $k \geq 3$ implies that the fifth state and beyond are zero. Hence the trellis is shown in the following figure.

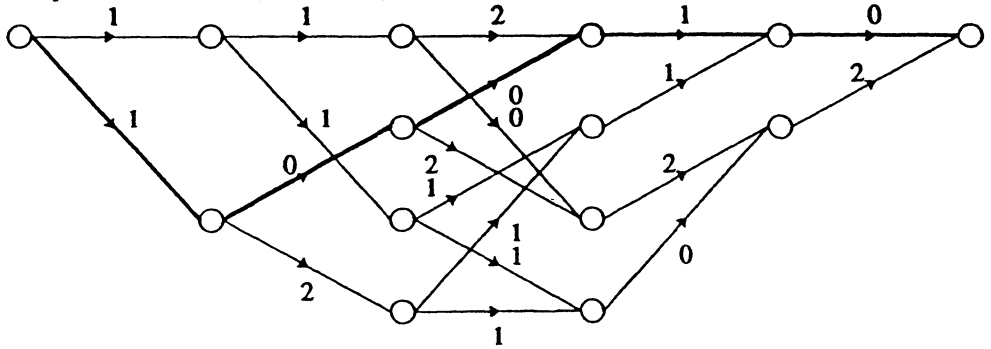

The transitions are labeled with their weights, which are the Hamming distances from the observation bit pairs. The minimum path metric corresponds to the bold path. Without errors introduced by the BSC the observation would have been {1,1,0,1,1,1,0,0,0,0,...}, implying that two bit errors were made. The decision $\hat{b}_k$ is {1,0,0,...}.

13-10.

(a) The state transition diagram and trellis are shown in the following figure:

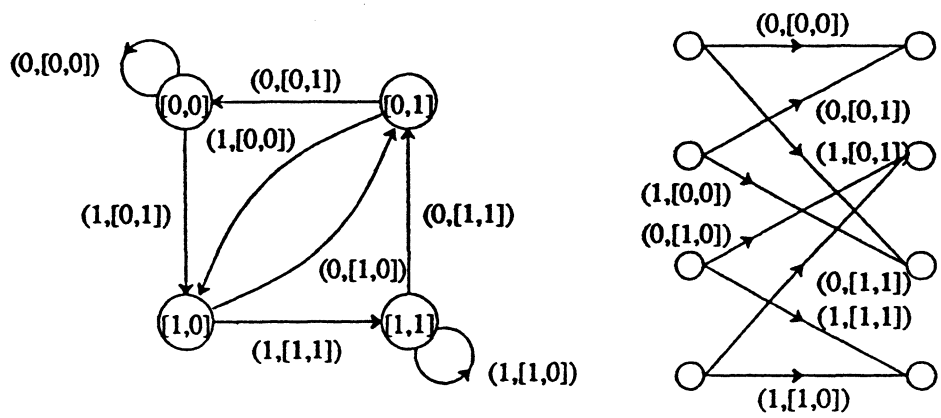

(b) The error event with the minimum Hamming distance is again an event with length $K = 2$, as shown in the following figure:

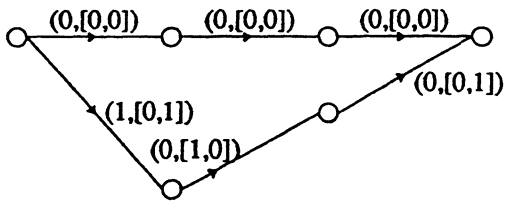

The minimum Hamming distance is therefore three. Assume a BSC with probability of correct transmission p. The probability of the error event is

$$\binom{3}{2} p^2(1-p) + \binom{3}{1} p^3 = 3p^2(1-p) + p^3 . \tag{13.153}$$

For p small this is approximately $3p^2$ which is significantly worse than the probability computed in (13.79), which for small p is approximately $10p^3$.

(c) The trellis is shown below re-labeled with the binary antipodal outputs.

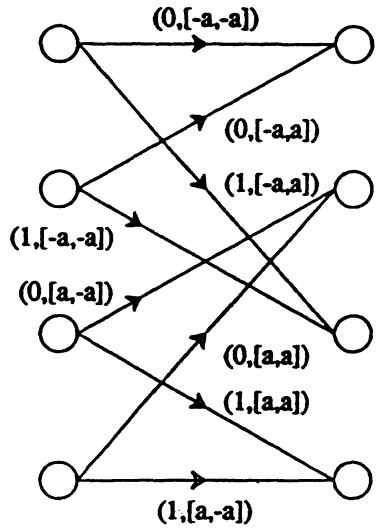

The minimum distance error event is shown below.

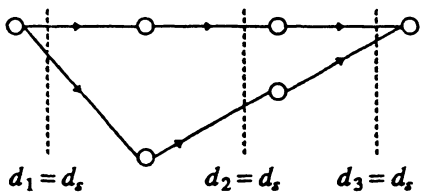

The ML soft decoder therefore has $d_{\min} = \sqrt{3}d_s$ where $d_s = 2a$. Hence, assuming the probability of error is dominated by this event,

$$\Pr[\textit{error event}] \simeq Q(\sqrt{3}a/\sigma_c) \tag{13.154}$$

where σ_c^2 is the variance of the noise of the coded system, which is twice the variance of the noise of the uncoded system, $\sigma_c^2 = 2\sigma_u^2$. Hence, the coded system is $10\log(3/2) \simeq 1.8$ *dB* better than the uncoded system. This is a full 2.2 dB worse than conv(1/2) in figure 13-8a. This is not surprising because the minimum distance is far worse.

13-11. One stage of the trellis is shown in figure 13-23.

(a) The minimum Hamming distance error event has distance 3, by inspection of figure 13-23a. Following the development of (13.79) we get that the probability of this error event is bounded by

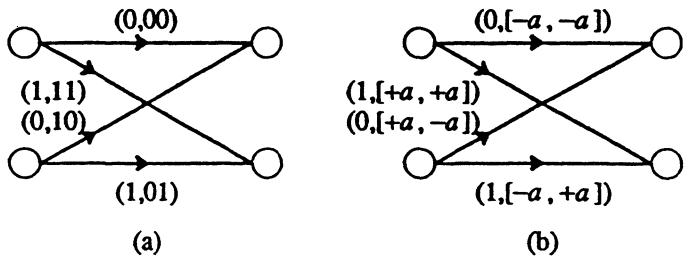

Figure 13-23. One stage of the trellis for the coder in figure 13-20. In (a) it is labeled with the binary output. In (b) it is labeled with the channel symbols, assuming binary antipodal signaling.

$$\Pr[\textit{this error event}] \le \binom{3}{2} p^2(1-p) + \binom{3}{3} p^3 = 3p^2(1-p) + p^3 . \tag{13.155}$$

(b) By inspection of figure 13-23b we see that the minimum Euclidean distance error event has distance $2a\sqrt{3}$. Hence

$$\Pr[\textit{this error event}] \approx Q\left[\frac{2a\sqrt{3}}{2\sigma_c}\right] = Q\left[\frac{2a\sqrt{3}}{2\sqrt{2}\sigma_u}\right] . \tag{13.156}$$

The uncoded system has probability of error

$$\Pr[\textit{error, uncoded system}] = Q\left[\frac{a}{\sigma_c}\right] \tag{13.157}$$

so the coding gain is approximately

$$20\log(\sqrt{3}/\sqrt{2}) \approx 1.8\ dB . \tag{13.158}$$

Note that this is the same coding gain achieved by the coder in figure 13-19 with a soft decoder. This coder is simpler, however, since its trellis has only two states.

13-12. The code is not linear because it does not include the zero vector.

13-13. $n = 7, k = 3, d_{H,min} = 4$, and the codewords are

0000000
1110100
0111010
1101001
1001110
0011101
1010011
0100111

Note that all the non-zero codewords have the same weight.

13-14. In figure 13-24 we show the state transition diagram with the zero state broken and the branches labeled with z raised to the square of the Euclidean distance of that branch from the zero branch. The path enumerator polynomial is therefore

$$T(z) = z^{12a^2} + z^{16a^2} + \cdots \tag{13.159}$$

In problem 13-11 we found that the error event with the minimum Euclidean distance had distance $2a\sqrt{3} = \sqrt{12a^2}$, consistent with this result. The compact form of this polynomial is

$$T(z) = \frac{z^{12a^2}}{1 - z^{4a^2}} . \tag{13.160}$$

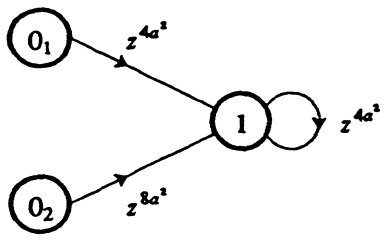

Figure 13-24. A state transition diagram with the zero state broken and the branches labeled with z raised to the square of the Euclidean distance of that branch from the zero branch.

13-15.

(a) By inspection,

$$T(x,y,z)=x^2yz^3+x^3y^2z^4+x^4y^3z^5+x^5y^4z^6+\cdots \tag{13.161}$$

or equivalently

$$T(x,y,z)=\frac{x^2yz^3}{1-xyz}. \tag{13.162}$$

(b) From (13.161) the length four error event (corresponding to x^5) has four bit errors and Hamming distance 6.

(c) The broken state transition diagram of figure 13-17 can be modified as shown in figure 13-25. Since we are only interested in length and distance (and not the number of bit errors) we need only two variables, x and z. The path enumerator polynomial is found using (13.109)

$$T(x,z)=\frac{x^3z^5}{1-x^2z-xz}. \tag{13.163}$$

By long division, we compute the first few terms

$$T(x,z)=x^3z^5+x^4z^6+x^5z^6+x^5z^7+x^6z^8+x^7z^7+\cdots \tag{13.164}$$

From this we see that there are two distance 6 error events, one with length 3 and one with length 4. (The length is the exponent of x minus one.) Also, there are two length four error events, one with distance 6 and one with distance 7.

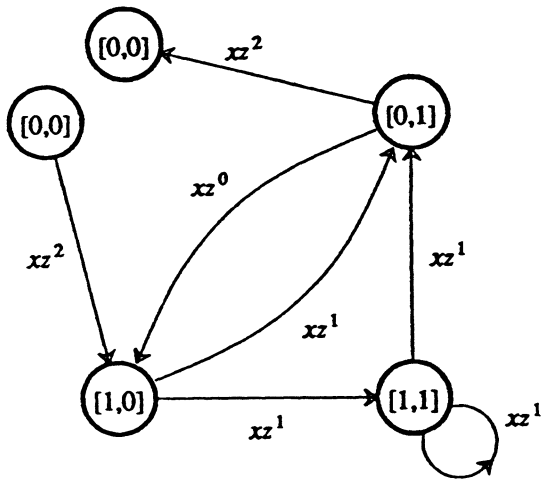

Figure 13-25. The state transition diagram of figure 13-17 is modified for enumerating the path lengths as shown.

CHAPTER 14: SOLUTIONS TO PROBLEMS

14-1. In the transmitter, generate two-dimensional symbols in the conventional way. Now group the transmitted baseband symbols into pairs, and transmit the real part of the two-dimensional symbol first, then the imaginary part. In the receiver, group the received samples at the slicer into pairs, and apply them to a complex slicer.

14-2.

(a) The coding gain is, of course, $\gamma_\Lambda = 1$. The shaping gain is

$$\gamma_S = \frac{2 \cdot \pi R^2}{12 \cdot R^2/2} = \frac{\pi}{3} . \tag{14.81}$$

(b) The coding gains are the same. The circular shaping provides $10 \log_{10} pi/3 = 0.2$ dB of shaping gain.

14-3. For the hexagonal constellation, the fundamental volume is the volume of a hexagon with inscribed radius $d_{\min}/2$. Hence,

$$V(\Lambda) = 6 (d_{\min}/2)^2 \tan\pi/6 \tag{14.82}$$

and the coding gain is

$$\gamma_\Lambda = \frac{2}{3 \tan\pi/6} = 1.155 . \tag{14.83}$$

This is 0.6 dB.

14-4. Clearly

$$d_{\min}(\alpha \cdot \Lambda) = \alpha \cdot d_{\min}(\Lambda) \tag{14.84}$$

and

$$V(\alpha \cdot \Lambda) = \alpha^N \cdot V(\Lambda) . \tag{14.85}$$

Thus, as a function of α, the coding gain is

$$\gamma_{\alpha \cdot \Lambda} = \frac{\alpha^2 d_{\min}^2}{\alpha^2 V^{2/N}(\Lambda)} = \frac{d_{\min}^2}{V^{2/N}(\Lambda)} = \gamma_\Lambda . \tag{14.86}$$

14-5. The volume is

$$V[C_N(R)] = \int_{C_N(R)} d\mathbf{x} . \tag{14.87}$$

The integral can be separated into the product of N integrals, each evaluating to $2R$, so $V[C_N(R)] = (2R)^N$. To evaluate the power, the uniform density function over the N-cube has height $(2R)^{-N}$, so the power is

$$P[C_N(R)] = (2R)^{-N} \int_{C_N(R)} \|\mathbf{x}\|^2 d\mathbf{x} = (2R)^{-N} \sum_{i=1}^{N} \int_{C_N(R)} x_i^2 d\mathbf{x} . \tag{14.88}$$

Each of the integrals evaluates to the same value,

$$\int_{C_{N'}(R)} x_i^2 dx = V[C_{N-1}(R)] \cdot \frac{2R^3}{3}, \tag{14.89}$$

and thus

$$P[C_N(R)] = N \cdot R^2/3. \tag{14.90}$$

Substituting the volume and power into the shaping gain, we get $\gamma_{C_{N'}(R)} = 1$.

14-6.

(a) Assuming the radius of the N-sphere is R, P is the power of $S_N(R)$ divided by the number of complex symbols, $N/2$. Hence $P = 2R^2/(N+2)$, and for fixed P the radius as a function of N is $R^2 = (N+2)P/2$. Assuming N is even, the volume of a sphere of this radius is

$$V(S_N(\sqrt{(N/2+1)P})) = \frac{(\pi(N/2+1)P)^{N/2}}{(N/2)!}. \tag{14.91}$$

The number of points in the signal constellation is proportional to the volume, since the fundamental volume is assumed to be constant, and hence ν is proportional to the logarithm of the volume divided by $N/2$, or

$$\nu \propto \frac{2}{N} \cdot \log_2 \left[\frac{(\pi(N/2+1)P)^{N/2}}{(N/2)!} \right] = \log_2(\pi P) + \log_2(N/2+1) - \frac{2}{N} \cdot \log_2(N/2)!. \tag{14.92}$$

Thus, the spectral efficiency is a constant plus a term that depends on N, where the latter is

$$\log_2\left(\frac{N}{2}+1\right) - \frac{2}{N} \cdot \log_2(N/2)! \tag{14.93}$$

When N goes from 2 to 4, the spectral efficiency increases by 0.085 bits. When N goes from 2 to 6, the spectral efficiency increases by 0.138 bits.

(b) By the Sterling approximation, the increase in spectral efficiency as $N \to \infty$ relative to $N = 2$ is $\log_2 e - 1 = 0.443$ bits per complex symbol. Of course, the absolute (as opposed to relative) spectral efficiency depends on Λ as well as N.

14-7. Let us assume that R is chosen such that $\mathbf{X}_N$ has unit variance components; that is, $R^2 = N+2$. The marginal density of $\mathbf{X}_K$ will be the density of $\mathbf{X}_N$ integrated over $N-K$ components. The integral is over a sphere of radius $\sqrt{R^2 - \|\mathbf{x}_K\|^2}$ and dimension $N-K$. The integrand is the density of $\mathbf{X}_N$, which is a constant $1/V_N(R)$, and thus the integral becomes proportional to the volume of an $(N-K)$-dimensional sphere. Thus,

$$f_{\mathbf{X}_K}(\mathbf{x}_K) = \frac{V_{N-K}(\sqrt{R^2 - \|\mathbf{x}_K\|^2})}{V_N(R)} = \frac{V_{N-K}(1)}{V_N(1)} \frac{\left[1 - \frac{\|\mathbf{x}_K\|^2}{R^2}\right]^{N/2}}{R^K \left[1 - \frac{\|\mathbf{x}_K\|^2}{R^2}\right]^{K/2}}. \tag{14.94}$$

Taking $R^2 = N+2$, or equivalently $R^2 = N$ when N is large, the only term that is a function of $\mathbf{x}_K$ as $N \to \infty$ is the numerator, which assumes the functional form $\exp\{-\|\mathbf{x}_K\|^2/2\}$, a Gaussian density with unit variance and independent components. The remaining constants are of course the normalization to unit area, and must equal $(2\pi)^{-K/2}$ asymptotically.

14-8. It is straightforward to calculate this probability,

$$\Pr\{\|\mathbf{X}\| \le R - \varepsilon\} = \frac{V(S_N[R-\varepsilon)]}{V[S_N(R)]} = \frac{(R-\varepsilon)^N}{R^N} = \left[1 - \frac{\varepsilon}{R}\right]^N \to 0. \tag{14.95}$$

14-9. The trellis for the convolutional coder is shown in the following figure:

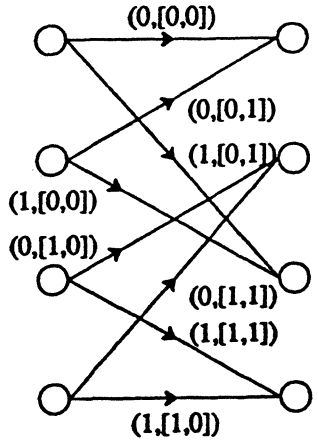

Comparing this to figure 14-9a, if we choose the mapping

$C_k^{(1)}$	$C_k^{(2)}$	A_k
0	0	a
0	1	$-a$
1	0	ja
1	1	$-ja$

then the trellis is identical. Thus with a line coder that implements this mapping, the code is equivalent.

14-10. The trellis for the convolutional coder is shown in the following figure:

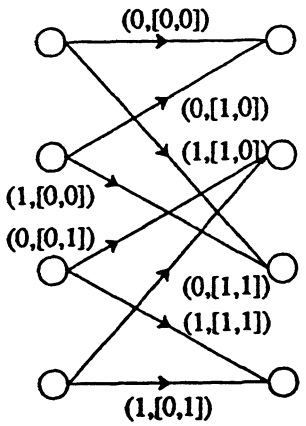

To get a trellis equivalent to that in figure 14-9 we select the mapping

$C_k^{(1)}$	$C_k^{(2)}$	A_k
0	0	a
0	1	ja
1	0	$-a$
1	1	$-ja$

14-11. One stage of the trellis is shown in figure 14-37a. The minimum-distance error event is shown in figure 14-37b for three different correct state trajectories. Also shown is the distance. The distance is different for all three.

14-12.

(a) Four bits per symbol are required, so the alphabet needs 16 symbols. 16-QAM will work.

(b) The required alphabet size is 32. The cross constellation in figure 14-23 will work, although there are others in Chapter 6.

(c) Coding is required. To get 4 dB total gain, using Ungerboeck's rule of thumb (see the first paragraph in Section 14.2.1), an eight state trellis code will work. The coder in figure 14-23 will do the job, and provide the additional benefit of 90 degree phase invariance. If phase invariance is not an issue, then the coder in figure 14-18 will also work, although one additional uncoded bit is required.

14-13. Consider the error events in figure 14-38. There are several error events represented here because of the parallel paths. To find the minimum-distance error event of these, first find the minimum distances between transitions in the same stage of the trellis. These are shown in the figure. For example, in the first stage, the upper parallel pair of transitions are taken from subset A in figure 14-13. The lower pair are taken from subset C. Hence the minimum distance in this stage is the minimum distance between symbols in A and C, or $\sqrt{2}$. The minimum distance in the third stage is similarly computed. The minimum distance in the second stage is the minimum distance between symbols in A and B, which with some simple

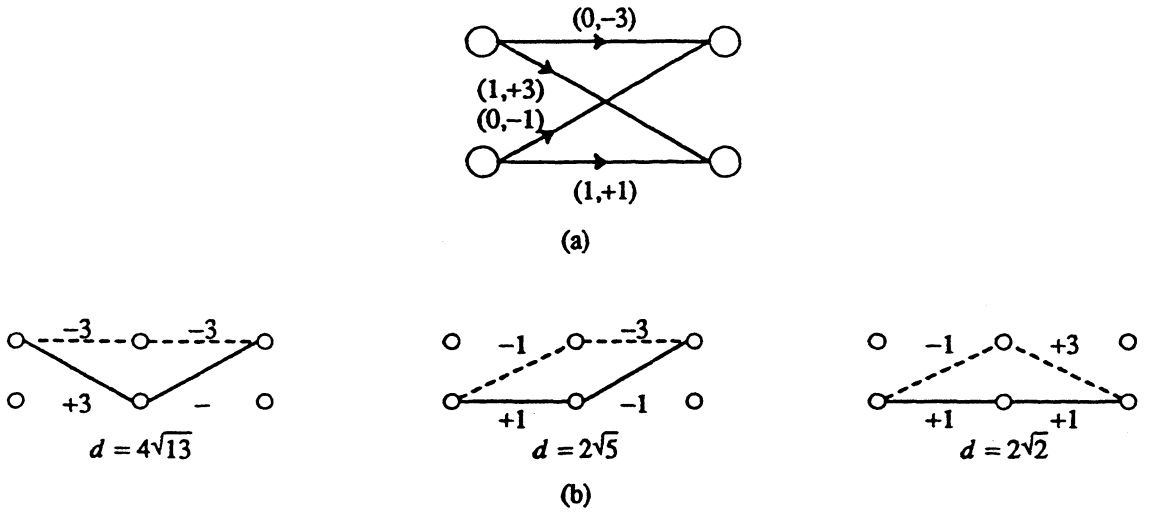

Figure 14-37. a. One stage of the trellis for the trellis coder in figure 14-33. b. The minimum-distance error events when the correct state trajectory is the path shown as a dashed line.

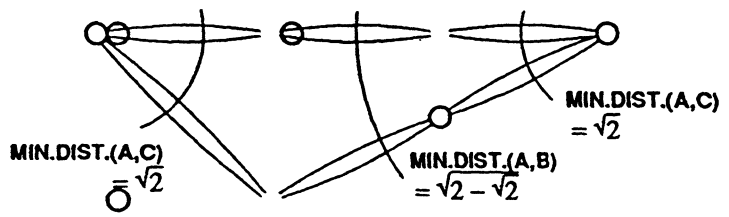

Figure 14-38. A set of error events and their minimum distance.

geometry can be shown to be $\sqrt{2-\sqrt{2}} \approx 0.77$. The minimum distance of all the error events shown is the square root of the sums of the squares of these stage distances, or

$$\sqrt{2+2-\sqrt{2}+2} = \sqrt{6-\sqrt{2}} \approx 2.14 . \tag{14.96}$$

It is easy to see that any error event with length greater than three stages will have a distance greater than these error events, so 2.14 is the distance of the second closest error event.

14-14.

(a) The partition is shown in figure 14-39, along with the minimum distances. Notice that at the final partitioning stage (into 16 subsets) there is no improvement in minimum distance for some of the subsets.

(b) The average power of the 16-QAM constellation has been computed elsewhere and is 10. The 32-cross constellation has all the same points, plus 16 additional points with average power

$$\frac{8}{16}(5^2+3^2)+\frac{8}{16}(5^2+1^2)=30 \tag{14.97}$$

so the overall average power is

$$\tfrac{1}{2}(10+30)=20 . \tag{14.98}$$

This is $10\log(2) = 3$ *dB* more power.

(c) It should be adequate to use the subsets in the third row of figure 14-39. The minimum distance between parallel transitions is 4. There are 4 such subsets, so $\bar{m} = 1$. Compared to the 16-QAM constellation in

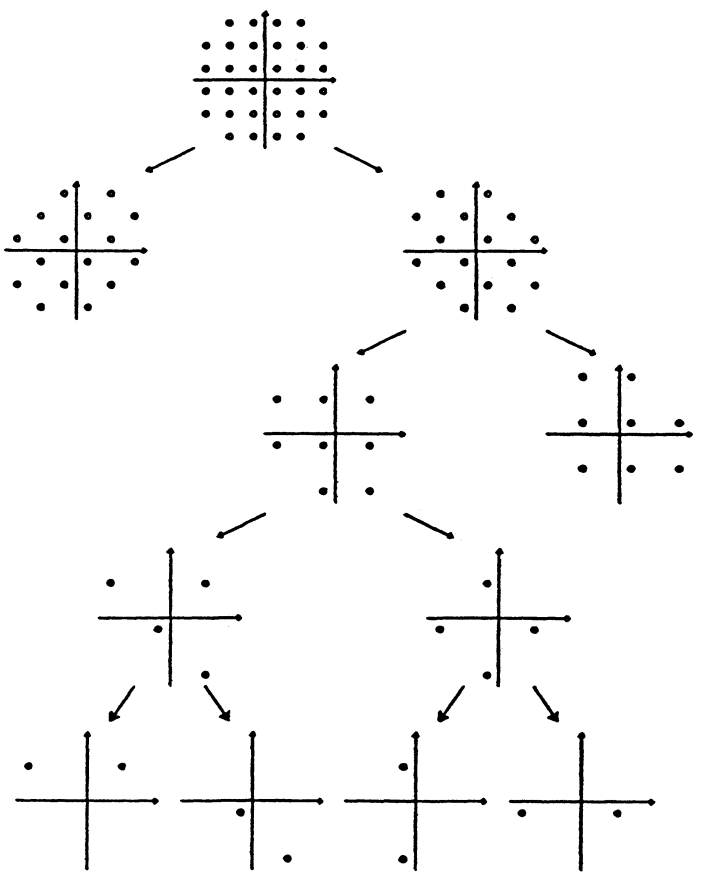

Figure 14-39. Set partitioning for a 32-cross constellation. The minimum distances between points in the subset are shown.

part (b), which has minimum distance 2, this is a 6 dB improvement. However, the power of the 32-cross constellation has to be reduced by 3 dB, so if the parallel transitions have the smallest distance (we can assure this with proper coder design) then the total gain will be about 3 dB. Using Ungerboeck's rule of thumb (see the first paragraph of Section 14.2.1), a coder with 4 states should work.

(d) It should be adequate to use the subsets in the fourth row of figure 14-39. There are 8 such subsets, so $\tilde{m} = 2$. The minimum distance between parallel transitions will be $4\sqrt{2}$, which is about 9 dB better than the minimum distance of 2 in the 16-QAM constellation. Again, of this 9 dB improvement, 3 dB must be sacrificed to normalize the power, leaving a 6 dB gain. This is more than we need, so we could use a 16 state trellis coder to get about 5 dB gain, and the minimum-distance error event will probably not be the parallel transitions.

14-15.

(a) The trick here is to compare to an uncoded system with the same average power. If the 8-PSK symbols have amplitude a, then it has average power a^2. If the 16-QAM symbols have real and imaginary parts that are $\pm b$ or $\pm 3b$, then they have average power $10b^2$. Hence, for the two systems to have the same average power, we require that $a = \sqrt{10}b \approx 3.16b$. The subsets that are used for parallel transitions are in the third row of figure 14-16. The symbols within each subset have minimum distance $4b$, so if the parallel transitions dominate the probability of error, then

$$\Pr[error] \approx Q\left[\frac{2b}{\sigma}\right]. \tag{14.99}$$

The minimum distance for the 8-PSK alphabet is $a\sqrt{2-\sqrt{2}} \approx 0.77a$, so for the uncoded system

$$\Pr[error] \approx Q\left[0.77\frac{a}{2\sigma}\right]. \tag{14.100}$$

The difference is

$$20\log\left[\frac{4b}{0.77a}\right] = 20\log\left[\frac{4}{0.77\sqrt{10}}\right] = 4.3\ dB, \tag{14.101}$$

which is very good indeed.

(b) The trellis is shown in figure 14-40. We can show that the error event with shape as in figure 14-38 is $\sqrt{20}b$, which is greater than the distance $4b$ of the parallel transitions. Hence the assumption in (a) seems reasonable.

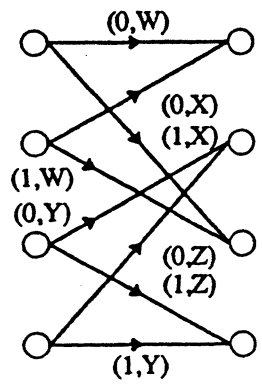

Figure 14-40. Yet another trellis.

14-16. First note that every error event is a minimum-distance error event for all possible actual paths through the trellis. Note further that every error event starts and ends with a symbol error, and has no symbol errors in between, so $w(e) = 2$ for all $e \in E$. Consequently, (9.150) becomes

$$R = 2 \sum_{e \in E} \Pr[\psi] . \tag{14.102}$$

Define $E(\psi)$ to be the set of error events for the actual path ψ through the trellis. Then the summation in (14.102) can be rewritten

$$\sum_{e \in E} \Pr[\psi] = \sum_{\psi} \sum_{e \in E(\psi)} \Pr[\psi] = \left[\sum_{\psi} \Pr[\psi] \right] \left[\sum_{e \in E(\psi)} 1 \right] . \tag{14.103}$$

The first summation is unity, and the second is infinite because every ψ has an infinite number of error events. Consequently, R is unbounded.

14-17.

(a) One stage of the trellis is shown in the following figure.

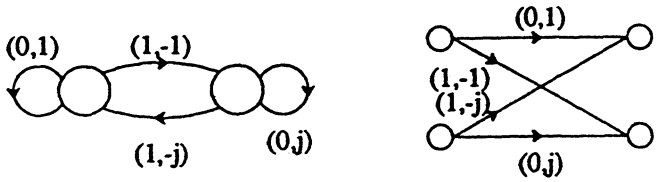

(b) For different assumed correct state trajectories, the minimum-distance error events are shown below.

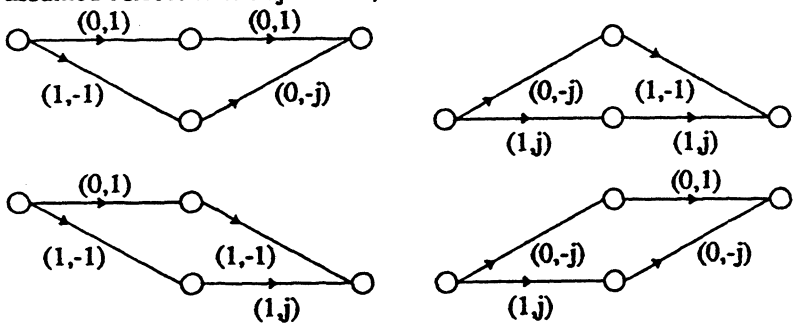

In each case the distance is $d_{E,min} = \sqrt{6}$. The probability of occurrence is therefore $Q(\sqrt{6}/2\sigma)$.

(c) The 2-PSK alphabet with the same power is $\Omega_A = \{-1, +1\}$ which has a minimum distance of 2. The coded system is therefore

$$20\log(\sqrt{6}/2) = 1.76\ dB \tag{14.105}$$

better.

(d) The set partioning is illustrated in the following figure.

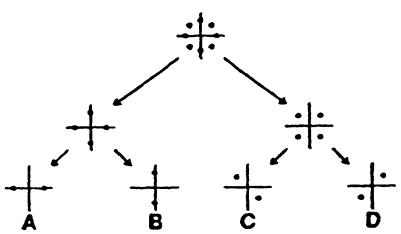

A suitable mapping is shown in the following trellis.

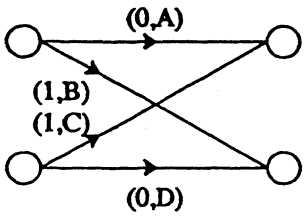

(e) The minimum-distance error event is shown in the following figure.

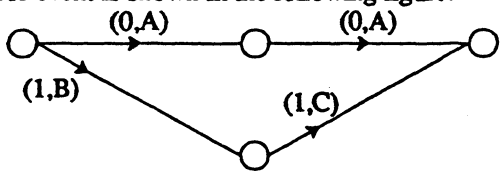

The minimum distance between points in A and points in B is $\sqrt{2}$. The minimum distance between points in A and points in C (find by simple geometry) is $\sqrt{2-\sqrt{2}}$. The total minimum distance is therefore

$$d_{E,min} = \sqrt{4-\sqrt{2}}\,. \tag{14.106}$$

The uncoded (4-PSK) system has a minimum distance $\sqrt{2}$ so the total gain is

$$20\log(\sqrt{4-\sqrt{2}}/\sqrt{2}) = 1.1\ dB\ , \tag{14.107}$$

a modest gain.

14-18. The trellis for the convolutional coder is shown below with the arcs labeled $(B_k^{(1)},[C_k^{(2)}, C_k^{(3)}])$.

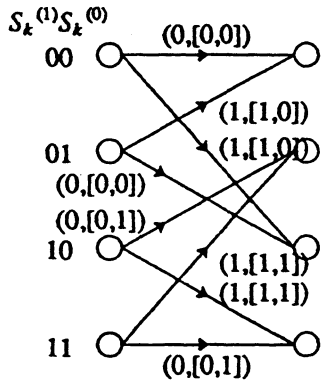

The same subsets of the 8-PSK constellation shown in figure 14-13 can be used in which case the trellis for the trellis code is identical if the mapping is given by the following table.

$C_k^{(2)}$	$C_k^{(2)}$	subset
0	0	A
0	1	B
1	0	C
1	1	D

CHAPTER 15: SOLUTIONS TO PROBLEMS

15-1.

(a) Two.

(b) The loop is unstable because

$$\frac{\Phi(s)}{\Theta(s)} = \frac{K_L}{K_L + s^2} \tag{15.99}$$

which has two poles on the $j\omega$ axis.

15-2. From (15.17)

$$\lim_{K_L \to \infty} \frac{\Phi(s)}{\Theta(s)} = \lim_{K_L \to \infty} \frac{K_L}{K_L + s} = 1 \tag{15.100}$$

so in the limit the output phase is identical to the input phase. The bandwidth of the PLL goes to infinity. This might be useful for carrier recovery, example 15-2, and not for timing recovery on point-to-point links, example 15-1. In either case, no noise on the input will be rejected.

15-3.

(a) Since the coefficients are real, the roots are complex conjugate pairs. We can write the two roots $Ae^{\pm j\theta}$, where $A > 0$. Then

$$s^2 + as + b = (s - Ae^{j\theta})(s - Ae^{-j\theta}) = s^2 - 2A\cos(\theta) + A^2 . \tag{15.101}$$

Noting that $b = A^2$ we observe that $b > 0$ unless $A = 0$, in which case the poles are both at zero and hence not in the open left half plane. Also note that $2A\cos(\theta) = a$. Hence the poles are in the open left half plane if and only if $a > 0$.

(b) The result follows trivially from part a.

15-4.

(a) From (15.15)

$$\frac{\Phi(s)}{\Theta(s)} = \frac{1}{s^2 + \sqrt{2}s + 1} , \tag{15.102}$$

which has poles at

$$s = \frac{-1}{\sqrt{2}} \pm \frac{j}{\sqrt{2}} . \tag{15.103}$$

The PLL is stable.

(b) For all ω,

$$\left| \frac{\Phi(j\omega)}{\Theta(j\omega)} \right|^2 = \frac{1}{1 + \omega^4} \leq 1 . \tag{15.104}$$

(c) From (b)

$$\left| \frac{\Phi(j\omega)}{\Theta(j\omega)} \right| = \frac{1}{\sqrt{1+\omega^4}}. \tag{15.105}$$

15-5.

(a) From (15.21)

$$\frac{\Phi(s)}{\Theta(s)} = \frac{s+0.5}{s^2+2s+0.5}. \tag{15.106}$$

(b) The conditions in problem 15-3 are satisfied so the PLL is stable.

(c) The poles are at $s = -1 \pm \sqrt{2}/2$ and the zero is at $s = -0.5$. This leads to the Bode plot below:

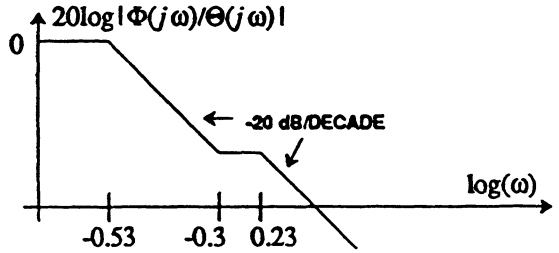

(d) We need to prove that for all ω

$$\left| \frac{\Phi(j\omega)}{\Theta(j\omega)} \right|^2 \le 1 \tag{15.107}$$

But

$$\left| \frac{\Phi(j\omega)}{\Theta(j\omega)} \right|^2 = \left| \frac{j\omega+0.5}{-\omega^2+2j\omega+0.5} \right|^2 = \frac{\omega^2+0.25}{\omega^4+3\omega^2+0.25} \tag{15.108}$$

Hence proving (15.107) is equivalent to proving

$$\omega^4+3\omega^2+0.25 \ge \omega^2+0.25 \tag{15.109}$$

or

$$\omega^2+2 \ge 0 \tag{15.110}$$

which is obviously true.

15-6.

(a)

$$\left| \frac{\Phi(j\omega)}{\Theta(j\omega)} \right|^2 = \left| \frac{K_L j\omega + K_L K_1}{-\omega^2+(K_L+K_2)j\omega+K_L K_1} \right|^2 = \frac{K_L^2\omega^2 + K_L^2 K_1^2}{(K_L+K_2)^2\omega^2+(K_L K_1-\omega^2)^2} \tag{15.111}$$

Peaking occurs if and only if for some ω

$$\left|\frac{\Phi(j\omega)}{\Theta(j\omega)}\right|^2 > 1 \tag{15.112}$$

or

$$K_L^2\omega^2 + K_L^2 K_1^2 > (K_L+K_2)^2\omega^2 + (K_L K_1-\omega^2)^2 \tag{15.113}$$

or

$$0 > K_2^2 - 2K_L K_1 + \omega^2 \tag{15.114}$$

so peaking occurs if and only if

$$\omega^2 < 2K_L K_1 - K_2^2 \,. \tag{15.115}$$

Hence there are frequencies at which the gain is greater than unity if and only if

$$K_2^2 < 2K_L K_1 \,. \tag{15.116}$$

(b) Given by (15.115).

(c) The lock range of the second-order loop is

$$\pi |K_{L2} K_1 / K_2| \tag{15.117}$$

from (15.20) so without peaking, since $K_2^2 \geq 2K_{L2}K_1$ or $K_2 \geq \sqrt{2K_{L2}K_1}$,

$$\text{lock range} \leq \frac{\pi}{\sqrt{2}} \sqrt{K_{L2} K_1} \,. \tag{15.118}$$

Using (15.73) we get that the lock range for the second-order loop satisfies

$$\text{lock range} \leq \frac{\pi}{\sqrt{2}} K_{L1} \,. \tag{15.119}$$

Comparing this to (15.18), the lock range of the first-order PLL, we see that it is smaller by a factor of $1/\sqrt{2}$.

15-7.

(a) Stability implies that $K_L K_1 > 0$, and since $K_2 = 0$, (15.72) is always true.

(b) From (15.21) we get

$$\left| \frac{\Phi(j\omega_n)}{\Theta(j\omega_n)} \right|^2 = \left| \frac{K_L K_1 + K_L j\sqrt{K_L K_1}}{K_L j\sqrt{K_L K_1}} \right|^2 = \frac{K_1 + K_L}{K_L} \,. \tag{15.120}$$

(c) From problem 15-3 we know that the type I PLL is stable if and only if $K_2 > -K_L$ and $K_L K_1 > 0$. Since in this case $K_2 = 0$, this is equivalent to the conditions stated in the exercise.

15-8.

(a) The transfer function is

$$\frac{\Phi(s)}{\Theta(s)} = \frac{K_1}{K_1 + K_2 s + s^2} \,. \tag{15.121}$$

This is an all pole transfer function, and hence is a lowpass filter. The d.c. gain is unity.

(b) This follows immediately from problem 15-3.

(c) Input $\Theta(j\omega)$ will be amplified for values of ω for which $|\Phi(j\omega)/\Theta(j\omega)|^2 > 1$. We can write

$$\left| \frac{\Phi(j\omega)}{\Theta(j\omega)} \right|^2 = \frac{K_1^2}{K_1^2 + (K_2^2 - 2K_1)\omega^2 + \omega^4} \,. \tag{15.122}$$

This is greater than or equal to unity when

$$\omega^2 \leq 2K_1 - K_2^2 \,. \tag{15.123}$$

Clearly if

$$2K_1^2 \leq K_2^2 \tag{15.124}$$

there is no amplification for any ω.

15-9.

(a) First note that $\Theta(s) = \beta/s$. From (15.31)

$$\varepsilon_{ss} = \lim_{s \to 0} \frac{s^2\Theta(s)}{L(s)+s} = \lim_{s \to 0} \frac{s\beta}{K_L + s} = 0 . \tag{15.126}$$

(b) Now $\Theta(s) = 2\beta/s^3$, so from (15.31)

$$\varepsilon_{ss} = \lim_{s \to 0} \frac{2\beta}{sK_L + s^2} = \infty . \tag{15.127}$$

15-10. The loop filter has the form

$$L(s) = \frac{N(s)}{D(s)} \tag{15.128}$$

where $N(0) \neq 0$ and $D(0) = 0$. From (15.31)

$$\varepsilon_{ss} = \lim_{s \to 0} \frac{\omega_0}{L(s)+s} = \lim_{s \to 0} \frac{\omega_0 D(s)}{N(s) + sD(s)} = 0 . \tag{15.129}$$

15-11. In each case

$$\left| \frac{\Phi(e^{j\omega T})}{\Theta(e^{j\omega T})} \right| = \frac{|K_L|}{|K_L - 1 + e^{j\omega T}|} = \frac{|K_L|}{\sqrt{K_L^2 + 2 - 2K_L + 2(K_L - 1)\cos(\omega T)}} . \tag{15.130}$$

(a)

$$\left| \frac{\Phi(e^{j\omega T})}{\Theta(e^{j\omega T})} \right| = \frac{0.5}{\sqrt{1.25 - \cos(\omega T)}} , \tag{15.131}$$

shown in figure 15-17a.

(b)

$$\left| \frac{\Phi(e^{j\omega T})}{\Theta(e^{j\omega T})} \right| = 1 , \tag{15.132}$$

shown in figure 15-17b.

(c)

$$\left| \frac{\Phi(e^{j\omega T})}{\Theta(e^{j\omega T})} \right| = \frac{1.5}{\sqrt{1.25 + \cos(\omega T)}} , \tag{15.133}$$

shown in figure 15-17c.

(d) The loop filter in (b) is not particularly useful because it results in an all-pass filter. The loop filter in (c) is even less useful because it amplifies the phase of the input at all frequencies.

15-12. Expanding we see that

$$D(z) = z^2 - (q+p)z + pq \tag{15.134}$$

so

$$pq = b \quad \text{and} \quad q + p = -a . \tag{15.135}$$

If p and q are inside the unit circle, $|p| < 1$ and $|q| < 1$, then

$$|pq| = b < 1 . \tag{15.136}$$

We now need to show that p and q inside the unit circle also imply that

$$|a| = |q + p| < 1 + pq . \tag{15.137}$$

15-13. From problem 15-12, the PLL is stable if and only if

$$\left| \frac{a_0 - b_0}{a_2 + b_1} \right| < 1 \tag{15.138}$$

and

$$\left| \frac{a_1 + b_0 - b_1}{a_2 + b_1} \right| < 1 + \frac{a_0 - b_0}{a_2 + b_1} . \tag{15.139}$$

15-14. Since $\theta(t) = \phi(t)$, $\cos(\theta(t) - \phi(t)) = 1$, so from (15.58)

$$\varepsilon(t) = \frac{A_v A_y}{2} . \tag{15.140}$$

This is a d.c. term so

$$c(t) = \frac{A_v A_y}{2} L(0) = \frac{d\phi(t)}{dt} . \tag{15.141}$$

Hence

$$\phi(t) = \int_0^t \frac{A_v A_y}{2} L(0) dt + K \tag{15.142}$$

for some constant K, so

$$\theta(t) = \phi(t) = \frac{A_v A_y}{2} L(0) t + K . \tag{15.143}$$

15-15. The VCO output frequency can range from 1 MHz/(N + 1) to 1 MHz/(N − 1), or about 9.9 kHz to 10.1 kHz. The lock range is therefore about 200 Hz.

15-16.

(a) 2,048 = 256×8 while 1,512 = 189×8. 256 and 189 are relatively prime, so N = 256 and M = 189.

(b) We can write

$$\frac{256}{189} = \frac{16}{9} \times \frac{16}{21} \tag{15.144}$$

(among many other factorizations). Hence we can used cascaded frequency dividers with $N_1 = N_2 = 16$ and $M_1 = 9$ and $M_2 = 21$. The first frequency synthesizer will produce a signal with frequency 2,688 kHz = 16×1,512 kHz/9, and its phase comparator will be comparing the phases of two signals with frequencies on the order of 168 kHz. The second phase comparator will be comparing signals with frequencies on the order of 128 kHz. The main advantage is the greatly relaxed design of the LPFs and faster response time (see example 15-15).

(c) The maximum number of cascaded frequency synthesizers is 8, evident from the prime factorization

$$\frac{256}{189} = \frac{2\times2\times2\times2\times2\times2\times2\times2}{3\times3\times3\times7} . \tag{15.145}$$

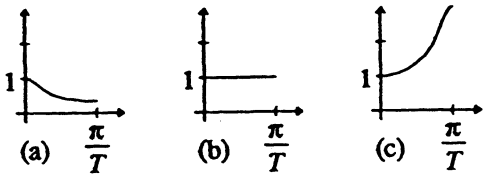

Figure 15-17. Frequency response of the first-order discrete-time PLL with three different values of the loop gain. The frequency response is symmetric and periodic so it is only shown over the region $0 \leq \omega \leq \pi/T$.

CHAPTER 16: SOLUTIONS TO PROBLEMS

16-1.

(a) We need

$$\theta_k - \phi_k = \theta_{k-1} - \phi_{k-1} + M\pi/2 \tag{16.30}$$

which corresponds to an offset frequency (in radians) of

$$\omega_0 = \frac{M}{T}\frac{\pi}{2}. \tag{16.31}$$

(b) The minimum offset frequency corrsponds to $M = 1$, so

$$\omega_0 = \frac{1}{T}\frac{\pi}{2}. \tag{16.32}$$

In this case, $(1/T) = 15\times10^6$, so the minimum offset if 15/4 MHz.

(c) If the channel frequency offset is constrained to be small, then the VCO output frequency range can also be constrained to be small enough that the sum of the two offsets is less than half that which leads to false lock.

16-2.

(a)

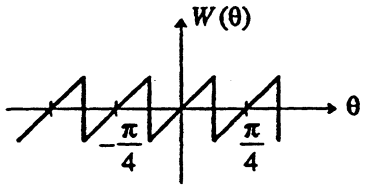

(b) Suppose that $A_k = 3 + j$, which has angle $\sin^{-1}(1/3) \approx 0.34$ radians. An decision error occurs if the phase error is less than –0.34 or greater than +0.22, half the angular difference between A_k and the symbol $3 + 3j$. $W(\cdot)$ is shown in the following figure:

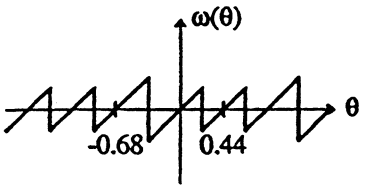

16-3.

(a) From (15.44) we have

$$\frac{\Phi(z)}{\Theta(z)} = \frac{0.1}{z - 0.9} \tag{16.33}$$

which has a pole at $z = 0.9$. The frequency response is similar to that in figure 15-17a, but with a stronger lowpass characteristic.

(b) From (15.44) we have

$$\frac{\Phi(z)}{\Theta(z)} = \frac{0.1z^{-1}}{0.1z^{-1}+z-1} = \frac{0.1}{z^2-z+0.1}, \tag{16.34}$$

which has poles at 0.89 and 0.11. The frequency response is still reasonable, although slightly compromised. Since the poles are all real there cannot be peaking.

(c) From (15.44) we have

$$\frac{\Phi(z)}{\Theta(z)} = \frac{0.1z^{-2}}{0.1z^{-2}+z-1} = \frac{0.1}{z^3-z^2+0.1}. \tag{16.35}$$

The poles can be found using a computer program, or by the following method. The system has at least one real pole, call it a, so

$$(z-a)H(z) = z^3 - z^2 + 0.1, \tag{16.36}$$

for some second-order polynomial $H(z)$. We can find $H(z)$ by long division

$$H(z) = \frac{z^3-z^2+0.1}{z-a} = z^2 + (a-1)z + a(a-1) + r(a) \tag{16.37}$$

where the remainder is

$$r(a) = 0.1 + a^2(a-1). \tag{16.38}$$

For a to be a pole, the remainder must be zero, so

$$a^3 - a^2 = -0.1 \tag{16.39}$$

which by successive approximation implies that

$$a \approx 0.87. \tag{16.40}$$

Consequently,

$$\frac{\Phi(z)}{\Theta(z)} = \frac{0.1}{(z-0.87)(z^2-0.13z-0.11)}. \tag{16.41}$$

The poles are at $z = 0.87, 0.40$, and -0.27. The system is stable.

(d)

$$\frac{\Phi(z)}{\Theta(z)} = \frac{0.1z^{-M}}{0.1z^{-M}+z-1} = \frac{0.1}{z^{M+1}-z^M+0.1}. \tag{16.42}$$

This goes unstable when M is 16 or larger. It exhibits peaking when M is 3 or larger.

16-4.

(a) There is no integer N such that

$$e^{jN\arg(A_m)} = 1 \tag{16.43}$$

because the angles of the symbols are not related by rational multiples.

(b) $N = 4$ will work.

16-5.

(a) $N = 4$, so $\omega_v = 2\pi\times2400\times4$. The smallest required lock range is ±2%,

$$|\omega_0| \le 1200 rad/sec \quad or \quad 192 Hz. \tag{16.44}$$

(b) Insert a "divide by N" between $(\cdot)^N$ and the phase detector in figure 16-8. The frequency divider might be preceded by a hard limiter for each of the real and imaginary parts.

16-6.

(a)

$$R(t)=\frac{1}{2}\left[e^{j(\omega_c t+\theta(t))}S(t)+e^{-j(\omega_c t+\theta(t))}S^*(t)\right]. \tag{16.45}$$

Hence

$$R^2(t)=\frac{1}{4}\left[e^{2j(\omega_c t+\theta(t))}S^2(t)+2|S(t)|^2+e^{-2j(\omega_c t+\theta(t))}S^{*2}(t)\right] \tag{16.46}$$

from which the result follows.

(b) The periodicity would come from the second term of (16.27). It is easy to show that for 4-PSK

$$E[\mathrm{Re}\{S^2(t)\}]=0 \tag{16.47}$$

so the expect value of the second term is zero.

(c) As long as

$$E[\mathrm{Re}\{S^2(t)\}]\neq 0 \tag{16.48}$$

there will be tone at $2\omega_c$. As long as A_m is white,

$$\mathrm{Re}\{S^2(t)\}=\sum_{m=-\infty}^{\infty}\left[[\mathrm{Re}\{A_m\}]^2-[\mathrm{Im}\{A_m\}]^2\right]p^2(t-mT) \tag{16.49}$$

which has nonzero expected value if

$$E\left[[\mathrm{Re}\{A_m\}]^2-[\mathrm{Im}\{A_m\}]^2\right]\neq 0. \tag{16.50}$$

CHAPTER 17: SOLUTIONS TO PROBLEMS

17-1. Using (17.48), and sampling $Q(t)$ at $t=kT+\alpha$, the summation is a convolution, and the filter impulse response is easily seen to be

$$h_n=\frac{\sin\frac{\pi}{T}(nT-\tau+\alpha)}{\frac{\pi}{T}(nT-\tau+\alpha)} \tag{17.72}$$

Clearly, an exact non-recursive implementation has infinite order. The impulse response can be approximated as FIR by truncation, but it falls off only linearly with n, so using a small number of taps will introduce substantial error.

17-2. First note that since the pulse has only 100% excess bandwidth, the Fourier series coefficients Z_m for $|m|\geq 2$ are zero. From (6.25), the pulse has Fourier transform

$$P(j\omega)=\begin{cases}\frac{T}{2}\{1-\sin[\frac{T}{2}(\omega-\frac{\pi}{T})]\}; & |\omega|\leq\frac{2\pi}{T}\\ 0; & \text{otherwise}\end{cases} \tag{17.73}$$

From (17.10),

$$Z_1 = \frac{E[|A_k|^2]}{T}\int_{-\infty}^{\infty} P(j\frac{2\pi}{T} - j\omega)P(j\omega)d\omega.$$
$$= E[|A_k|^2]\frac{T}{4}\int_0^{2\pi/T}\{1-\sin\left[\frac{T}{2}(\frac{\pi}{T}-\omega)\right]\}\{1-\sin\left[\frac{T}{2}(\omega-\frac{\pi}{T})\right]\}d\omega. \quad (17.74)$$

Using trigonometric identities, we find that

$$Z_1 = E[|A_k|^2]\left[\frac{\pi}{2} + \frac{T}{8}\int_0^{2\pi/T}\{\cos[\pi - T\omega] - 1\}d\omega\right]$$
$$= E[|A_k|^2]\left[\frac{\pi}{4} - \frac{T}{8}\sin(\pi - T\omega)|_0^{2\pi/T}\right] = E[|A_k|^2]\frac{\pi}{4} \quad (17.75)$$

From (17.11)

$$z(t) = E[|R(t)|^2] = E[|A_k|^2]\left[Z_0 + \frac{\pi}{2}\cos(\frac{2\pi}{T}t)\right] \quad (17.76)$$

implying a strong timing tone. Square law timing recovery works well with PAM signals with raised cosine Nyquist pulses with large excess bandwidth.

17-3. The 0% excess bandwidth pulse is

$$g(t) = \frac{\sin \pi t/T}{\pi t/T}$$

and has the Fourier transform

$$G(\omega) = \begin{cases} \frac{T}{2}; & |\omega| \le \frac{\pi}{T} \\ 0; & \text{otherwise} \end{cases}.$$

From (17.10),

$$X_1 = \frac{1}{T}\int_{-\infty}^{\infty} G(\frac{2\pi}{T} - \omega)G(\omega)d\omega = 0$$

17-4. Write the autocorrelation function

$$R_R(\tau) = E[R(t+\Theta+\tau)R^*(t+\Theta)]$$
$$= E[\sum_{m=-\infty}^{\infty}\sum_{n=-\infty}^{\infty} A_m A_n^* p(t+\Theta+\tau-mT)p(t+\Theta-nT)]$$
$$= a\sum_{m=-\infty}^{\infty} E[p(t+\Theta+\tau-mT)p(t+\Theta-nT)]$$
$$= a\sum_{m=-\infty}^{\infty}\frac{1}{T}\int_0^T p(t+\theta+\tau-mT)p(t+\theta-nT)d\theta$$
$$= a\sum_{m=-\infty}^{\infty}\frac{1}{T}\int_{-mT}^{-mT+T} p(t+\theta+\tau)p(t+\theta)d\theta \quad (17.77)$$
$$= a\frac{1}{T}\int_{-\infty}^{\infty} p(t+\theta+\tau)p(t+\theta)d\theta$$
$$= a\frac{1}{T}\int_{-\infty}^{\infty} p(\theta+\tau)p(\theta)d\theta.$$

The Fourier transform of this is

$$S_R(j\omega) = \frac{a}{T}|P(j\omega)|^2 \tag{17.78}$$

which has no spectral lines at the symbol frequency if $p(t)$ is not periodic with period T.

17-5. The Fourier transforms that are used to compute the timing tone are shown in figure 17-15. Note that the entire signal is used. There is no useful prefiltering.

17-6. The conditions in (17.54) imply that $\omega_v t + \phi(t)$ evaluated at $kT + \tau_k$ is $3\pi/2$ plus any multiple of 2π. Hence we can write

$$\omega_v kT + \omega_v \tau_k + \phi(kT + \tau_k) = \frac{3\pi}{2} + k2\pi . \tag{17.79}$$

17-7.

(a) Write

$$\begin{aligned} f(\tau_k) &= \mathrm{E}[-A_k Q_{k-1}(\tau_k) + A_{k-1} Q_k(\tau_k)] \\ &= \mathrm{E}[-\sum_{m=-\infty}^{\infty} A_k A_m p((k-m-1)T + \tau_k) + A_k N_k \\ &\quad + \sum_{m=-\infty}^{\infty} A_k A_m p((k-m)T + \tau_k) + A_k N_k] \\ &= \mathrm{E}[|A_k|^2][p(\tau_k - T) - p(\tau_k + T)] . \end{aligned} \tag{17.80}$$

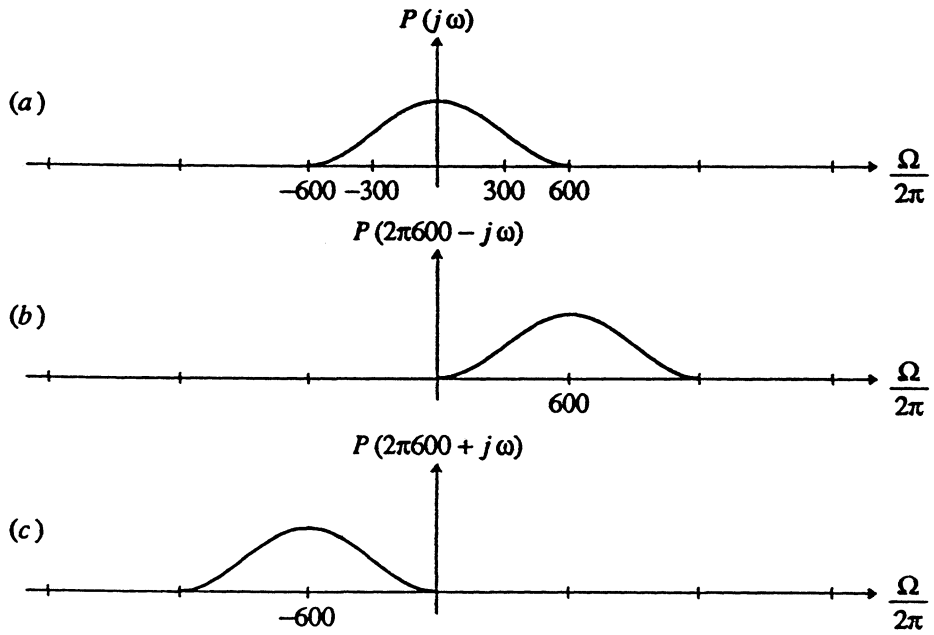

Figure 17-15. An illustration of prefiltering for recovering timing of a 600 baud, 100% excess bandwidth raised cosine signal. The Fourier transform of the pulse is shown in (a). The Fourier transforms in (b) and (c) are multiplied by the one in (a) and integrated to get the timing tone. Note that the whole signal contributes to the timing tone.

(b) The timing function is plotted in the following figure:

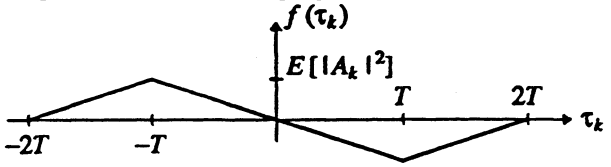

17-8.

(a) Write

$$Z_k = A_{k-1}Q_k(\tau_k) = \sum_{m=-\infty}^{\infty} A_{k-1}A_m p((k-m)T + \tau_k). \tag{17.82}$$

Then

$$f(\tau_k) = \mathrm{E}[Z_k] = \mathrm{E}[|A_k|^2]p(\tau_k + T). \tag{17.83}$$

(b) For the triangular pulse, the timing function is just a shifted and scaled version of the triangular pulse.

(c) The method does not look good for triangular pulses (no unique zero crossing of the timing function) but will work for raised cosine pulses, especially if the excess bandwidth is low.

(d)

$$f(\tau_k) = \mathrm{E}[Z_k] = \mathrm{E}[|A_k|^2]p(\tau_k - T). \tag{17.84}$$

This again will work for raised cosine pulses with low excess bandwidth.

17-9. The only frequencies that will contribute to the jitter power are those where $H(j\omega)$ is near unity in magnitude, or $\omega \ll K_L$. Investigating this region further, let $\varepsilon = \omega/K_L \ll 1$, and do a Taylor series expansion,

$$\frac{1}{(}1 + j\varepsilon)^N \approx jN\varepsilon - \tfrac{1}{2}N(N+1)\varepsilon^2, \tag{17.85}$$

and hence

$$H_T(jK_L\varepsilon) \approx N\left[1 - j\frac{N+1}{2}\varepsilon\right]. \tag{17.86}$$

We see that $|H_{\mathrm{TOTAL}}(j\omega)|$ is a lowpass filter with cutoff frequency at approximately $\varepsilon = 2/N$ or $\omega = 2K_L/N$. An ideal lowpass filter with this cutoff would have a jitter power twice that predicted in example 17-13; the difference is due to the deviation from an ideal filter.

CHAPTER 18: SOLUTIONS TO PROBLEMS

18-1.

(a) One superframe of 1176 bits corresponds to 6·48 = 288 bits on each input. The bit rate is thus 1176·1544/288 = 6,304.7 kb/s.

(b) One superframe corresponds to 288 bits at 1,544 kb/s, which is 186.53 μsec. A frame is one-quarter this, or 46.6 μsec.

18-2. The traffic burst contains 2 ms · 1.544 kb/s = 3088 information bits. The information portion of a traffic burst consumes 25.56 μsec, and there is room for 78 time-slots in the absence of overhead. Since there are more time-slots required in the G.733 case, overhead is going to be more of a factor, and therefore in practice a fewer number of voiceband channels will be accommodated.

18-3.

(a) Regardless of the location of the error, we will fail to recognize the start of the link-frame. In fact, we will incorrectly infer the end-flag to be a start-flag, since the end-flag cannot occur in the information packet. In the absence of a recovery procedure or additional bit-errors, we will perpetually detect each idle period as a link frame and each link frame as an idle period!

(b) We will erroneously detect the start flag of the next link frame as the end flag of the current packet. The end effect will be the same as in a.

(c) Most locations of errors will not cause a loss of link frame synchronization, although some will. In particular, it is possible for a bit-error to create an end flag within the information packet. The effect will be to shorten that packet, and then cause the same major problem as in a. and b.; namely, reversal of the link frames and idle periods.

Clearly these problems suggest the need for a means of detecting the reversal of link frames and idle periods, as well as indicate that individual packets will be "lost", meaning that they will not be recognized at the receiver.

18-4. There are an infinite number of possibilities, but here are two:

- Poll each buffer in order, but if more than one packet is waiting in a buffer take only one packet, the oldest, for transmission.

- At each cycle take a packet from the buffer the closest to overflow; that is, the one with the largest number of packets stored.

18-5. The probability of j packets sitting in the buffer is given by (3.129), $\rho^j(1-\rho)$.

(a) The average number of packets in the queue is given by

$$M = \sum_{j=0}^{\infty} j\rho^j(1-\rho) = \frac{\rho}{1-\rho} \quad . \tag{18.17}$$

The summation of this series can be obtained by differentiating the series $\sum_{j=0}^{\infty} \rho^j$.

(b) This follows from the summation

$$\sum_{j=M}^{\infty} \rho^j(1-\rho) = \rho^M \quad . \tag{18.18}$$

(c) With a finite buffer the multiplex is no longer modeled as an M/M/1 queue, so the previous results are not directly applicable. However, the probability of a buffer that can hold M packets overflowing should be approximately the same as an infinite buffer exceeding M packets waiting for transmission.

18-6.

(a) The average length of a packet is 500 bits divided by 1 Mb/s, or 0.5 msec. The utilization is therefore 0.5/3.0 = 0.17.

(b) The utilization of the output link must be 5 times the incoming links, or 0.833.

(c) The average service time on the outgoing link is the time it takes to transmit 500 bits at 2 Mb/s, or 0.25 msec. The queueing delay is therefore

$$0.25 \cdot \frac{0.833}{1-0.833} = 1.25 \text{ msec} . \tag{18.19}$$

18-7. If we transmit our packet at time t_0, constrained to be the beginning of a time-slot, a collision occurs only if a packet (including retransmissions) arrives at another node in the interval $[t_0 - 1/\mu, t_0]$. The probability of this occurring is $e^{-\rho_{in}}$, and hence we get the load equation $\rho_X = \rho_{out} e^{-\rho_{in}}$ leading to a doubling of throughput. This equation is plotted in figure 18-9.

CHAPTER 19: SOLUTIONS TO PROBLEMS

19-1. If we use the precoder plus $(1 - D)$ filter, we must connect the echo canceler after the precoder, since it is nonlinear in the sense that it cannot be modeled as a continuous-amplitude transversal filter. We can connect the echo canceler before the filter, since it is linear, and the filter will simply be a part of the echo path. It is in fact advantageous to do so, since for binary transmission the filter output has three levels and the input two, simplifying the "multipliers" in the echo canceler. An alternative would be to directly code the input signal to a three-level signal (zero-bits to zero level, one-bits to alternating positive and negative levels). In this case, the coder output, a three-level signal, would be connected to the echo canceler. Thus, the precoder realization is probably more attractive because of the simplification to the echo canceler.

19-2.

(a) Either 7200 ($R = 3$) or 9600 Hz ($R = 4$) could be used. The tradeoff is that the former rate would allow a lower multiply rate in the canceler, and the latter would result in simpler anti-alias and phase-splitter filter designs since there would be a greater guard-band between the highest signal frequency and filter cutoff frequency.

(b) Assume $R = 4$. For interleaved cancelers, each canceler would require 32×2.4 = 76.8 thousand complex multiplies per second, and all four cancelers would require 307.2 thousand complex multiplies per second. For the single canceler connected to the transmitter output, the canceler would have 32×4 = 128 taps, and would calculate its output at a rate of 9600 Hz, for a multiply rate of 1228.8 thousand multiplies per second (four times higher than the interleaved cancelers).

19-3.

(a) As discussed in Chapter 6, we can use a phase splitter followed by demodulator as shown below:

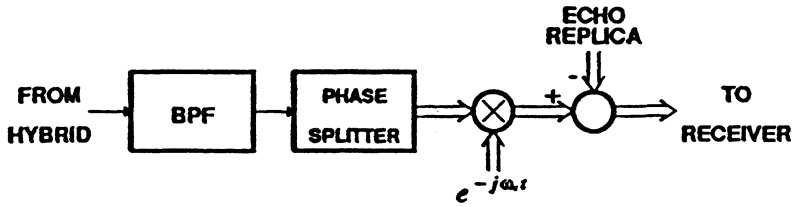

Alternatively, we can use the demodulator followed by bandpass filter as shown below:

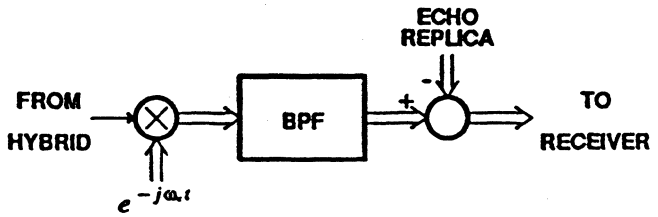

In this case the bandpass filter serves two purposes — elimination of out-of-band noise and rejection of double frequency components. Both configurations generate a baseband complex envelope signal, allowing us to do complex-error cancellation and giving us a demodulated signal ready to be fed into the receiver.

(b) No, because the signal is baseband we need both real and imaginary parts. We could modulate to passband again after cancellation and take the real part, but this would be silly.

(c) A baseband transversal filter echo canceler with complex coefficients and no modulator will be appropriate.

(d) This configuration would be identical to the complex-error canceler described in the chapter.

(e) This configuration eliminates the modulator in the echo canceler, which is an advantage. It is probably the appropriate configuration for the case where the two directions are synchronous. But where they are not synchronous, it requires interpolation of the complex envelope, which requires two lowpass filters rather than one.

19-4. Four cases must be considered:

1. *Complex-error and baseband transversal filter.* The transversal filter requires N multiplies, each with four real-valued multiplies, and the modulator requires four multiplies, for a total of $R\,(4N+4)$ real-valued multiplications per baud.

2. *Complex-error and passband transversal filter.* The transversal filter requires N multiplies, each with four real-valued multiplies, and the modulator requires no multiplies, for a total of $R\,(4N)$ real-valued multiplications per baud.

3. *Real-error and baseband transversal filter.* The transversal filter requires N multiplies, each with four real-valued multiplies, and the modulator requires two multiplies (since only the real part of the output is required), for a total of $R\,(4N+2)$ real-valued multiplications per baud.

4. *Real-error and passband transversal filter.* The transversal filter requires N multiplies, each with two real-valued multiplies (since only the real part of the output is required), and the modulator requires no multiplies, for a total of $R\,(2N)$ real-valued multiplications per baud.

Clearly, assuming that it meets the other system requirements the real-error canceler with passband transversal filter is the most attractive. It has approximately half the multiplication rate of the other configurations.

19-5. One possible configuration is shown below:

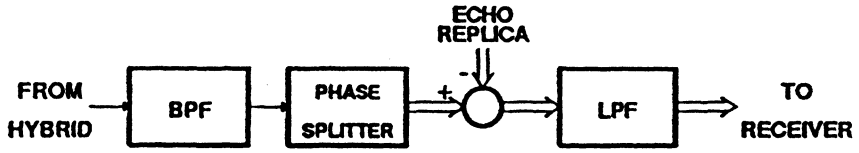

We use a complex-error canceler, which generates an analytic signal representation of the far-end data signal. We can interpolate this far-end signal using a complex lowpass filter, followed by sampler synchronous with the far-end data signal. Another possibility would be to put the receive demodulation after the phase splitter and before cancellation (problem 19-3), thereby simplifying the canceler.

19-6. If we approach this problem intelligently it is trivial. First we draw the channel model and corresponding baseband transversal filter model below:

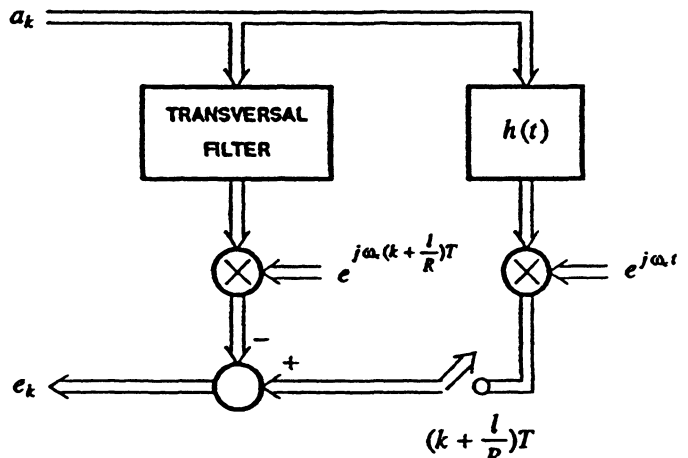

Then note that the two modulators can be moved through the difference operation and combined into a single modulator as shown below:

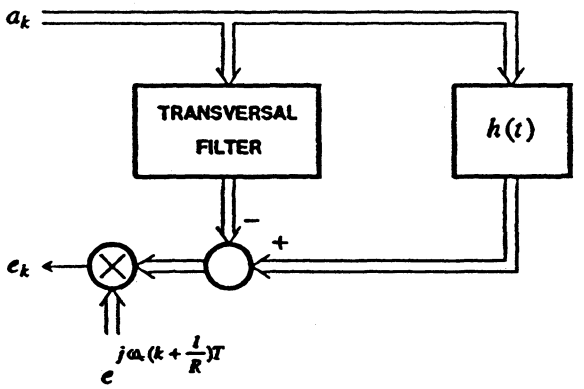

Since

$$|E_k| = |e^{-j\omega_c(k+\frac{l}{R})T} E_k| \tag{19.114}$$

minimizing $|E_k|^2$ is equivalent to minimizing the variance of the difference operation output. But the latter problem is identical to the passband transversal filter case with $\tilde{A}_k$ replaced by A_k and $\tilde{h}_k$ replaced by h_k. Hence the solution is the same with a simple redefinition of Φ and $\mathbf{p}$.

19-7. As long as we deal with ($e^{-j\omega_c(k+\frac{1}{R})T}E_k$) rather than E_k for the baseband transversal case, there is an equivalence between the two echo canceler structures (exercise 19-2). The convergence formulas will all apply as long as we replace $\tilde{a}_k$ by a_k and $\tilde{h}_k$ by h_k. The convergence rate and asymptotic MSE are not affected by h_k, so that substitution makes no difference. If the transmitted data symbols are uncorrelated and have uncorrelated real and imaginary components, then $\tilde{a}_k$ and a_k have the same second order statistics, and thus that substitution will not affect the convergence rate and asymptotic error. Of course we do have to assume that the two cancelers have the same number of coefficients!

19-8.

(a) The effective step-size of the algorithm is proportional to the norm-squared of the echo impulse response $\|\mathbf{c}_k\|^2$.

(b) We could calculate this norm squared, and normalize the step-size by this value. In fact, since we expect the echo impulse response to vary slowly, we need recalculate this norm-squared only occasionally.

19-9.

(a) We get

$$\frac{\partial(\mathrm{Re}\{E_k\})^2}{\partial\hat{\theta}} = 2\mathrm{Re}\{E_k\}\frac{\partial\mathrm{Re}\{E_k\}}{\partial\hat{\theta}} \tag{19.115}$$

where the second term is

$$\begin{aligned}\frac{\partial\mathrm{Re}\{E_k\}}{\partial\hat{\theta}} &= \tfrac{1}{2}\frac{\partial}{\partial\hat{\theta}}(E_k + E_k^*)\\ &= \tfrac{1}{2}(-je^{j\hat{\theta}}\mathbf{c}_k'\tilde{\mathbf{a}}_k + je^{-j\hat{\theta}}\mathbf{c}_k^{*\prime}\tilde{\mathbf{a}}_k^*)\\ &= -\mathrm{Im}\{e^{-j\hat{\theta}}\mathbf{c}_k^{*\prime}\tilde{\mathbf{a}}_k^*\} = \mathrm{Im}\{e^{j\hat{\theta}}\mathbf{c}_k'\tilde{\mathbf{a}}_k\}.\end{aligned} \tag{19.116}$$

(b) Subtracting a constant times the derivative from last phase estimate, we get

$$\hat{\theta}_k = \hat{\theta}_{k-1} - \beta\,\mathrm{Re}\{E_k\}\,\mathrm{Im}\{e^{j\hat{\theta}}\mathbf{c}_k'\tilde{\mathbf{a}}_k\}. \tag{19.117}$$

This can be interpreted as shown below:

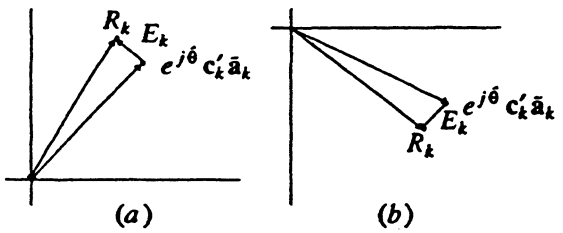

Shown are two cases, where the echo replica is above and below the real-axis. In both cases the real-error is negative, but the interpretation as to whether the phase estimate should be increased or decreased is opposite. We therefore multiply by a quantity which is positive if the echo replica is above the axis and negative if below, $\mathrm{Im}\{e^{j\hat{\theta}}\mathbf{c}_k'\tilde{\mathbf{a}}_k\}$.

(c) The correction is

$$\begin{aligned}&\mathrm{Re}\{(e^{j\theta_k} - e^{j\hat{\theta}})\mathbf{c}_k'\tilde{\mathbf{a}}_k\}\,\mathrm{Im}\{e^{-j\hat{\theta}}\mathbf{c}_k^{*\prime}\tilde{\mathbf{a}}_k^*\} =\\ &[(e^{j\theta_k} - e^{j\hat{\theta}})\mathbf{c}_k'\tilde{\mathbf{a}}_k + (e^{-j\theta_k} - e^{-j\hat{\theta}})\mathbf{c}_k^{*\prime}\tilde{\mathbf{a}}_k^*][e^{-j\hat{\theta}}\mathbf{c}_k^{*\prime}\tilde{\mathbf{a}}_k^* - e^{j\hat{\theta}}\mathbf{c}_k'\tilde{\mathbf{a}}_k].\end{aligned} \tag{19.118}$$

The expectation of the cross terms in (19.118) is zero in view of exercise 19-7. Hence the expectation of (19.118) becomes

$$\tfrac{1}{2}\sigma_a^2\|c_k\|^2\sin(\theta_k - \hat{\theta}_k). \tag{19.119}$$

As might be expected, the correction is half as large as in the complex-error case, and hence for the same step-size β the convergence is slower.